FLOWERING LOCUS C Mediates Natural Variation in the High-Temperature Response of the *Arabidopsis* Circadian Clock [W]

Kieron D. Edwards,[a] Paul E. Anderson,[b,c] Anthony Hall,[d,1] Neeraj S. Salathia,[d,2] James C.W. Locke,[c,d,e]
James R. Lynn,[f] Martin Straume,[g] James Q. Smith,[b,c] and Andrew J. Millar[a,c,3]

[a] Institute of Molecular Plant Sciences, University of Edinburgh, Edinburgh, EH9 3JH United Kingdom
[b] Department of Statistics, University of Warwick, Coventry, CV4 7AL United Kingdom
[c] Interdisciplinary Program for Cellular Regulation, University of Warwick, Coventry, CV4 7AL United Kingdom
[d] Department of Biological Sciences, University of Warwick, Coventry, CV4 7AL United Kingdom
[e] Department of Physics, University of Warwick, Coventry, CV4 7AL United Kingdom
[f] Warwick HRI, Wellesbourne, CV35 93F United Kingdom
[g] Center for Biomathematical Technology, University of Virginia, Charlottesville, Virginia 22903

Temperature compensation contributes to the accuracy of biological timing by preventing circadian rhythms from running more quickly at high than at low temperatures. We previously identified quantitative trait loci (QTL) with temperature-specific effects on the circadian rhythm of leaf movement, including a QTL linked to the transcription factor *FLOWERING LOCUS C* (*FLC*). We have now analyzed *FLC* alleles in near-isogenic lines and induced mutants to eliminate other candidate genes. We showed that *FLC* lengthened the circadian period specifically at 27°C, contributing to temperature compensation of the circadian clock. Known upstream regulators of *FLC* expression in flowering time pathways similarly controlled its circadian effect. We sought to identify downstream targets of *FLC* regulation in the molecular mechanism of the circadian clock using genome-wide analysis to identify *FLC*-responsive genes and 3503 transcripts controlled by the circadian clock. A Bayesian clustering method based on Fourier coefficients allowed us to discriminate putative regulatory genes. Among rhythmic *FLC*-responsive genes, transcripts of the transcription factor *LUX ARRHYTHMO* (*LUX*) correlated in peak abundance with the circadian period in *flc* mutants. Mathematical modeling indicated that the modest change in peak *LUX* RNA abundance was sufficient to cause the period change due to *FLC*, providing a molecular target for the crosstalk between flowering time pathways and circadian regulation.

INTRODUCTION

Circadian clocks provide organisms with a means of temporally organizing their daily metabolic and physiological activities relative to the day/night cycle. Such organization is believed to impart a selective advantage (Ouyang et al., 1998; Dodd et al., 2005). Nearly all eukaryotes and some prokaryotes possess circadian clocks, and comparison between diverse model species shows that although their components and construction are varied, they do share a unified set of defining properties: all circadian clocks are self-sustaining, entrainable, and temperature compensated (Pittendrigh, 1960). Transcription-translation

[1] Current address: School of Biological Sciences, University of Liverpool, Liverpool, L69 3BX UK.
[2] Current address: Bauer Center for Genomics Research, Harvard University, Cambridge, MA 02138.
[3] To whom correspondence should be addressed. E-mail andrew.millar@ed.ac.uk; fax 44-0131-650-5392.
The author responsible for distribution of materials integral to the findings presented in this article in accordance with the policy described in the Instructions for Authors (www.plantcell.org) is: Andrew J. Millar (andrew.millar@ed.ac.uk).
[W] Online version contains Web-only data.

feedback loops involving multiple positive and negative interacting components are important in the clock mechanisms of these model species (reviewed in Young and Kay, 2001). The *Arabidopsis thaliana* clock is putatively based on the feedback loop involving the genes *TIMING OF CAB EXPRESSION1* (*TOC1*), *CIRCADIAN CLOCK ASSOCIATED1* (*CCA1*), and *LATE ELONGATED HYPOCOTYL* (*LHY*), where *TOC1* induces the transcription of *LHY* and *CCA1*, which are translated into proteins that feed back to repress the expression of *TOC1* (Alabadi et al., 2001). Modeling of this clock suggested that it was insufficient to explain the experimental data (Locke et al., 2005a). As a result, Locke et al. (2005b) added two further components to the model: a gene *X*, which lies between *TOC1* and *LHY/CCA1*, and a gene *Y*, which forms a coupled loop and is likely to correspond to the evening-expressed gene *GIGANTEA* (*GI*).

Temperature compensation, a defining feature of circadian rhythms, results in the period of the clock changing very little when measured over a broad range of constant temperatures (Pittendrigh, 1954; Rensing and Ruoff, 2002). Natural genetic variation in the *Drosophila melanogaster* central clock gene *period* was shown to affect the temperature compensation of the fly clock (Sawyer et al., 1997). Analysis of circadian period in *Arabidopsis* accessions revealed natural genetic variation in the temperature compensation of the plant clock (Edwards et al.,
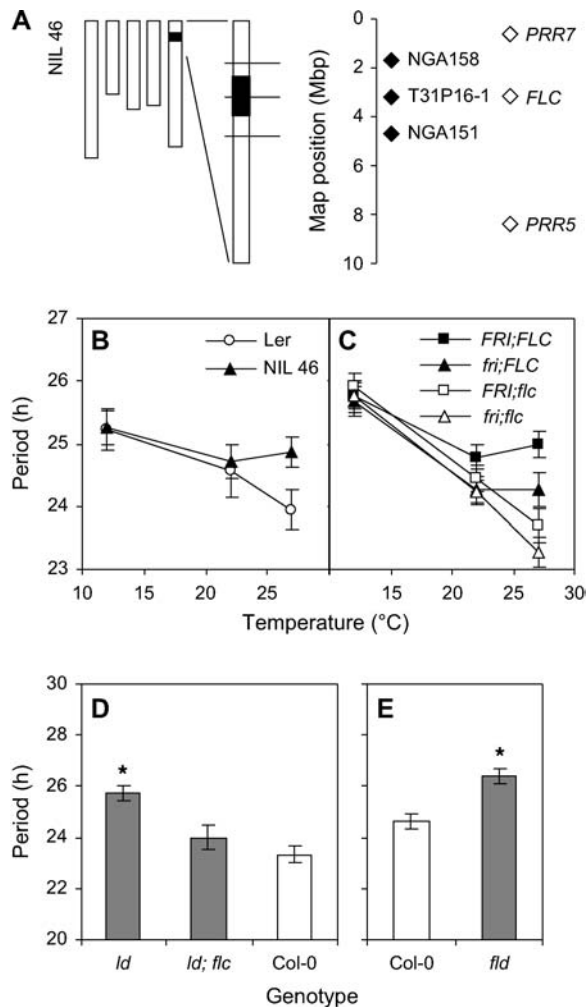
Figure 1. *FLC* Alters the Period of the Clock in a Temperature-Dependent Manner.

(A) NIL46 summary map showing the five *Arabidopsis* chromosomes and an expanded view of the top of Chromosome 5. Genotype of chromosomal regions is displayed graphically for L*er* (white) and Cvi (black), with recombination break points indicated at the midpoint between molecular markers. Position of molecular markers (closed diamonds) and clock-related genes (open diamonds) are shown at right. The leaf movement period of NIL46 and L*er* **(B)** and the *fri* and *flc* single and double mutant combinations **(C)** were assayed at 12, 22, and 27°C. Symbols are indicated in inset legends. Bars represent SE. Leaf movement period of *ld*, *ld*; *flc* **(D)**, and *fld* **(E)** mutants along with wild-type Col-0 seedlings at 27°C. Bars represent variance-weighted SE of period estimates. Asterisks **(D)** and **(E)** indicate *t* test P value < 0.05 compared with Col-0.

2005). This variation was used to map quantitative trait loci (QTL) for circadian period in recombinant inbred lines (RILs) derived from a cross between the accessions Landsberg *erecta* (L*er*) and Cape Verde Islands (Cvi) (Edwards et al., 2005).

FLOWERING LOCUS C (*FLC*) was suggested as a candidate for the period QTL *PerCv5b*, mapped on the upper arm of chromosome 5 (Edwards et al., 2005). FLC is a MADS box transcription factor that inhibits the transition to flowering by repressing

the expression of the floral integrators *AGAMOUS LIKE20* (*AGL20*) and *FLOWERING LOCUS T* (Samach et al., 2000; Michaels et al., 2005). Prolonged cold treatment, such as a winter, represses the expression of *FLC* in a process called vernalization, allowing plants to flower in the subsequent warmer conditions (reviewed in Bastow et al., 2004; Sung and Amasino, 2004). *FLC* is also regulated by a suite of autonomous pathway genes, including *FRIGIDA* (*FRI*), *LUMINIDEPENDENS* (*LD*), and *FLOWERING LOCUS D* (*FLD*; Michaels and Amasino, 1999; He et al., 2003).The L*er* allele of *flc* was shown to be weakly expressed as the result of a transposable element within the first intron of the gene (Gazzani et al., 2003), making it a strong candidate for a QTL in the Cvi crossed with L*er* RILs. Indeed, Swarup et al. (1999) previously identified a circadian period QTL (named *ANDANTE*) linked to *FLC* and showed a slight (~0.8 h) short circadian period phenotype in *flc* mutant seedlings, indicating that *FLC* could also affect the circadian clock. The molecular target of *FLC* function was unknown.

Microarray assays have enabled the large-scale identification of transcripts regulated by the circadian clock in *Arabidopsis*, *Drosophila*, and mouse (Harmer et al., 2000; Ceriani et al., 2002; Panda et al., 2002). Identifying rhythmic patterns in the short time courses and sparse samples typical of circadian array data has been challenging; a number of approaches have been adopted for different experimental designs (Akhtar et al., 2002; Langmead et al., 2002; Straume, 2004). Harmer et al. (2000) suggested that ~6% of the *Arabidopsis* genome was regulated by the circadian clock. Clustering the rhythmic expression patterns using the time of the peak allowed the identification of an overrepresented regulatory sequence (the evening element) and of functional relationships among some coexpressed genes, though this study tested only ~8000 genes (Harmer et al., 2000).

We now pursue the analysis of the *PerCv5b* QTL, using near-isogenic lines (NILs) and mutants to identify natural variation at *FLC* as the cause of the 27°C-specific QTL effect on circadian period. Using genome-wide transcriptomic analysis, we identify the likely mechanism by which *FLC* alters the period of the circadian clock at this higher temperature. Our results illustrate the benefits of functional genomics approaches, combined with dedicated data analysis methods and mathematical modeling, in understanding the quantitative molecular mechanisms downstream of a QTL of moderate effect.

Table 1. Mapping PerCv5b to FLC: NIL and Mutant Periods

Line	12°C		22°C		27°C	
	Period (h)	SE	Period (h)	SE	Period (h)	SE
L*er*	25.22	0.32	24.56	0.41	23.94	0.32
NIL46	25.27	0.29	24.72	0.27	24.86**	0.25
FRI; *FLC*	25.76	0.21	24.78	0.20	24.99	0.22
fri; *FLC*	25.69	0.24	24.26*	0.20	24.26*	0.27
FRI; *flc*	25.91	0.23	24.43	0.21	23.69**	0.26
fri; *flc*	25.76	0.25	24.22*	0.20	23.27**a	0.24

Leaf movement period estimates for NIL46 and *fri* and *flc* mutant combinations. Asterisks indicate P values of *t* test of period versus L*er* for NIL46 and *FRI*; *FLC* for mutants at * <0.05 and ** <0.01.
[a] P value <0.01 of Student's *t* test of *fri*; *flc* versus *fri*; *FLC*.
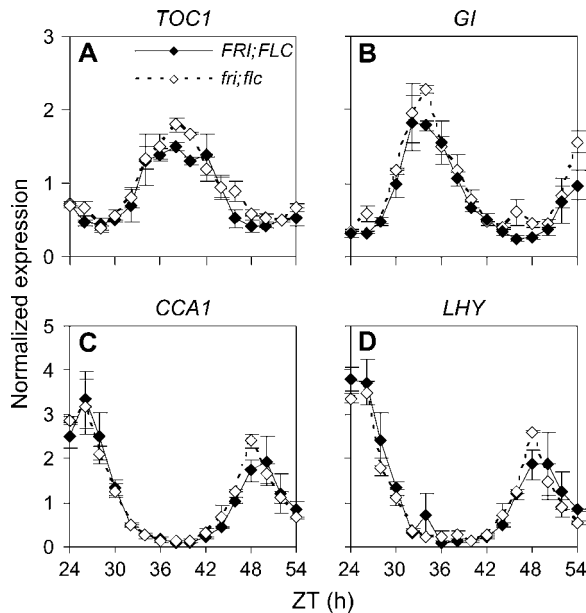
Figure 2. Temporal Expression of Clock Genes in the *FRI*; *FLC* and *fri*; *flc* Genotypes at 27°C.

The temporal pattern in transcript abundance of the clock genes *TOC1* **(A)**, *GI* **(B)**, *CCA1* **(C)**, and *LHY* **(D)** was analyzed by real-time PCR in *FRI*; *FLC* (closed diamonds) and *fri*; *flc* (open diamonds) genotype seedlings. Expression levels for each gene were normalized to the average for the *fri*; *flc* genotype with respect to *ACTIN2* (*ACT2*). Data shown are the average of two biological replicates, with error bars representing the range.

RESULTS

FLC Causes the *PerCv5b* QTL

We previously mapped six temperature-dependent QTL for circadian period in the Cvi crossed with L*er* RILs (Edwards et al., 2005). *PerCv5b* mapped to the top of Chromosome 5. The Cvi allele of this QTL was estimated to cause a 0.75-h period lengthening effect specifically at 27°C (Edwards et al., 2005). Figure 1 summarizes the mapping of the *PerCv5b* QTL to the MADS box transcription factor *FLC*.

NILs, containing a small Cvi genomic region around the *PerCv5b* locus in an otherwise isogenic L*er* background were constructed to isolate and confirm the effect of the QTL. NIL46 contained a Cvi introgression of <3 Mbp around *PerCv5b* (Figure 1A). Analysis of rhythmic leaf movement in this line showed a 27°C-specific period lengthening effect of 0.9 h relative to L*er*, consistent with the QTL effect (Figure 1B, Table 1; Edwards et al., 2005). A second independently derived NIL with an equivalent Cvi introgression to NIL46 showed the same phenotype (data not shown). The clock-affecting genes *PSEUDORESPONSE REGULATOR 7* (*PRR7*) and *PRR5* (Nakamichi et al., 2005) were considered as candidates for the multiple Chromosome 5 QTL mapped in our work and a previous study (Michael et al., 2003). Neither of these genes lay within the Cvi introgression of NIL46, ruling them out as the cause of the QTL effect contained within

this NIL (Figure 1A). *FLC* was an alternative candidate gene within the Cvi introgression of NIL46 (Figure 1A).

Period phenotypes in *flc* mutants (Swarup et al., 1999) and natural variation in the L*er* allele of the gene (Gazzani et al., 2003) supported *FLC* as a candidate for *PerCv5b*. To test this possibility, we measured the period of *flc* mutant seedlings in combination with mutant or wild-type alleles of *FRI*, a positive regulator of *FLC* expression (Michaels and Amasino, 2001). No major period differences were shown between the lines at 12°C, but small differences were shown at 22°C, and by 27°C *flc* mutant seedlings had significantly shorter periods than plants with wild-type *FLC* alleles (Figure 1C, Table 1). This response was opposite to that shown by NIL46, and both data sets suggested that stronger expression of *FLC* resulted in longer circadian period at higher temperatures (Figures 1B and 1C).

Plants of *FRI*; *FLC* genotype showed a longer period than those of *fri*; *FLC*, suggesting that the upregulation of *FLC* by *FRI* might contribute toward the period lengthening (Figure 1C). To test this, we measured the circadian period of leaf movement in plants mutated in *LD* or *FLD*, genes that normally repress the expression of *FLC* (Michaels and Amasino, 1999; He et al., 2003). Figures 1D and 1E show that the period of *ld* and *fld* mutant seedlings at 27°C was significantly longer than wild-type seedlings. The period change was prevented when the *ld* mutant was combined with a mutant allele of *flc*, indicating that period lengthening in the *ld* mutant required *FLC* and was presumably mediated by increased *FLC* expression levels in the *ld* background (Figure 1D).

Mechanisms of *FLC* Effects on the Clock

We tested whether *FLC* expression levels increased with temperature, thereby mediating the temperature-dependent period lengthening in *FLC*-expressing genotypes, but found little difference in the level of *FLC* transcript between 22 and 27°C (see Supplemental Figure 1 online). This suggested that altered *FLC* function rather than expression level caused the temperature dependence of the effect of *FLC* on the circadian clock. A simple possibility was that *FLC* might alter the period of the clock by regulating the transcription of a clock gene. To test this, the temporal expression patterns of *TOC1*, *GI*, *CCA1*, and *LHY* were compared between *fri*; *flc* and *FRI*; *FLC* seedlings at 27°C. The timing of expression of all rhythmic genes was expected to alter owing to the *FLC*-dependent change in period, but the target of *FLC* might additionally show altered expression levels. Figure 2

Table 2. Genes Scored Rhythmic by COSOPT

pMMC-β	No. Rhythmic	Rhythmic (%)	Harmer et al. (2000) (%)
<0.10	5127	22.54	88.94
<0.05	3504	15.40	82.80
<0.02	1729	7.60	61.43

Number of rhythmic genes shown as total and percentage of genes on the array as well as the percentage of genes scored rhythmic by Harmer et al. (2000) at three pMMC-β thresholds.
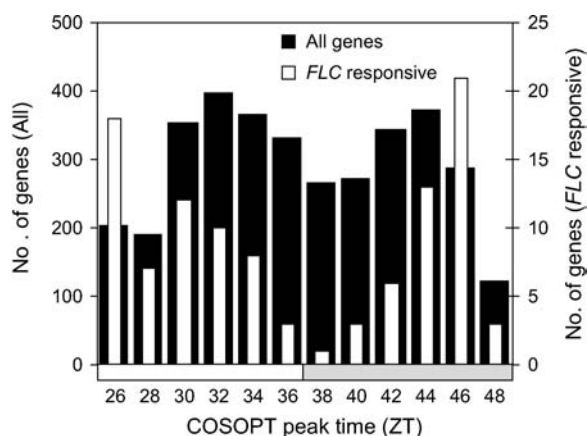
Figure 3. Distribution of COSOPT Peak Phases.

Microarray time course expression profiles of *Arabidopsis* genes were scored for circadian rhythmicity with the program COSOPT. Phase estimates for all rhythmic genes (pMMC-β <0.05; closed bars) and rhythmic *FLC*-responsive genes (open bars) were binned into 2-h intervals. The number of genes was plotted for each bin, labeled with the lower period bound of the bin. Primary *y* axis (left) represents total number of genes and secondary axis (right) represents number of *FLC*-responsive genes. The bar on the *x* axis represents subjective day (white) and night (gray).

shows that neither the mean nor the peak level of transcript abundance at 27°C was clearly affected by *FLC* expression. It was therefore unlikely that one of these central clock genes was an early target of *FLC* regulation.

Candidate Targets for *FLC* Regulation

To identify genes that might mediate the effect of *FLC* on the clock, global transcript profiles were compared in the *fri*; *flc* and *FRI*; *FLC* genotypes using the Affymetrix ATH1 microarray. RNA samples were taken from the two genotypes, under the conditions used for the leaf movement experiments at 27°C, and pooled from four time points spaced equidistantly across one circadian cycle (see Methods), in case *FLC*-dependent regulation was detectable only at specific circadian phases. Pooling may have reduced the effect shown by such genes, but it enabled a broader screen of genes peaking at different circadian phases. In the *fri*; *flc* genotype, *FLC* showed very low expression and *AGL20* showed more than threefold increased expression compared with *FRI*; *FLC* (see Supplemental Table 1 online). As *AGL20* is transcriptionally repressed by *FLC* in other conditions (Hepworth et al., 2002), this confirmed our ability to identify *FLC*-regulated genes.

Transcripts were ranked according to change in expression between the *fri*; *flc* and *FRI*; *FLC* genotypes, and the 1000 genes showing the greatest fold changes were termed *FLC* responsive (see Supplemental Table 1 online). This level was selected as an arbitrary cutoff to allow focus on potential candidate genes in the following microarray experiment. The *FLC*-responsive genes did not include any of the clock genes tested in Figure 2 nor any other genes thought to be important to circadian function at the time.

Global Analysis of Rhythmic Gene Expression

Regulators of the circadian clock are often themselves rhythmically regulated, so identifying rhythmic transcripts among the *FLC*-responsive genes could highlight possible targets of *FLC* regulation in the circadian clock mechanism. We therefore identified rhythmically regulated transcripts using the Affymetrix ATH1 array. Eight-day-old Columbia (Col-0) seedlings grown under 12-h-light/12-h-dark cycles (LD 12:12) were transferred to

Figure 4. Bayesian Clustering of Rhythmic Genes.
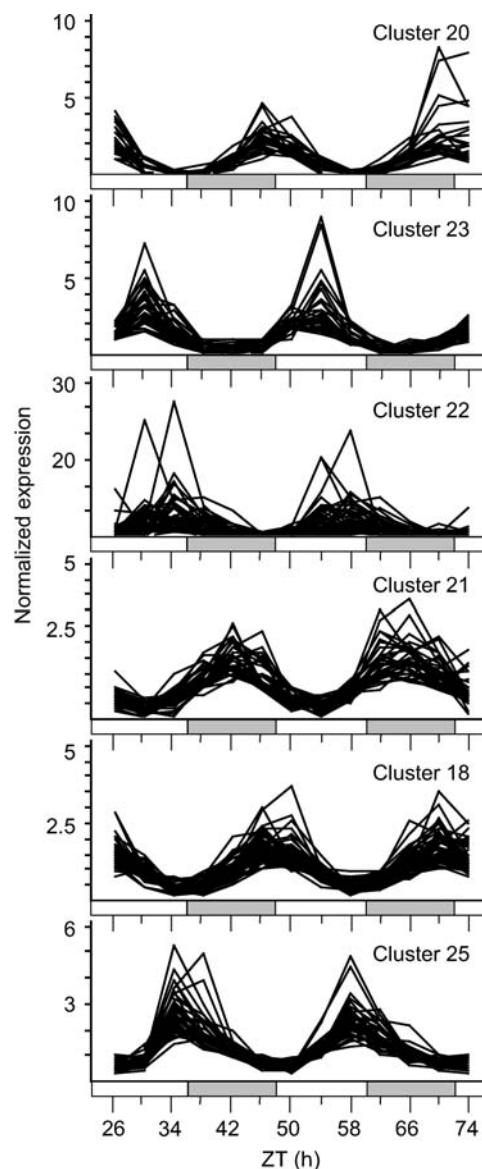
BFC was applied to microarray time course data to identify rhythmic genes. Graphs in vertical order showing expression profiles of genes in the six clusters scored with the highest amplitude. Cluster numbers are shown in the top right of each graph. Bars on *x* axes represent subjective day (white) and night (gray). The full analysis results are available from www.amillar.org.

constant light at 22°C and harvested at 13 time points, covering two circadian cycles in 4-h intervals, starting 26 h after the last dark–light transition. This time is referred to as Zeitgeber time (ZT) 26, where ZT0 is the time of the last dark–light transition. Expression values were scored for circadian regulation using the modified cosinor analysis program COSOPT (Straume, 2004), which was previously used to score circadian expression of genes in *Drosophila* and mouse (Ceriani et al., 2002; Panda et al., 2002), and is similar to the algorithm used in the earlier array study in *Arabidopsis* (Harmer et al., 2000).

Previous studies using this method employed a threshold of 0.1 for the probability (pMMC-β) that the best-fit rhythm had a significant amplitude (Harmer et al., 2000; Panda et al., 2002). pMMC-β cutoff values of 0.10, 0.05, and 0.02 were considered to score rhythmic transcripts in our data (Table 2), and all three scored the putative central oscillator components *TOC1*, *CCA1*, and *LHY* as rhythmic. The remaining *PRR* genes were all scored rhythmic at pMMC-β <0.1, but *PRR9* was not included at <0.05, and further circadian genes were also excluded at the cutoff of <0.02, suggesting this threshold was too stringent. Visual inspection of the expression patterns of genes around the threshold suggested that 0.1 might be too liberal for our data; thus, the threshold of <0.05 was selected for scoring rhythmic transcripts.

At this threshold, 3503 genes were scored as rhythmic out of 22,746 probe sets represented on the array, suggesting that ∼16% of the *Arabidopsis* genome was regulated by the circadian clock. This rhythmic set included 83% of the rhythmic genes identified by Harmer et al. (2000) using an 8000-gene array (Table 2).

All circadian phases were well represented based on COSOPT estimates of peak phase times (Figure 3). As in Harmer et al. (2000), an increased number of genes peaked around the end of the subjective day (ZT30 to ZT36 h; subjective dawns are ZT24 and ZT48, subjective dusk is ZT36) and the second half of the subjective night (ZT42 to ZT46 h). However, fewer transcripts were shown to peak around the subjective dawns (ZT26 to ZT28 and ZT48), which was not observed in the previous study (Harmer et al., 2000). Of the *FLC*-responsive genes, 105 were included in the rhythmic set. The distribution of their peak phases followed the overall pattern but also showed an increased number peaking around ZT26 and ZT46 (Figure 3).

Promoter analysis of the COSOPT phase clusters supported the suggested role of the evening element regulatory sequence

Table 3. BFC Identified Clusters

No.	Circadian Score	Amplitude	Phase (ZT)	No. Genes	Rhythmic Circadian Score (%)	Rhythmic COSOPT (%)	Clock-Related Genes
1	0.54	0.11	35.3	181	56	51	
2	0.45	0.11	42.8	311	45	32	
3	0.71	0.24	43.3	208	81	72	*PHYE*
4	0.76	0.18	43.7	72	97	94	*PHYB*
5	0.61	0.20	47.7	280	78	68	*SPA1*
6	0.60	0.25	50.0	54	81	74	
7	0.64	0.19	29.5	306	74	59	
8	0.62	0.24	30.3	53	94	75	*CRY1*
9	0.78	0.29	32.0	292	87	73	*PHYA, WNK1*
10	0.56	0.24	42.7	98	77	79	
11	0.67	0.34	41.3	46	100	100	
12	0.46	0.24	34.2	47	49	38	
13	0.71	0.35	35.4	60	100	100	
14	0.50	0.23	34.5	325	41	34	*ELF4, ELF3*
15	0.69	0.44	48.9	26	100	100	
16	0.70	0.38	45.7	63	100	97	
17	0.73	0.53	45.0	126	97	85	
18*	0.76	0.73	46.8	59	100	95	*COL1*
19	0.67	0.54	50.0	20	95	100	
20*	0.80	1.60	46.9	24	100	100	*LHY, CCA1*
21*	0.70	0.84	42.4	34	100	94	
22*	0.76	0.96	34.1	58	74	57	*GI, PRR5*
23*	0.78	1.06	30.2	30	100	87	*PRR7, PRR9, PIF4, PIL6, EPR1*
24	0.39	0.37	26.0	21	0	5	
25*	0.64	0.70	35.1	38	100	97	*TOC1, PRR3, FKF1, LUX, CCR2*
26	0.72	0.62	33.2	131	89	77	
27	0.70	0.52	30.2	100	97	87	*NPH1*

BFC clusters, showing the circadian score, amplitude, and phase estimates for the average trace for each cluster, the number of genes as a total and percentage scored rhythmic by circadian score (>0.4) and COSOPT (pMMC-β <0.05), and a list of clock-associated genes in each cluster. The asterisks indicate the six highest-amplitude clusters.

(AAAATATCT; Harmer et al., 2000; Harmer and Kay, 2005), with this sequence, and a one base variant (AAATATCT), being overrepresented in genes peaking late in the subjective day (ZT34 to ZT38; P < 2 × 10^{-6}). Also, the G-box core sequence (CACGTG) was overrepresented in genes peaking at the end of the subjective night (ZT44 to ZT46; P < 0.004), suggesting that G-box binding factors may play a role in determining this phase of expression.

COSOPT expression phase clusters were also tested for overrepresentation of groups of functionally related genes using Gene Ontology (GO) annotations. Among the most significant patterns, genes involved in photosynthesis were overrepresented around the middle of the subjective day (ZT30; P < 0.001), while genes involved in phenylpropanoid metabolism were overrepresented just before subjective dawn (ZT46; P < 0.001), consistent with previous findings (Harmer et al., 2000). Conversely, genes involved in glucose and alcohol catabolism (P = 0.001 and 0.002, respectively) and carbon utilization (P = 0.011) showed overrepresentation in the middle of the subjective night (ZT42), ∼6 h later than previously suggested for genes involved in carbon metabolism (Harmer et al., 2000).

The COSOPT analysis provided a robust method of detecting rhythmic genes and their associated properties but has limited capacity to discriminate among rhythmic waveforms. To assist the identification of candidate circadian regulators, rather than downstream clock-regulated targets, we applied a complementary clustering method.

Clustering of Expression Patterns Using Fourier Series

Fourier analysis provides a well-understood, rapid, and flexible means of characterizing rhythmic waveforms in terms of a combination of sine and cosine waves. The Fourier coefficients measure the contribution of sine and cosine waves with differing periods (for our time series, the six harmonics used are 48, 24, 16, 12, 9.6, and 8 h) to the rhythmic patterns in the data. This efficiently captures the rhythmic properties of interest to us, so we developed an agglomerative, hierarchical method of clustering our gene expression patterns based on the Fourier coefficients using a Bayesian statistical approach (see Methods). Bayesian Fourier clustering (BFC) can discriminate among circadian-regulated patterns based on the amplitude and waveform of the rhythm, in addition to the phase. Circadian-regulated expression profiles were identified by the dominant contribution of the sine and cosine waves with a 24-h period. For our data, this was reflected in the Fourier coefficients for the second harmonic, which we measured using the circadian score (see Methods).

We identified 27 circadian-regulated clusters comprising 3063 genes (13% of transcripts represented on the array). These accounted for ∼70% of the genes scored rhythmic by Harmer et al. (2000). Of the genes in circadian clusters, 65% were also scored as rhythmic by COSOPT. This rose to 86% in the six clusters with highest amplitude and fell to 50% in the six lowest amplitude clusters. Figure 4 shows the expression patterns of all genes in the six clusters of highest amplitude. All of the clusters are summarized in Table 3 and are shown in Supplemental Figure 2 online; the distribution of cluster phases, amplitudes, and gene numbers around the circadian cycle are shown in Figure 5. The

clusters varied significantly in the similarity of the individual expression profiles and in the robustness of their circadian rhythmicity but readily discriminated between genes with different amplitudes at the same peak phase (Figure 5; see Supplemental Figure 2 online).

As each cluster includes a range of expression patterns around the average, we performed a Fourier analysis of individual gene expression patterns. A total of 783 genes had a circadian score below our threshold (0.4; see Methods) despite being placed in the circadian clusters, indicating a potentially high number of false positives. The vast majority of these fell in the clusters with low amplitude: 75% of these were in the six lowest-amplitude clusters (40% of all the genes in these clusters), whereas only 2% were in the six clusters of highest amplitude (6% of all genes in these clusters).

None of the BFC clusters were scored as peaking between ZT36 and ZT40 (Figure 5). This gap in phase expression was not indicated by the phase estimates from COSOPT (Figure 3). Comparison of the expression profiles of genes in BFC clusters either side of this window suggests that genes peaking between ZT36 and ZT40 may have been pulled into the surrounding clusters. The spread of phases estimated by COSOPT in the clusters supports this (see Supplemental Figure 3 online), suggesting that the lack of genes peaking between ZT36 and ZT40 may be an artifact of the clustering.
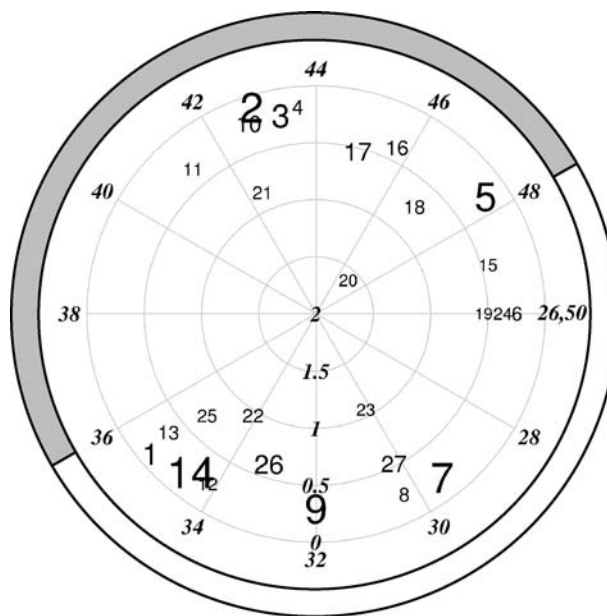
Figure 5. Phase and Amplitude of BFC-Identified Clusters.

Polar plot of phase versus amplitude for each of the rhythmic clusters identified. Clusters are represented by their identity numbers (as in Table 3). Phase estimates for clusters are shown clockwise in italics around the circumference from ZT26 to ZT50, and amplitudes are shown in italics on the radial axis. Size of cluster identity numbers represents number of genes in each cluster. Subjective night (gray) and day (white) represented by the band around the outside of the plot.
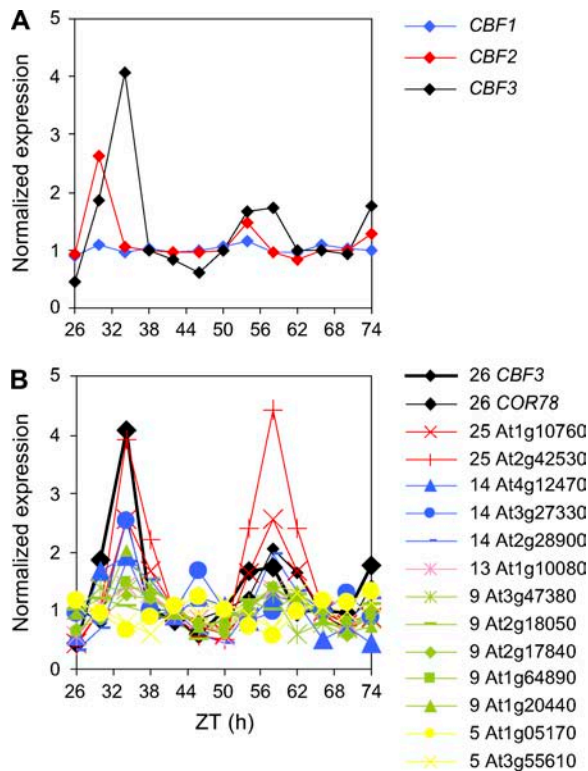
Figure 6. Circadian Expression of *CBF* Genes and Their Targets.

Microarray expression profiles of *CBF1* (blue), *CBF2* (red), and *CBF3* (black) genes **(A)** plus *CBF3* and *CBF* target genes (identified in Fowler and Thomashow, 2002) in BFC clusters **(B)**. See keys to right of graphs for gene identification. Cluster numbers shown as prefix to Arabidopsis Genome Initiative numbers in keys **(B)** and gene profiles colored by cluster.

BFC clusters were also tested for functionally related groups of genes based on GO terms and showed similar patterns for genes involved in photosynthesis and phenylpropanoid biosynthesis as COSOPT. No overrepresentation of carbon metabolism genes was seen in the middle of the subjective night for BFC, but sulfate assimilation was overrepresented in clusters peaking around the end of the subjective night (clusters 5, ZT48, $P < 0.02$ and 17, ZT45, $P < 0.001$) as suggested previously by Harmer et al. (2000). Water channel activity genes were overrepresented in the middle of the subjective day (cluster 7, ZT30, $P < 0.001$) followed by genes responsive to water and water deprivation ~3 h later (cluster 26, ZT33, $P < 0.05$). This pattern in water responses suggests a possible selective advantage of circadian clocks in plants.

Another interesting result was the overrepresentation of transcription factors in clusters 20 (seven transcription factors out of 24 genes), 23 (10 out of 30 genes), and 27 (16 out of 100 genes), suggesting that these genes may play a regulatory role in the clock or in output from it. Clusters 20 and 23 were scored with the two highest amplitudes of all the clusters. The high amplitude clusters tended to include fewer genes, whereas several of the low amplitude clusters were much larger (Figure 5, Table 3). This is consistent with the notion that genes in the smaller, higher-amplitude clusters might regulate the expression of genes in

lower-amplitude clusters, particularly those at a similar phase. This is supported by the location of genes clustered by BFC and identified as regulated by the cold response transcription factor *C REPEAT BINDING FACTOR3* (*CBF3*) primarily in clusters of lower amplitude and/or later phase than this gene.

CBF3 (also called *DREB1a*) is part of the three-gene *CBF* family (*CBF1-3*), which regulates a large number of cold-responsive genes (Fowler and Thomashow, 2002; Vogel et al., 2005). Harmer et al. (2000) showed this gene to be rhythmically expressed previously and suggested that this regulation might explain the circadian rhythm in cold resistance of cold-sensitive plants. Cold induction of all three *CBF* genes, along with two of their known targets, was recently shown to be gated by the circadian clock (Fowler et al., 2005), suggesting that clock control of the *CBF* genes may indeed be important to induction of cold resistance. *CBF3* was placed in BFC cluster 26, along with the known *CBF* target gene *COLD REGULATED78* (*COR78*; Jaglo-Ottosen et al., 1998). However, neither *CBF1* nor *CBF2* was clustered by BFC or scored rhythmic by COSOPT, although *CBF2* did appear potentially rhythmic by eye (Figure 6A). Fourteen genes, including *COR78*, from a list of 41 previously identified as *CBF* responsive (Fowler and Thomashow, 2002), were located in BFC clusters. Of these, only two genes were in a cluster with a markedly different peak phase to *CBF3*. Of the remaining 12, four were in clusters 13 and 14 (later phased and lower amplitude than *CBF3*'s cluster), two were in cluster 25 (later phased but higher amplitude), and five were in the lower amplitude but slightly earlier phased cluster 9. Visual inspection of the genes' profiles supported the suggestion that *CBF3* may be regulating the output of the other genes (Figure 6B). The earlier phasing of the five genes in cluster 9 could be explained by coregulation by the other *CBF* genes, particularly as the expression of *CBF2* showed an earlier peak in expression than *CBF3* (Figure 6A).
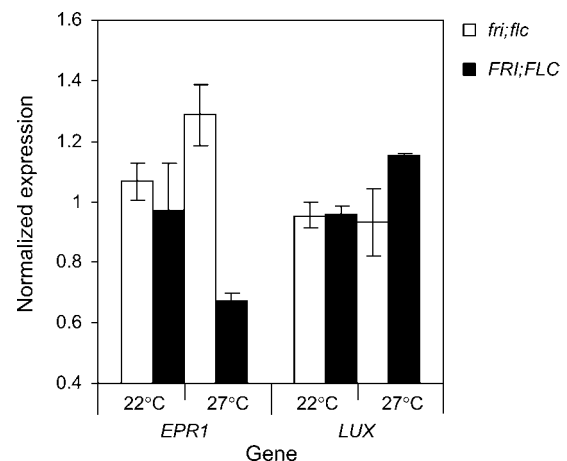
Figure 7. *EPR1* and *LUX* Expression in the *FRI*; *FLC* Genotypes.

The average expression of *EPR1* and *LUX* was analyzed by real-time PCR in pooled samples for *FRI*; *FLC* (closed bars) and *fri*; *flc* (open bars) genotype seedlings at 22 and 27°C. Expression levels for each gene are based on the average of two independent biological replicates and normalized to the average for all samples with respect to *ACT2*. Error bars show range of the replicates.
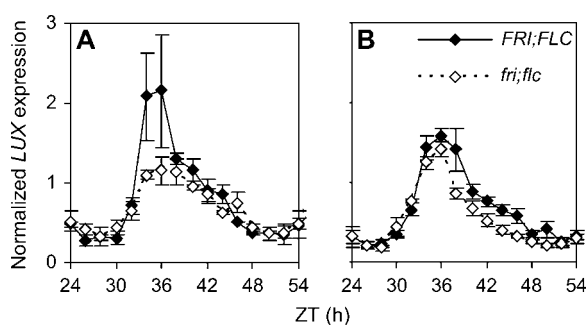
Figure 8. *FLC* Alters the Peak Level of *LUX* in a Temperature-Specific Manner.

The temporal pattern in *LUX* transcript abundance was analyzed by real-time PCR in *FRI*; *FLC* (closed diamonds) and *fri*; *flc* (open diamonds) genotype seedlings at 27°C **(A)** and at 22°C **(B)**. *LUX* expression levels were normalized with respect to *ACT2*, and the average for the *fri*; *flc* genotype at each temperature across ZT32 to ZT40 was set to 1. Data shown are the average of two to three biological replicates, with technical triplicates (see Methods). Error bars represent SE.

Many known clock genes (including *LHY*, *CCA1*, *GI*, and *TOC1*) were placed within the six clusters of highest amplitude (Table 3). Two notable absentees from this list included *EARLY FLOWERING3* (*ELF3*) and *ELF4*, in which mutations can cause arrhythmic circadian phenotypes (Hicks et al., 1996; Doyle et al., 2002). Similarly, other genes, such as *ZEITLUPE*, are known to affect the function of the clock but are not clock regulated at the transcript level (Somers et al., 2000). Thus, the high-amplitude clusters did not provide a comprehensive list of important clock genes, but they did provide a means of identifying a subset of potentially important clock genes from our list of *FLC*-responsive genes. The results of our COSOPT and BFC analyses are available from www.amillar.org.

Testing *FLC*-Responsive Genes

Of the *FLC*-responsive genes, 132 were in BFC clusters, with 32 falling in the six highest amplitude clusters (see Supplemental Table 2 online). Four of the 32 genes were transcription factors, highlighting them as candidates to potentially affect clock function. Three of the transcription factors were SHAQKYF-type MYB genes, like the core clock components *LHY* and *CCA1* (Schaffer et al., 1998; Wang and Tobin, 1998), and the other was a member of the WRKY family. One of the MYB genes, *EARLY PHYTOCHROME RESPONSIVE1* (*EPR1*), was previously shown to be rhythmically regulated and suggested as a component of a slave oscillator regulating some output pathways from the circadian clock (Kuno et al., 2003). *EPR1* transcript abundance in *fri*; *flc* and *FRI*; *FLC* seedlings was tested by quantitative PCR of the pooled samples used in the microarray experiments at 27°C, along with a comparative set grown at 22°C. Figure 7 shows that, as suggested by the array data, *FLC* downregulated the expression of *EPR1* at 27°C. Overexpression of *EPR1*, however, reportedly did not show any period effects (Kuno et al., 2003), and similarly little or no period phenotype was shown by leaf movement analysis of the *epr1* T-DNA insertion mutant SALK_047716

at either 22 or 27°C (see Supplemental Figure 4 online), suggesting that *EPR1* did not mediate *FLC*'s effect on the clock.

A more likely candidate was offered by another of the MYB transcription factors, At3g46640. This gene was recently identified as *LUX ARRHYTHMO* (*LUX*; also called *PHYTOCLOCK1*). Arrhythmic circadian phenotypes were shown by *lux* mutants, suggesting that the gene is important to the function of the clock (Hazen et al., 2005; Onai and Ishiura, 2005). As for *EPR1*, the expression of *LUX* in *fri*; *flc* and *FRI*; *FLC* seedlings was tested by quantitative PCR. *LUX* showed increased expression in the *FRI*; *FLC* genotype at 27°C, but no difference was apparent in its expression levels between the lines at 22°C (Figure 7). Figure 8 shows the temporal expression of *LUX* in the *fri*; *flc* and *FRI*; *FLC* genotypes at 27 and 22°C. *LUX* was clustered along with *TOC1* by BFC (cluster 25; Table 3), and this was supported by the temporal expression pattern shown for both genes by real-time PCR (Figures 2A and 8). Trough levels of *LUX* expression were comparable between the two genotypes at both temperatures. The peak in *LUX* expression was approximately twofold higher in the *FRI*; *FLC* seedlings at 27°C but only slightly higher at 22°C (Figure 8). This small increase in *LUX* RNA at 22°C was nonetheless consistently observed over multiple time points in replicated experiments. Thus, *FLC*-dependent *LUX* expression correlated with period change at both 22 and 27°C, with only small differences in peak *LUX* expression level (Figure 8) and period (Figure 1C, Table 1) between the *FRI*; *FLC* genotypes at 22°C compared with the larger changes at 27°C. We could not test the requirement for *LUX* to mediate the period change caused by *FLC* by constructing the *flc lux* double mutant because the *lux* single mutant was already arrhythmic (Hazen et al., 2005). We therefore sought an alternative quantitative test.

The evening phase of *LUX* expression and its role as a transcription factor suggests it may help to close the loop between *TOC1* and *LHY/CCA1* in the clock mechanism (Hazen et al., 2005). Locke et al. (2005b) proposed a *TOC1*-activated factor, modeled as a gene *X*, to explain the delay between peak
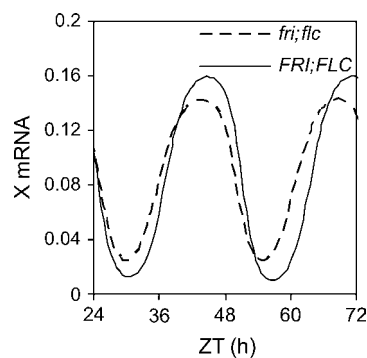
Figure 9. Modeling the Effect of *LUX* on the Clock.

Graph showing temporal expression of *X* (mRNA abundance) for *fri*; *flc* (dashed line) and *FRI*; *FLC* (solid line) genotypes as predicted by the model by Locke et al. (2005b). Initial parameters were taken from this model, and maximum transcription rate of *X* mRNA was increased by 10% under constant light conditions to simulate the increased peak expression of *LUX* mRNA in the *FRI*; *FLC* genotype compared with *fri*; *flc*. This resulted in a 1.6-h increase to free running period of the model.

expression of *TOC1* and the increase in expression of *LHY/ CCA1*. *LUX* alone is unlikely to be *X*, as the expression pattern of *LUX* RNA is similar to *TOC1* RNA; however, *LUX* may contribute to the synthesis or assembly of active X. We therefore modeled the increase in peak expression of *LUX* by increasing the parameter that specifies the maximum transcription rate of gene *X* by 10% in the model by Locke et al. (2005b). This elevated the peak levels of *X* RNA by 12% and caused a 1.6-h period lengthening in the model under constant light (Figure 9), similar to the period lengthening in *FRI*; *FLC* plants relative to *fri*; *flc* at 27°C.

DISCUSSION

FLC's involvement in the circadian clock was first suggested by QTL mapping (Swarup et al., 1999), and further analysis revealed the *PerCv5b* QTL overlapping *FLC*'s map location, with a high-temperature-specific effect on circadian period (Edwards et al., 2005). The similarity of temperature specificity, direction, and extent of the period phenotype in the QTL, in NILs carrying the weak *FLC*-L*er* allele or functional *FLC*-Cvi allele, as well as in single or double mutant combinations of induced *flc* and *fri* alleles strongly support *FLC* as the cause of the *PerCv5b* QTL. Temperature compensation keeps the circadian period relatively constant over a wide temperature range and is a ubiquitous property of circadian rhythms. Shorter periods are commonly observed at the upper end of the physiological temperature range due to increased biochemical reaction rates (Rensing and Ruoff, 2002). *FLC* expression contributes to normal temperature compensation of the *Arabidopsis* circadian clock by counteracting the period shortening observed in *flc* mutants at 27°C.

As aberrant circadian timing impairs plant growth (Dodd et al., 2005), this suggests that the circadian function of *FLC* is likely to be relevant to fitness in some habitats. The period change caused by *FLC* at 27°C is at least as great as the effects of natural allelic variants in *Drosophila* that are distributed in a latitudinal cline (Sawyer et al., 1997). *FLC* expression could be lost either by epigenetic repression of *FLC* following vernalization (Bastow et al., 2004; Sung and Amasino, 2004) or in the early flowering accessions that carry mutations of *FLC* or its activator *FRI* (Michaels and Amasino, 1999; Johanson et al., 2000; Gazzani et al., 2003). Selective pressure for such downregulation of *FLC* function in flowering time appears to have overridden secondary effects of altered circadian timing, at least in these cases. The multiple QTL that affect circadian period at 27°C (Edwards et al., 2005) might in part reflect compensating mechanisms to balance selection on flowering time and circadian timing.

Transcriptomic analysis comparing the *fri*; *flc* and *FRI*; *FLC* genotypes at 27°C was used to identify *FLC*-responsive genes. A list of 1000 candidate genes showing greatest change in expression between the two genotypes included *FLC* and *AGL20*, but few other genes known to be involved in the regulation of flowering time or, for that matter, of the circadian clock. Further microarray assays were used to identify circadian-regulated transcripts and highlight a subset of candidate genes to mediate *FLC*'s effect on the clock. Some differences were apparent between the two methods of scoring rhythmic transcripts, COSOPT and BFC. Overall, COSOPT gave a more reliable indication of rhythmicity, which suggested that ~16% of the *Arabidopsis* genome was

clock regulated. Clustering by BFC enabled identification of genes with higher amplitude profiles, similar to those of known important clock genes, as a means of targeting potentially important rhythmic regulators. Even the high-amplitude BFC clusters included several genes that were not scored as rhythmic by COSOPT (Table 3). A consensus of the two methods indicated that a minimum of 8.7% of the genes on the array showed a circadian expression pattern under our experimental conditions.

GO and promoter analysis of the genes scored rhythmic by COSOPT and clustered by BFC revealed that the data contained considerable information on functional clustering and potential regulatory sequences. Both methods used in concert enabled wider sampling of this information. Clearly, not all the important clock-affecting genes are rhythmically regulated at the transcript level, but BFC provides a means of targeting a few genes from a large number, as is often required from array data. This identified *LUX* as a strong candidate to mediate *FLC*'s effect on the clock. Mathematical modeling suggested that a modest increase in peak *LUX* expression, as observed in *FRI*; *FLC*, would be sufficient to explain *FLC*'s effect on the clock at 27°C. One caveat to this is that plants constitutively overexpressing *LUX* did not show a long period phenotype but rather wild-type period oscillations that damped into arrhythmia (Onai and Ishiura, 2005). However, rhythmic overexpression of *LUX*, as in *FRI*; *FLC*, may alter the clock in a different way to constitutive overexpression of the gene. Indeed, increasing rhythmically expressed *LUX* gene dosage does appear to increase circadian period, consistent with our prediction, because plants heterozygous for a *lux* mutation have a shorter period than wild-type *LUX* homozygotes (Onai et al., 2004).

Natural genetic variation is a valuable resource, and its importance for understanding plant biology is increasingly being recognized (reviewed in Koornneef et al., 2004). Pinpointing the mechanisms of small effect QTL, starting with the identification of the underlying genes, is not a trivial matter (Weigel and Nordborg, 2005). As demonstrated for *FLC*, mathematical modeling provides a useful complement to experiments in understanding quantitative changes in plant response networks.

METHODS

Plant Materials and Growth Conditions

NIL46 was produced by genotypic selection from a backcross of NIL187 (donated by M. Koornneef) to L*er*. The *fri*; *flc*, *FRI*; *FLC*, *fri*; *FLC*, and *FRI*; *flc* genotypic combinations used for leaf movement and RNA time courses are in the Col background with combinations of either wild-type Col or *flc*-3 and *FRI*-SF2 alleles (Michaels and Amasino, 1999, 2001). The *ld*-1 and *ld*-1; *flc*-3 mutants have been described (Michaels and Amasino, 2001), as have the *fld*-3 mutants (He et al., 2003). Wild-type Col-0 seedlings were used for the microarray circadian time-course experiment. Unless otherwise stated, seedlings were sterilized and grown as described (Edwards et al., 2005).

Measuring Circadian Rhythms

Circadian rhythms were measured by video imaging of leaf movement under constant light and analyzed in the BRASS interface (Edwards et al., 2005; http://www.amillar.org/Downloads.html). Mean period estimates for each genotype in Figures 1B and 1C are based on 10 to 50 leaf traces

from two to four independent experiments at each temperature, analyzed using REML (Patterson and Thompson, 1971) in the statistical package GENSTAT 5 (Payne et al., 1993). Mean period estimates in Figures 1D and 1E are from representative experiments analyzed in BRASS.

Quantitative RT-PCR

Approximately 100 seedlings were ground under liquid nitrogen per time point, and total RNA was extracted using a Plant RNeasy kit and RNase-free DNase (Qiagen) according to the manufacturer's instructions. cDNA samples for real-time PCR applications were reverse transcribed from 1 μg of RNA using the RevertAid first-strand cDNA synthesis kit (Fermentas, Helena Biosciences) according to the manufacturer's instructions, and the cDNA product was diluted 1:5 in RNase-free water. Transcript abundance of *TOC1*, *CCA1*, *LHY*, *GI*, *EPR1*, and *LUX* were assessed by quantitative real-time PCR in either an ABI PRISM 7700 (Applied Biosystems) or Bio-Rad iCycler IQ using ABI SYBR Green PCR Master Mix (Applied Biosystems) in 15-μL reactions. Transcript levels were normalized to *ACT2* using a cDNA dilution series for each primer set in each experiment. Each RNA sample was assayed in triplicate. Primers for *GI* and *ACT2* have been described previously (Locke et al., 2005b). Primer sequences to assess other transcripts are shown below: *TOC1* forward, 5′-ATCTTCGCAGAATCCCTGTGATA-3′; *TOC1* reverse, 5′-GCACCTAGCTTCAAGCACTTTACA-3′; *CCA1* forward, 5′-CTGTGT-CTGACGAGGGTCGAA-3′; *CCA1* reverse, 5′-ATATGTAAAACTTTGCGG-CAATACCT-3′; *LHY* forward, 5′-CAACAGCAACAACAATGCAACTAC-3′ *LHY* reverse, 5′-AGAGAGCCTGAAACGCTATACGA-3′; *EPR1* forward, 5′-CCAAGATGGCTCAGGAAGCT-3′; *EPR1* reverse, 5′-AAGGATGTGC-CGGTTTTCTCT-3′; *LUX* forward, 5′-GACGATGATTCTGATGATAAGG-3′; *LUX* reverse, 5′-CAGTTTATGCACATCATATGGG-3′.

Data presented in Figure 8 are based on the average of three independent biological replicates for all time points aside from ZT24 to ZT30 and ZT42 to ZT54 in Figure 8A, which are based on independent biological duplicates.

Microarrays

Total RNA was extracted as described above. Seedlings for the *fri*; *flc* versus *FRI*; *FLC* microarray were grown as described for leaf movement and placed into constant conditions at 27°C. Four samples were taken at 6-h intervals starting from 24 h into constant conditions (ZT24, ZT30, ZT36, and ZT42), and equal amounts of RNA were pooled from each time point for each genotype. An independent biological repeat was performed for both genotypes. Seedlings for the Col-0 time course were sterilized and grown as described above, with the exception that they were placed immediately into LD 12:12 and grown for 7 d at 22°C. At dawn on the 8th day, they were placed into constant 60 to 65 μmol m^{-2} s^{-1} cool white fluorescent light. Samples were taken over two circadian cycles at 4-h intervals starting from ZT26. Samples were assayed on the Affymetrix GeneChip oligonucleotide ATH1 array (Affymetrix) according to the manufacturer's instructions. Background correction and normalization and gene expression analysis of the array data were performed using the GC-RMA routine (Wu et al., 2004) in GeneSpring version 7.2 (Silicon Genetics). This results in the normalization of expression values to the average expression of all time points for that probe set. The normalized values are then used to detect rhythms using COSOPT or BFC. Promoter analysis of the immediate upstream regions (1000 bp from start codon) of the transcripts was performed in GeneSpring, and GO terms were analyzed using FuncAssociate (Berriz et al., 2003).

Scoring Circadian Transcripts Using COSOPT

COSOPT was used as previously described (Straume, 2004), with the exception of the removal of the initial sampling-density-weighted linear regression detrending. The sparse time points and short time course, covering only two cycles of circadian period, enabled the linear regression to skew the data. An increased number of genes were scored rhythmic at the same pMMC-β threshold when no detrending of the data occurred, but ~80% of the rhythmic genes for a given pMMC-β were common to both methods. Phase estimates presented in Figure 3 and Supplemental Figure 3 online have been translated into ZT within the first circadian cycle of the real array data.

Scoring Circadian Transcripts Using BFC

BFC employs Bayesian techniques to cluster time series data according to a standard linear model (Heard et al., 2006). Curves were clustered together by BFC if they appear to have been drawn from a joint distribution with parameters β and σ², where Y = Bβ + ε and Y holds the expression levels. ε is a noise term, which is normally distributed with mean zero and variance σ². Design matrix B was chosen to contain Fourier basis functions for identification of rhythmic genes. β holds the Fourier coefficients for the average profile of each cluster (these values produce the average profile, seen as the blue line in Supplemental Figure 2 online, and the circadian score, amplitude, and phase values in Table 3). Thus, each cluster of genes is characterized by a different β and σ². The clustering is exceptionally fast because σ² was chosen to be inverse γ distributed and, given σ², β is multivariate normal. The algorithm was used to perform an agglomerative hierarchical clustering; each gene expression profile was initially put in a separate cluster and then the two clusters most similar in covariance structure were merged repeatedly until all profiles formed one cluster. At each merger, the clustering was scored; the highest score was obtained for 27 clusters for 3063 genes. To search the massive space of potential clusters effectively (Anderson et al., 2005), the 22,810 gene profiles were arbitrarily split into four groups. Each of the groups was clustered as described, then clusters from each group that contained rhythmic genes were clustered with the rhythmic clusters from another group, until all remaining gene profiles could be clustered in a single group.

Circadian clusters were identified by dominance of the second harmonic (24-h period). This dominance was measured by the circadian score, which might more accurately be termed the second harmonic ratio: $\sqrt{a_2^2 + b_2^2} / \sum_{i=2}^{6} \sqrt{a_i^2 + b_i^2}$, where a_i is the coefficient of the ith cosine term and b_i the coefficient of the ith sine term. Thus, a cluster with a high circadian score indicated that the 24-h period characterized the average expression pattern more than the shorter periods. A circadian score of >0.4 was used as a guide to determine which clusters were retained at each stage of the hierarchical clustering. On this basis, BFC identified 26 clusters of circadian genes together with a 27th cluster with a circadian score of 0.38 that appeared circadian regulated by eye. Amplitude of rhythms was provided by the second harmonic ($\sqrt{a_2^2 + b_2^2}$), and phase was determined as the maximum point of the average expression profile within the first cycle of data.

Accession Numbers

Data for the microarray experiments described in Methods are available from the NASCArrays database (http://affymetrix.arabidopsis.info/narrays/experimentbrowse.pl) under the accession numbers NASCAR-RAYS-334 (*FRI*; *FLC* versus *fri*; *flc*) and NASCARRAYS-108 (circadian time course).

Supplemental Data

The following materials are available in the online version of this article.

   Supplemental Figure 1. *FLC* mRNA Expression at 22 and 27°C.

   Supplemental Figure 2. BFC Clusters.

Supplemental Figure 3. COSOPT and BFC Peak Time Comparisons.

Supplemental Figure 4. *EPR1* Leaf Movement.

Supplemental Table 1. *FLC*-Responsive Genes.

Supplemental Table 2. *FLC* Clock Candidate Genes.

REFERENCES

Akhtar, R.A., Reddy, A.B., Maywood, E.S., Clayton, J.D., King, V.M., Smith, A.G., Gant, T.W., Hastings, M.H., and Kyriacou, C.P. (2002). Circadian cycling of the mouse liver transcriptome, as revealed by cDNA microarray, is driven by the suprachiasmatic nucleus. Curr. Biol. **12,** 540–550.

Alabadi, D., Oyama, T., Yanovsky, M.J., Harmon, F.G., Mas, P., and Kay, S.A. (2001). Reciprocal regulation between *TOC1* and *LHY/CCA1.* Science **293,** 880–883.

Anderson, P.E., Smith, J.Q., Edwards, K.D., and Millar, A.J. (2005). Bayesian Clustering and Model Exploration. (Coventry, UK: University of Warwick).

Bastow, R., Mylne, J.S., Lister, C., Lippman, Z., Martienssen, R.A., and Dean, C. (2004). Vernalization requires epigenetic silencing of FLC by histone methylation. Nature **427,** 164–167.

Berriz, G.F., King, O.D., Bryant, B., Sander, C., and Roth, F.P. (2003). Characterizing gene sets with FuncAssociate. Bioinformatics **19,** 2502–2504.

Ceriani, M.F., Hogenesch, J.B., Yanovsky, M., Panda, S., Straume, M., and Kay, S.A. (2002). Genome-wide expression analysis in Drosophila reveals genes controlling circadian behavior. J. Neurosci. **22,** 9305–9319.

Dodd, A.N., Salathia, N., Hall, A., Kevei, E., Toth, R., Nagy, F., Hibberd, J., Millar, A.J., and Webb, A.A. (2005). Plant circadian clocks increase photosynthesis, growth, survival, and competitive advantage. Science **309,** 630–633.

Doyle, M.R., Davis, S.J., Bastow, R.M., McWatters, H.G., Kozma-Bognar, L., Nagy, F., Millar, A.J., and Amasino, R.M. (2002). The *ELF4* gene controls circadian rhythms and flowering time in *Arabidopsis thaliana.* Nature **419,** 74–77.

Edwards, K.D., Lynn, J.R., Gyula, P., Nagy, F., and Millar, A.J. (2005). Natural allelic variation in the temperature-compensation mechanisms of the *Arabidopsis thaliana* circadian clock. Genetics **170,** 387–400.

Fowler, S., and Thomashow, M.F. (2002). Arabidopsis transcriptome profiling indicates that multiple regulatory pathways are activated during cold acclimation in addition to the CBF cold response pathway. Plant Cell **14,** 1675–1690.

Fowler, S.G., Cook, D., and Thomashow, M.F. (2005). Low temperature induction of Arabidopsis CBF1, 2, and 3 is gated by the circadian clock. Plant Physiol. **137,** 961–968.

Gazzani, S., Gendall, A.R., Lister, C., and Dean, C. (2003). Analysis of the molecular basis of flowering time variation in Arabidopsis accessions. Plant Physiol. **132,** 1107–1114.

Harmer, S.L., Hogenesch, J.B., Straume, M., Chang, H.S., Han, B., Zhu, T., Wang, X., Kreps, J.A., and Kay, S.A. (2000). Orchestrated transcription of key pathways in Arabidopsis by the circadian clock. Science **290,** 2110–2113.

Harmer, S.L., and Kay, S.A. (2005). Positive and negative factors confer phase-specific circadian regulation of transcription in Arabidopsis. Plant Cell **17,** 1926–1940.

Hazen, S.P., Schultz, T.F., Pruneda-Paz, J.L., Borevitz, J.O., Ecker, J.R., and Kay, S.A. (2005). *LUX ARRHYTHMO* encodes a Myb domain protein essential for circadian rhythms. Proc. Natl. Acad. Sci. USA **102,** 10387–10392.

He, Y., Michaels, S.D., and Amasino, R.M. (2003). Regulation of flowering time by histone acetylation in Arabidopsis. Science **302,** 1751–1754.

Heard, N.A., Holmes, C.C., and Stephens, D.A. (2006). A quantitative study of gene regulation involved in the immune response of Anopheline mosquitoes: An application of Bayesian hierarchical clustering of curves. J. Am. Stat. Assoc., in press.

Hepworth, S.R., Valverde, F., Ravenscroft, D., Mouradov, A., and Coupland, G. (2002). Antagonistic regulation of flowering-time gene *SOC1* by CONSTANS and FLC via separate promoter motifs. EMBO J. **21,** 4327–4337.

Hicks, K.A., Millar, A.J., Carré, I.A., Somers, D.E., Straume, M., Meeks-Wagner, D.R., and Kay, S.A. (1996). Conditional circadian dysfunction of the Arabidopsis *early-flowering 3* mutant. Science **274,** 790–792.

Jaglo-Ottosen, K.R., Gilmour, S.J., Zarka, D.G., Schabenberger, O., and Thomashow, M.F. (1998). Arabidopsis CBF1 overexpression induces COR genes and enhances freezing tolerance. Science **280,** 104–106.

Johanson, U., West, J., Lister, C., Michaels, S., Amasino, R., and Dean, C. (2000). Molecular analysis of *FRIGIDA*, a major determinant of natural variation in Arabidopsis flowering time. Science **290,** 344–347.

Koornneef, M., Alonso-Blanco, C., and Vreugdenhil, D. (2004). Naturally occurring genetic variation in *Arabidopsis thaliana.* Annu. Rev. Plant Biol. **55,** 141–172.

Kuno, N., Moller, S.G., Shinomura, T., Xu, X., Chua, N.H., and Furuya, M. (2003). The novel MYB protein EARLY-PHYTOCHROME-RESPONSIVE1 is a component of a slave circadian oscillator in Arabidopsis. Plant Cell **15,** 2476–2488.

Langmead, C.J., McClung, C.R., and Donald, B.R. (2002). A maximum entropy algorithm for rhythmic analysis of genome-wide expression patterns. Proc. IEEE Comput. Soc. Bioinform. Conf. **1,** 237–245.

Locke, J.C.W., Millar, A.J., and Turner, M.S. (2005a). Modelling genetic networks with noisy and varied experimental data: The circadian clock in *Arabidopsis thaliana.* J. Theor. Biol. **234,** 383–393.

Locke, J.C.W., Southern, M.M., Kozma-Bognar, L., Hibberd, V., Brown, P.E., Turner, M.S., and Millar, A.J. (June 28, 2005b).

Extension of a genetic network model by iterative experimentation and mathematical analysis. Mol. Syst. Biol. **1,** http://dx.doi.org/10.1038/msb4100018.

Michael, T.P., Salome, P.A., Yu, H.J., Spencer, T.R., Sharp, E.L., McPeek, M.A., Alonso, J.M., Ecker, J.R., and McClung, C.R. (2003). Enhanced fitness conferred by naturally occurring variation in the circadian clock. Science **302,** 1049–1053.

Michaels, S.D., and Amasino, R.M. (1999). *FLOWERING LOCUS C* encodes a novel MADS domain protein that acts as a repressor of flowering. Plant Cell **11,** 949–956.

Michaels, S.D., and Amasino, R.M. (2001). Loss of *FLOWERING LOCUS C* activity eliminates the late-flowering phenotype of *FRIGIDA* and autonomous pathway mutations but not responsiveness to vernalization. Plant Cell **13,** 935–941.

Michaels, S.D., Himelblau, E., Kim, S.Y., Schomburg, F.M., and Amasino, R.M. (2005). Integration of flowering signals in winterannual Arabidopsis. Plant Physiol. **137,** 149–156.

Nakamichi, N., Kita, M., Ito, S., Sato, E., Yamashino, T., and Mizuno, T. (2005). The *Arabidopsis* pseudo-response regulators, PRR5 and PRR7, coordinately play essential roles for circadian clock function. Plant Cell Physiol. **46,** 609–619.

Onai, K., and Ishiura, M. (2005). *PHYTOCLOCK 1* encoding a novel GARP protein essential for the *Arabidopsis* circadian clock. Genes Cells **10,** 963–972.

Onai, K., Okamoto, K., Nishimoto, H., Morioka, C., Hirano, M., Kami-ike, N., and Ishiura, M. (2004). Large-scale screening of *Arabidopsis* circadian clock mutants by a high-throughput real-time bioluminescence monitoring system. Plant J. **40,** 1–11.

Ouyang, Y., Andersson, C.R., Kondo, T., Golden, S.S., and Johnson, C.H. (1998). Resonating circadian clocks enhance fitness in cyanobacteria. Proc. Natl. Acad. Sci. USA **95,** 8660–8664.

Panda, S., Antoch, M.P., Miller, B.H., Su, A.I., Schook, A.B., Straume, M., Schultz, P.G., Kay, S.A., Takahashi, J.S., and Hogenesch, J.B. (2002). Coordinated transcription of key pathways in the mouse by the circadian clock. Cell **109,** 307–320.

Patterson, H.D., and Thompson, R. (1971). Recovery of interblock information when block sizes are unequal. Biometrika **58,** 545–554.

Payne, R.W., Lane, P., Digby, P., Harding, S., Leech, P., Morgan, G., Todd, A., Thompson, R., Tunnicliffe, W., Welham, S., and White, R. (1993). Genstat 5 Release 3 Reference Manual. (Oxford: Oxford University Press).

Pittendrigh, C.S. (1954). On temperature independance in the clock system controlling emergence time in Drosophilla. Proc. Natl. Acad. Sci. USA **40,** 1018–1029.

Pittendrigh, C.S. (1960). Circadian rhythms and the circadian organisation of living systems. Cold Spring Harb. Symp. Quant. Biol. **25,** 159–184.

Rensing, L., and Ruoff, P. (2002). Temperature effect on entrainment, phase shifting, and amplitude of circadian clocks and its molecular bases. Chronobiol. Int. **19,** 807–864.

Samach, A., Onouchi, H., Gold, S.E., Ditta, G.S., Schwarz-Sommer, Z., Yanofsky, M.F., and Coupland, G. (2000). Distinct roles of CONSTANS target genes in reproductive development of Arabidopsis. Science **288,** 1613–1616.

Sawyer, L.A., Hennessy, J.M., Peixoto, A.A., Rosato, E., Parkinson, H., Costa, R., and Kyriacou, C.P. (1997). Natural variation in a Drosophila clock gene and temperature compensation. Science **278,** 2117–2120.

Schaffer, R., Ramsay, N., Samach, A., Corden, S., Putterill, J., Carre, I.A., and Coupland, G. (1998). The late elongated hypocotyl mutation of Arabidopsis disrupts circadian rhythms and the photoperiodic control of flowering. Cell **93,** 1219–1229.

Somers, D.E., Schultz, T.F., Milnamow, M., and Kay, S.A. (2000). *ZEITLUPE* encodes a novel clock-associated PAS protein from Arabidopsis. Cell **101,** 319–329.

Straume, M. (2004). DNA microarray time series analysis: Automated statistical assessment of circadian rhythms in gene expression patterning. Methods Enzymol. **383,** 149–166.

Sung, S., and Amasino, R.M. (2004). Vernalization and epigenetics: How plants remember winter. Curr. Opin. Plant Biol. **7,** 4–10.

Swarup, K., Alonso-Blanco, C., Lynn, J.R., Michaels, S.D., Amasino, R.M., Koornneef, M., and Millar, A.J. (1999). Natural allelic variation identifies new genes in the *Arabidopsis* circadian system. Plant J. **20,** 67–77.

Vogel, J.T., Zarka, D.G., Van Buskirk, H.A., Fowler, S.G., and Thomashow, M.F. (2005). Roles of the CBF2 and ZAT12 transcription factors in configuring the low temperature transcriptome of Arabidopsis. Plant J. **41,** 195–211.

Wang, Z.Y., and Tobin, E.M. (1998). Constitutive expression of the *CIRCADIAN CLOCK ASSOCIATED 1* (*CCA1*) gene disrupts circadian rhythms and suppresses its own expression. Cell **93,** 1207–1217.

Weigel, D., and Nordborg, M. (2005). Natural variation in Arabidopsis. How do we find the causal genes? Plant Physiol. **138,** 567–568.

Wu, Z., Irizarry, R.A., Gentleman, R., Murillo, F.M., and Spencer, F. (2004). A Model Based Background Adjustment for Oligonucleotide Expression Arrays. (Baltimore, MD: Johns Hopkins University), http://www.bepress.com/jhubiostat/paper1.

Young, M.W., and Kay, S.A. (2001). Time zones: A comparative genetics of circadian clocks. Nat. Rev. Genet. **2,** 702–715.

Supplementary Figure Legends

Supplementary Figure 1 – *FLC* mRNA expression at 22°C and 27°C
FLC transcript abundance was measured across a circadian cycle by quantitative real time PCR in *FRI*; *FLC* genotype seedlings at 22°C (closed bars) or 27°C (open bars). Expression values are the average of two independent biological replicates and normalised to the mean of all samples. Error bars show the range of the two replicates.

Supplementary Figure 2 – BFC Clusters
Expression versus time for genes in the 27 circadian BFC clusters. Expression of individual genes (dashed black lines) and cluster average (solid blue line) shown for each cluster. Clock related genes (solid coloured lines; see legends for gene identity) indicated where appropriate. Gene number, Circadian Score (Second Harmonic Ratio, SHR), Amplitude (Second Harmonic Amplitude, SHA) and Phase (Phase by Maximum, PBM) values indicated for each cluster.

Supplementary Figure 3 – COSOPT and BFC peak time comparisons
Scatter plot of cluster peak phase time for genes in BFC clusters versus COSOPT peak phase time estimates of the individual genes.

Supplementary Figure 4 - *EPR1* leaf movement
Leaf movement period estimates for Col-0 (back bars) and the *epr1* T-DNA insertion line SALK_047716 (white bars). Three independent experiments shown at 22°C and two at 27°C. Error bars show variance weighted SEM of period estimates.
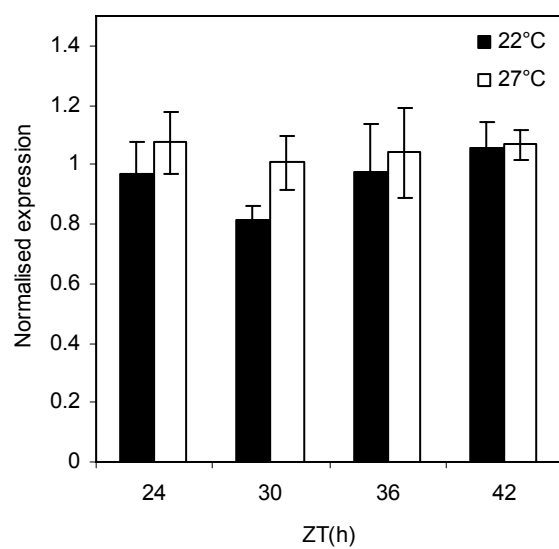
Cluster 1 (181 genes). SHR=0.538.

Time
SHA=0.105. PBM=35.312 hours.
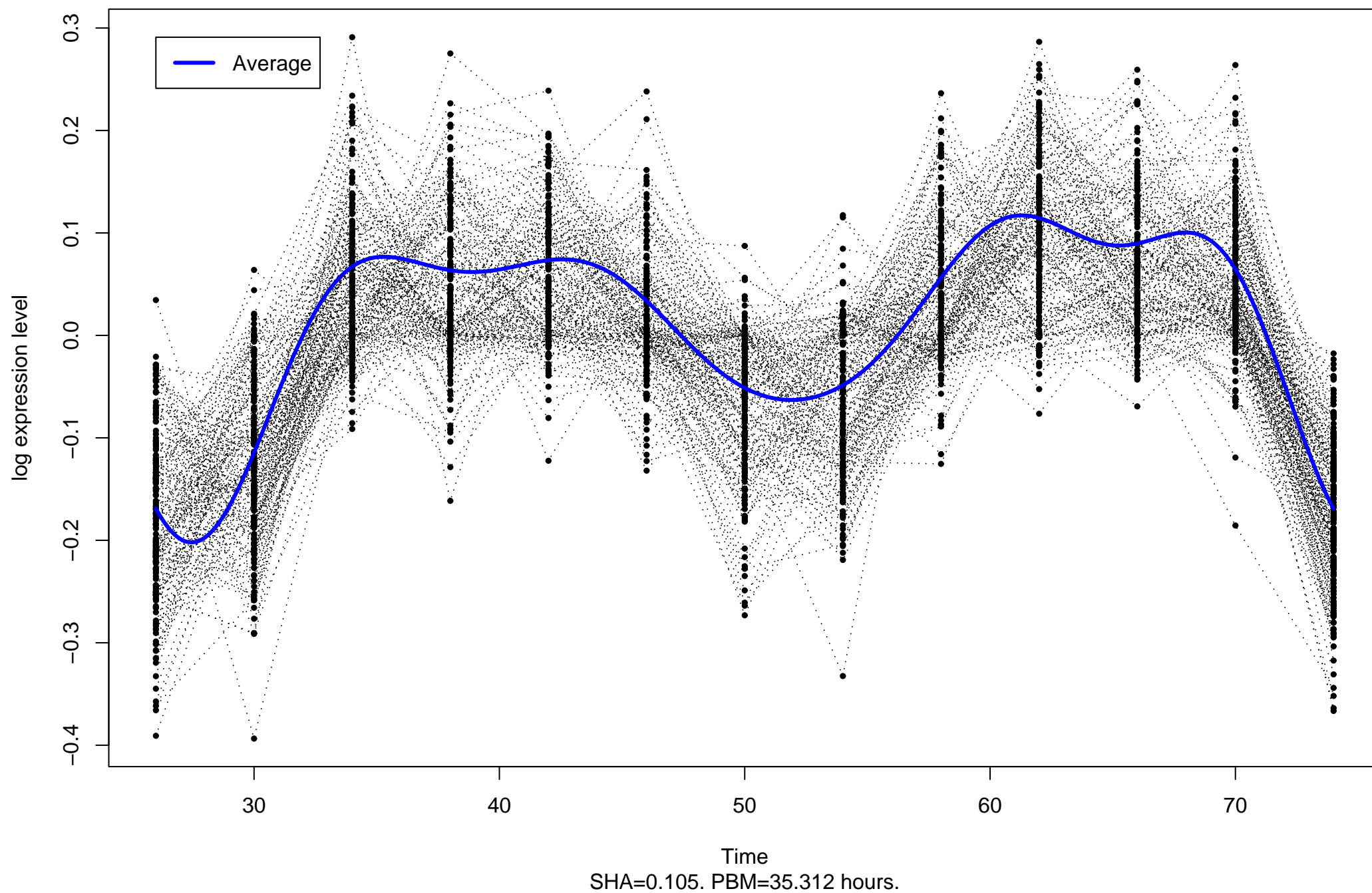
Cluster 2 (311 genes). SHR=0.452.

Time
SHA=0.107. PBM=42.848 hours.
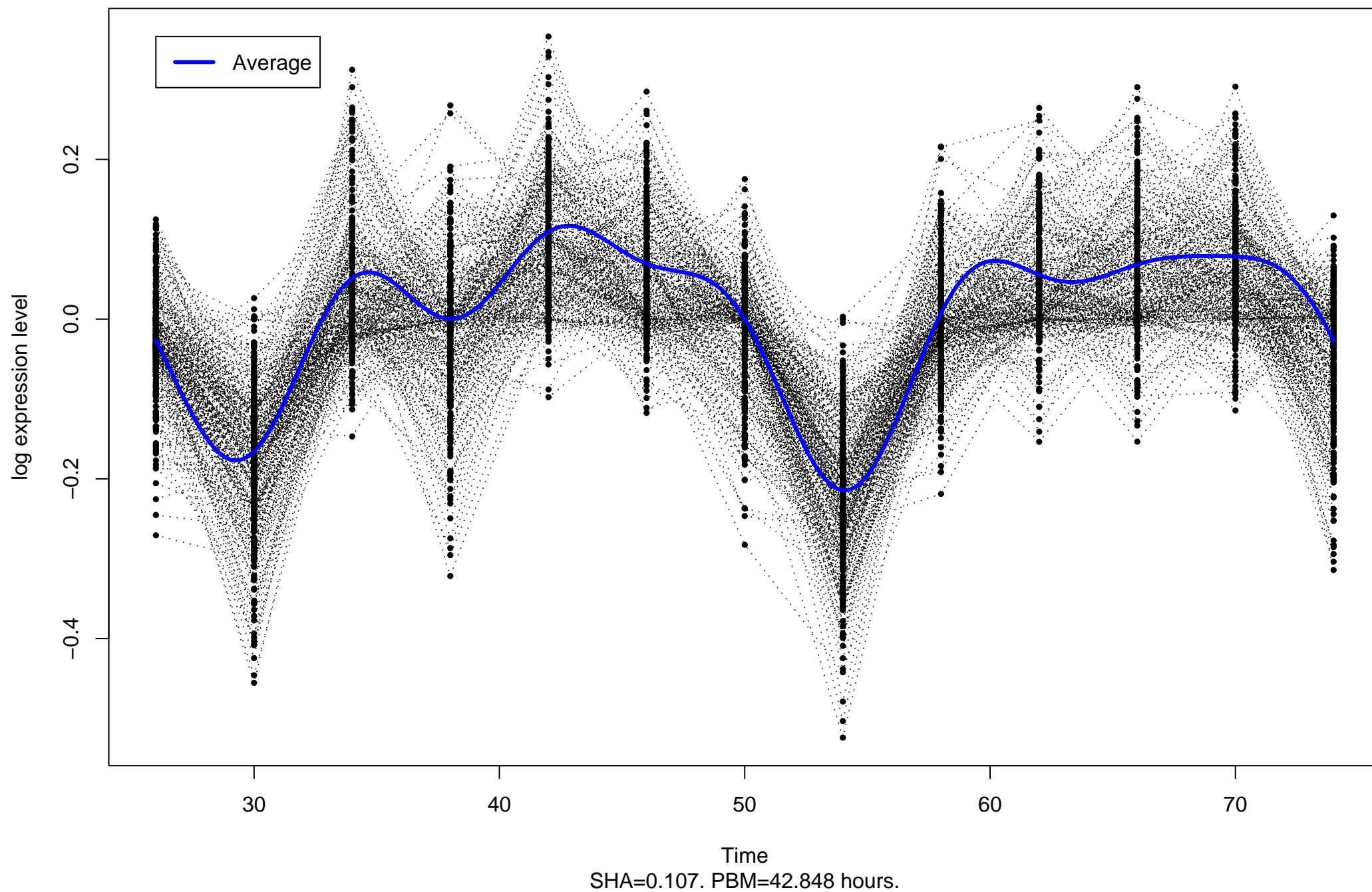
Cluster 3 (208 genes). SHR=0.711.

Time

SHA=0.24. PBM=43.328 hours.
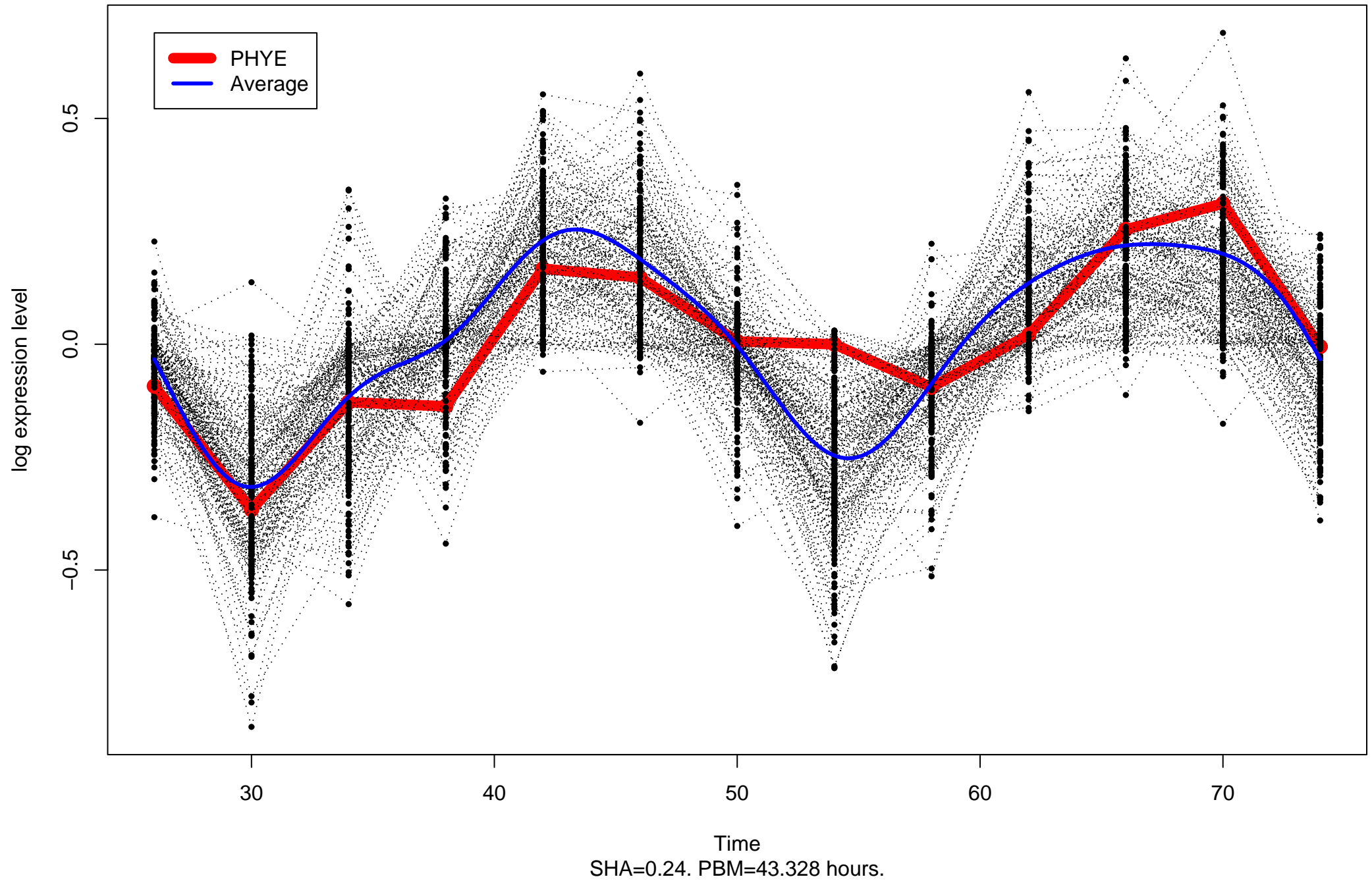
Cluster 4 (72 genes). SHR=0.763.

Time
SHA=0.182. PBM=43.664 hours.
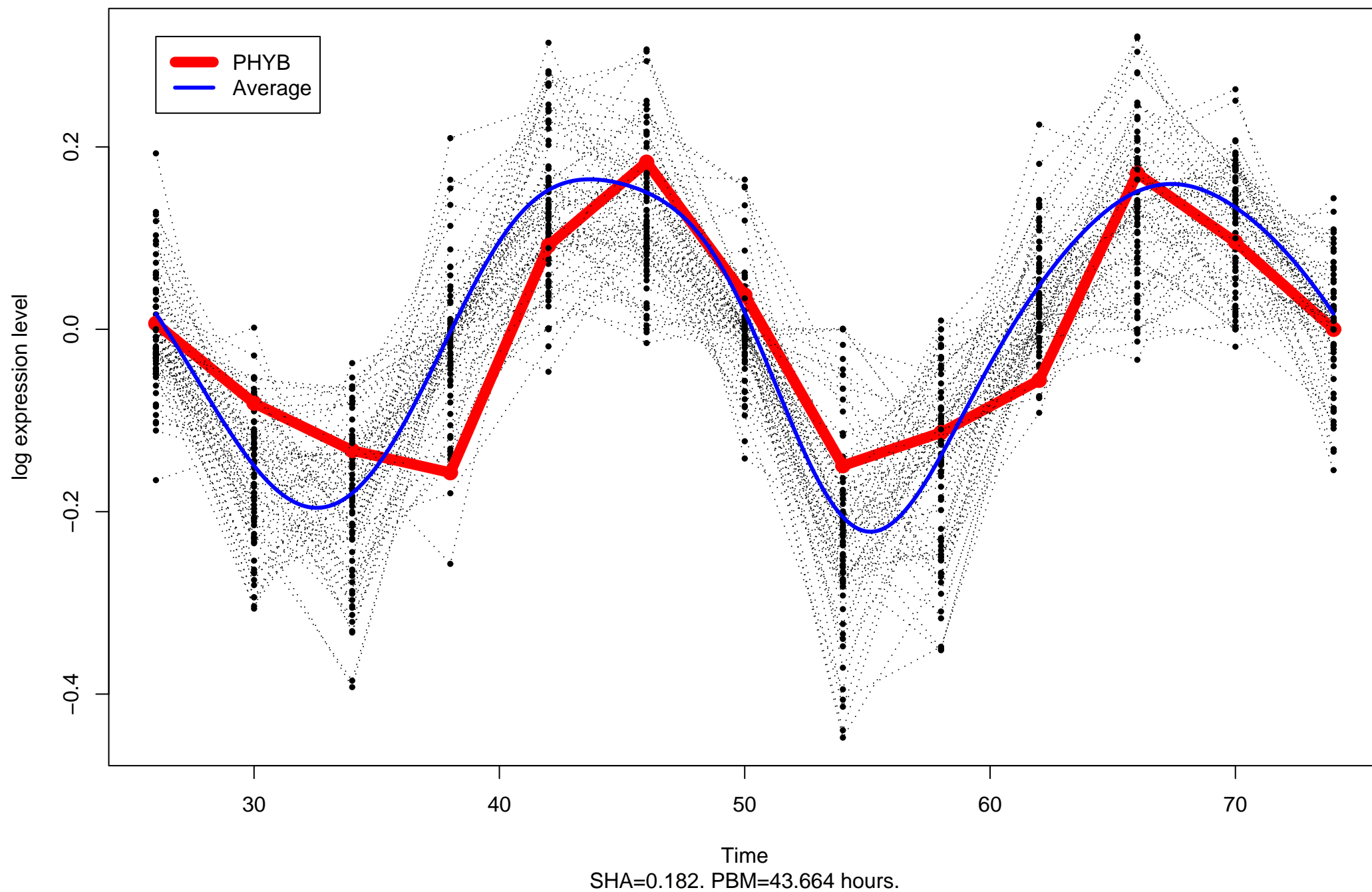
Cluster 5 (280 genes). SHR=0.608.

Time
SHA=0.203. PBM=47.696 hours.
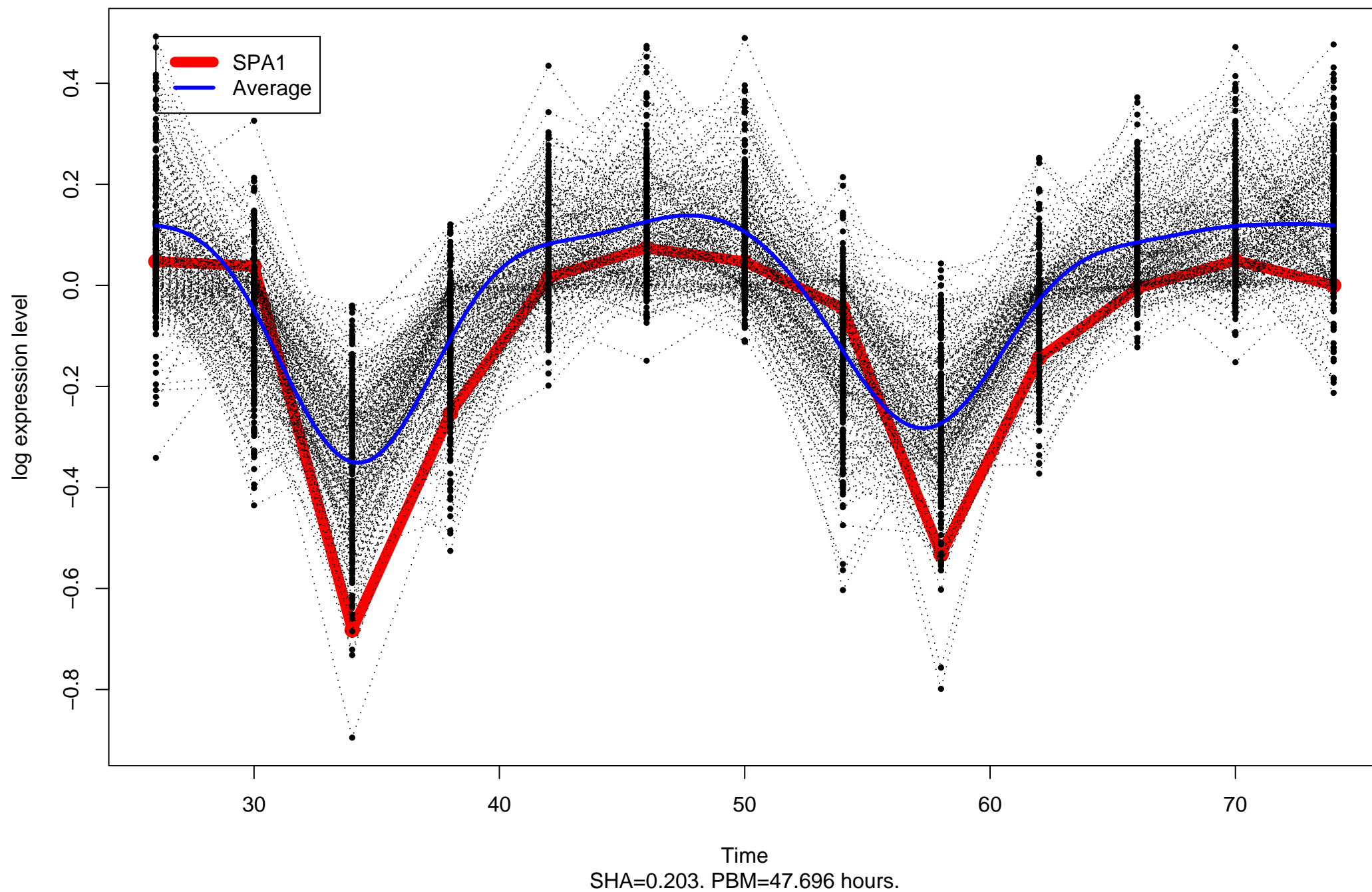
Cluster 6 (54 genes). SHR=0.603.

log expression level

Time
SHA=0.247. PBM=50 hours.
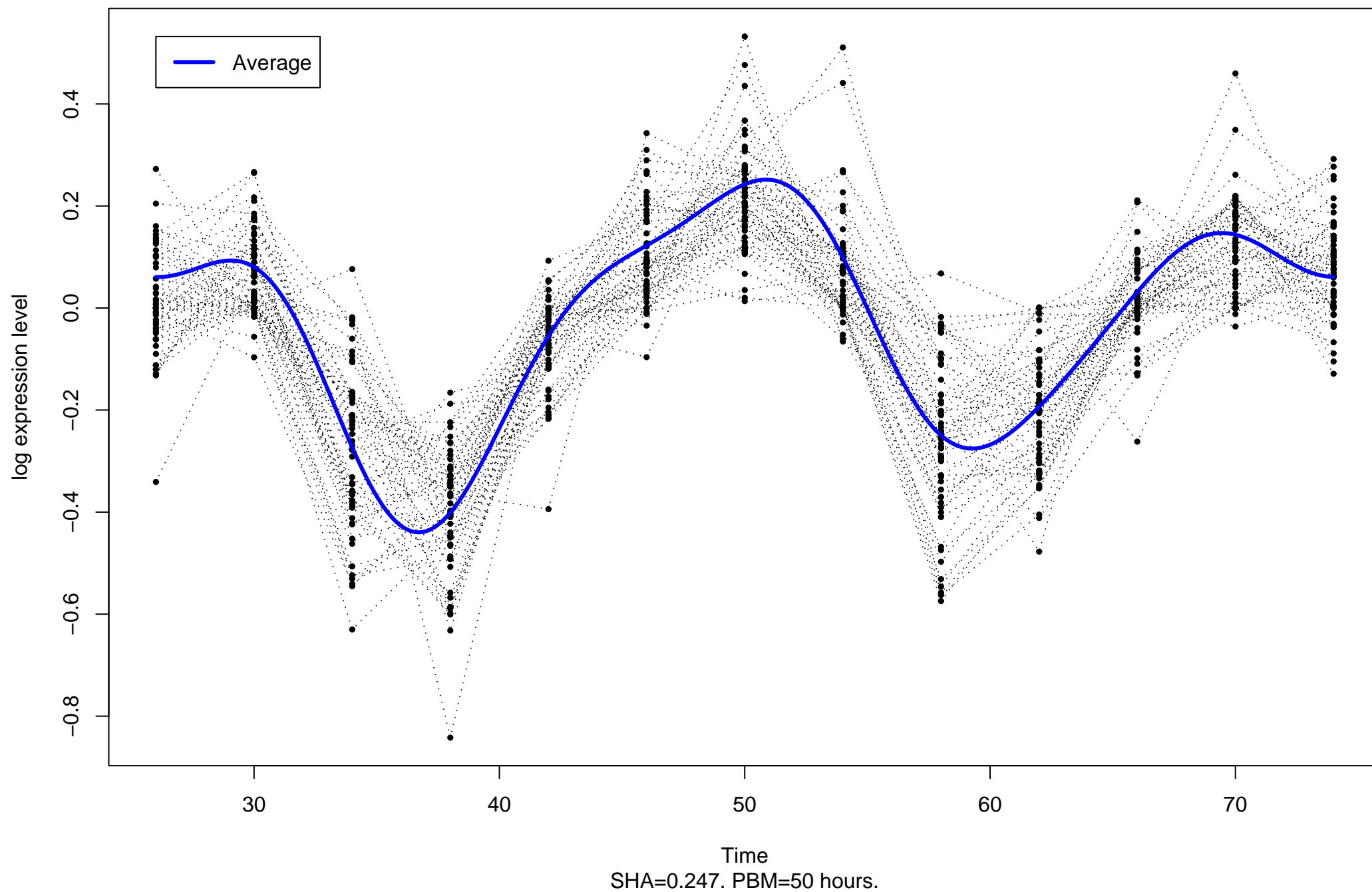
Cluster 7 (306 genes). SHR=0.639.

Time
SHA=0.189. PBM=29.504 hours.
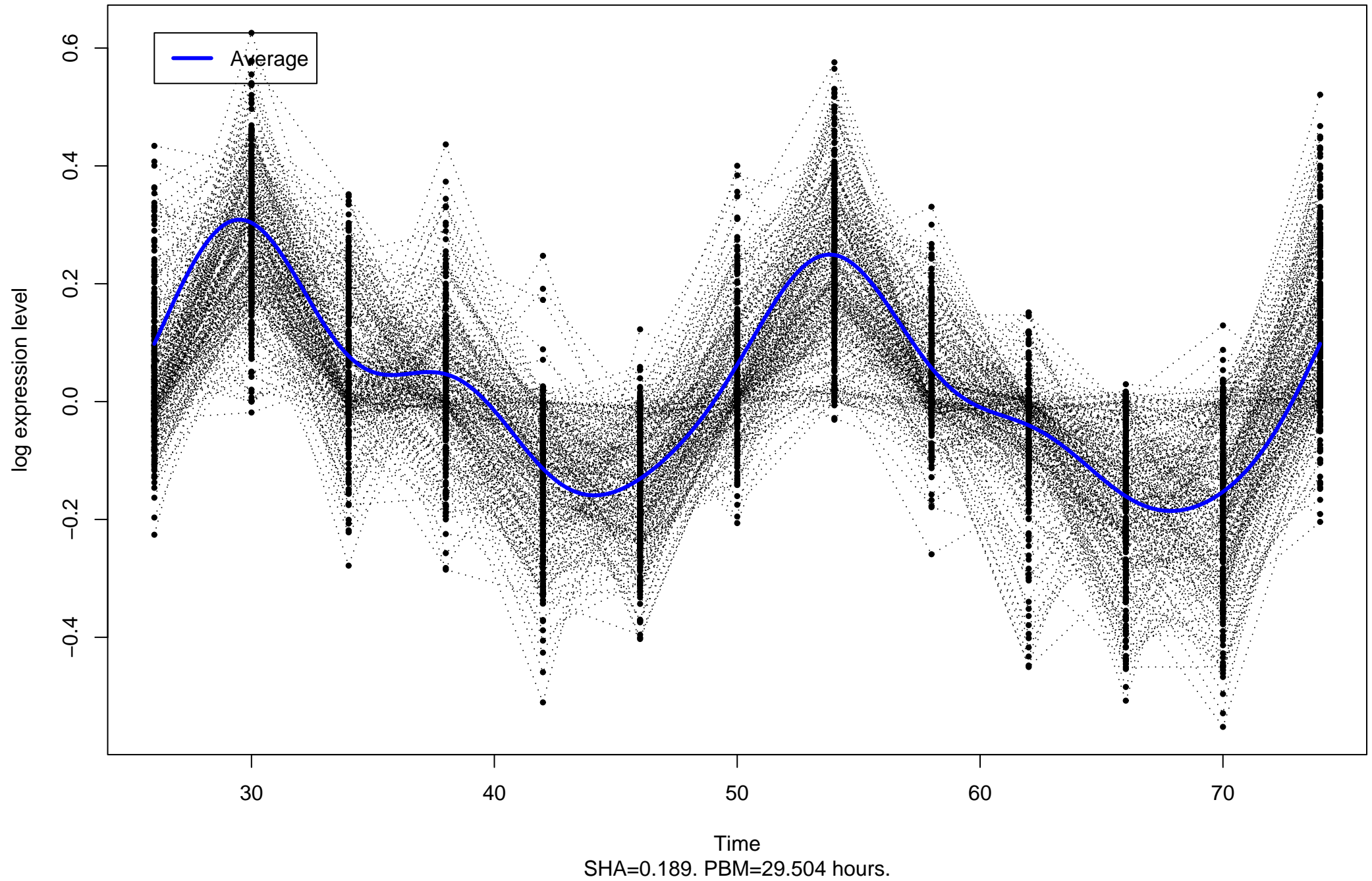
Cluster 8 (53 genes). SHR=0.619.

Time
SHA=0.241. PBM=30.272 hours.
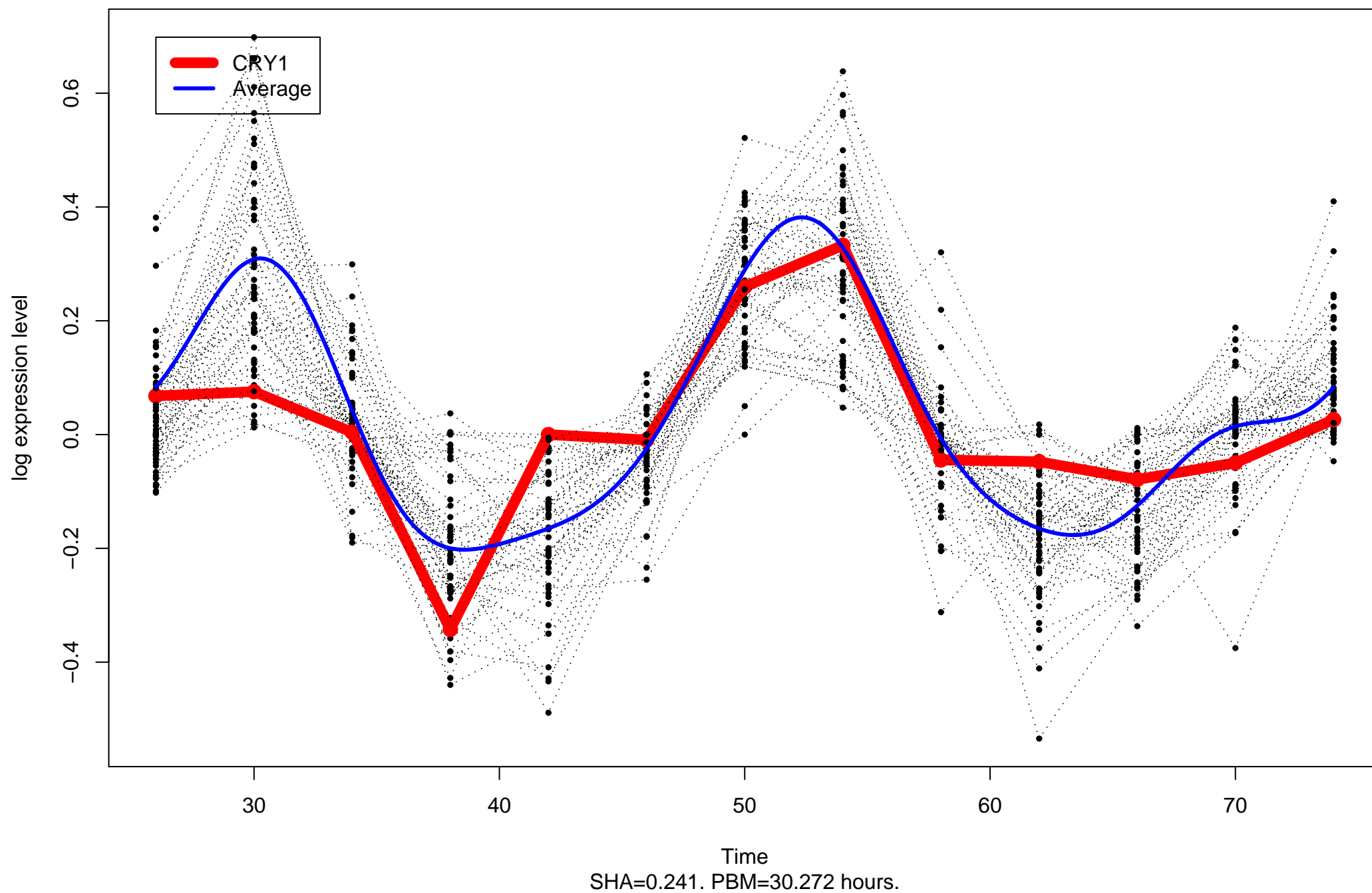
Cluster 9 (292 genes). SHR=0.779.

Time
SHA=0.291. PBM=32 hours.
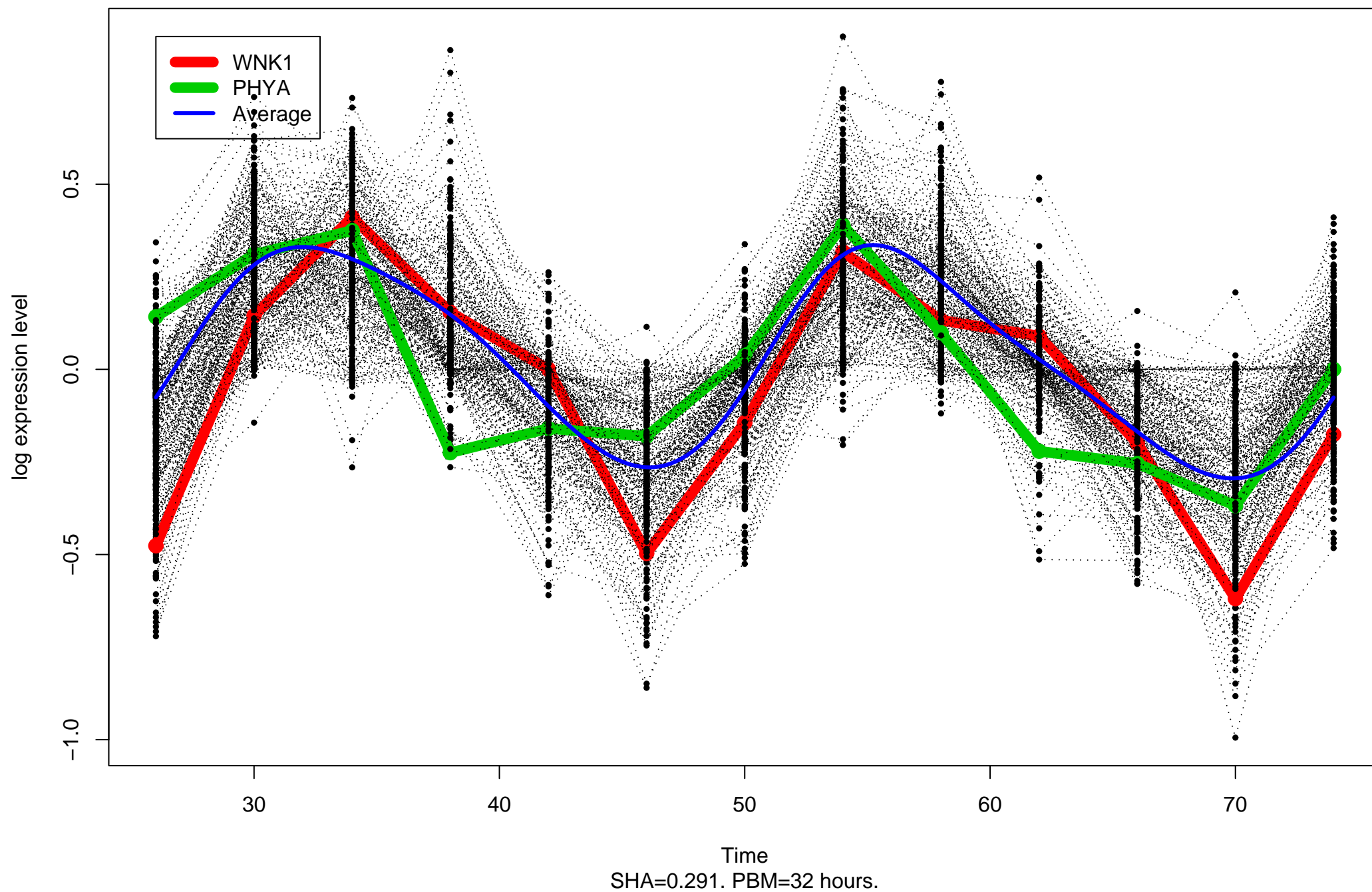
Cluster 10 (98 genes). SHR=0.555.

Time
SHA=0.235. PBM=42.704 hours.
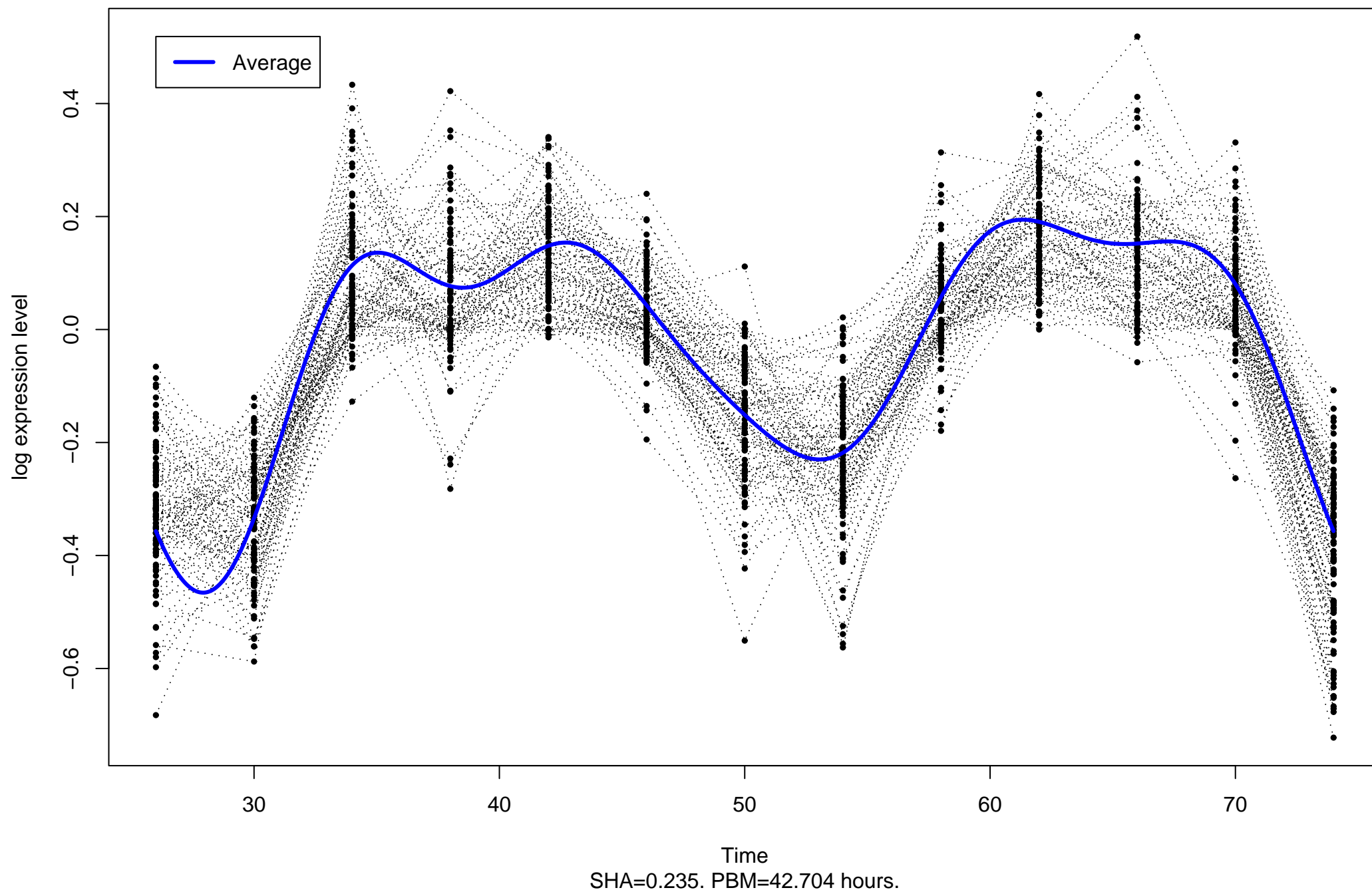
Cluster 11 (46 genes). SHR=0.665.

SHA=0.339. PBM=41.312 hours.
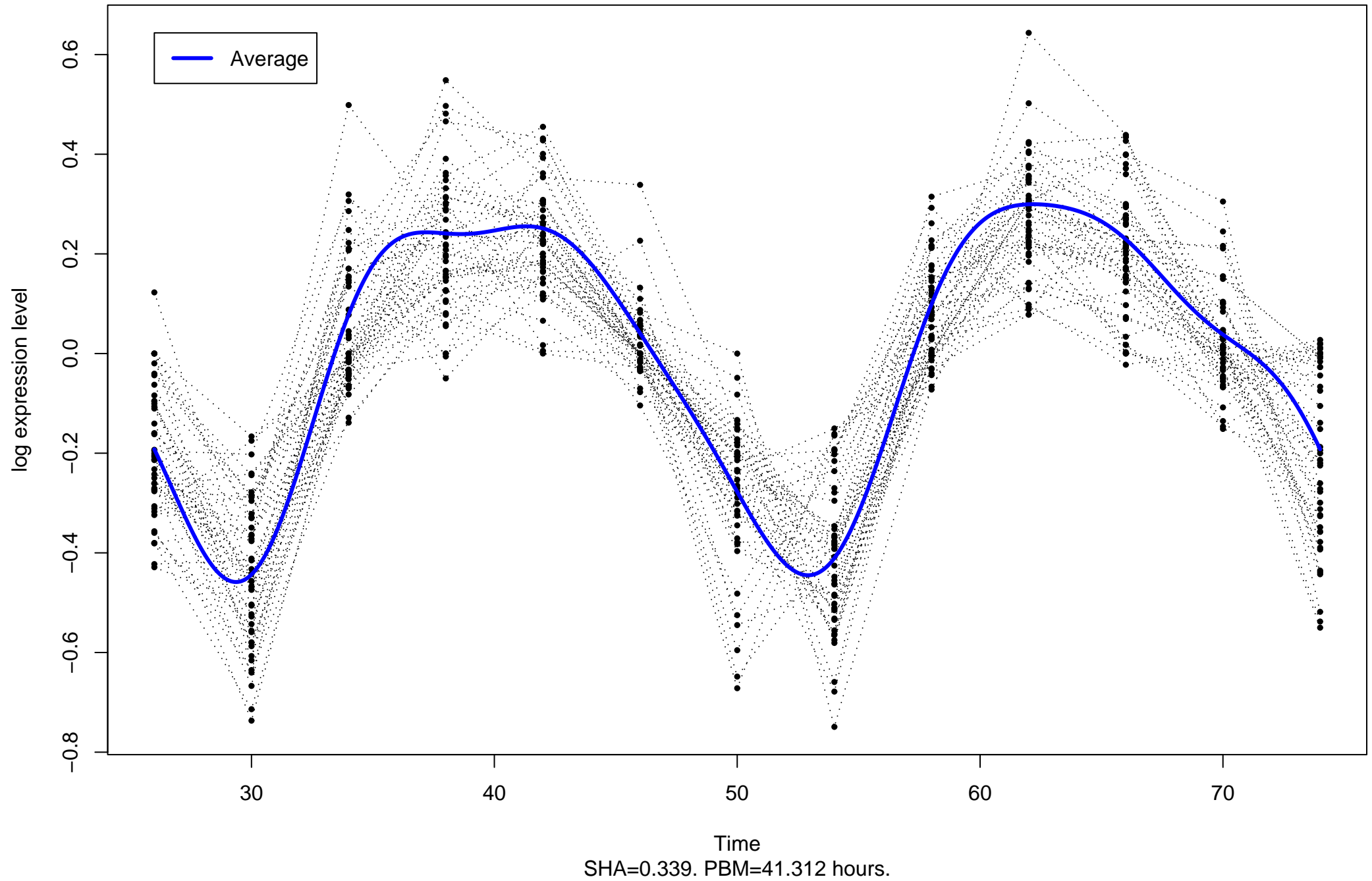
Cluster 12 (47 genes). SHR=0.46.

Time
SHA=0.236. PBM=34.16 hours.
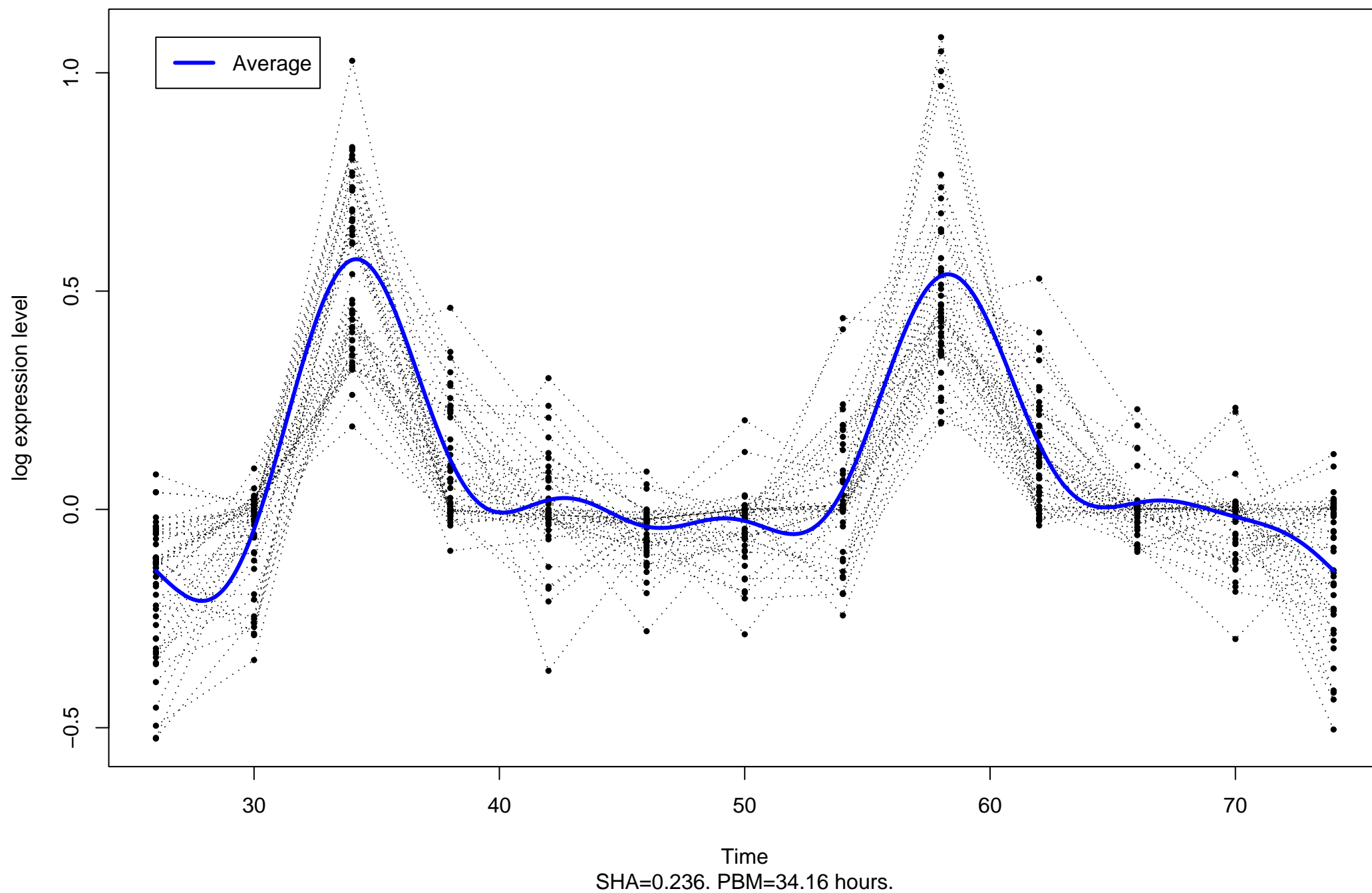
Cluster 13 (60 genes). SHR=0.713.

Time
SHA=0.346. PBM=35.408 hours.
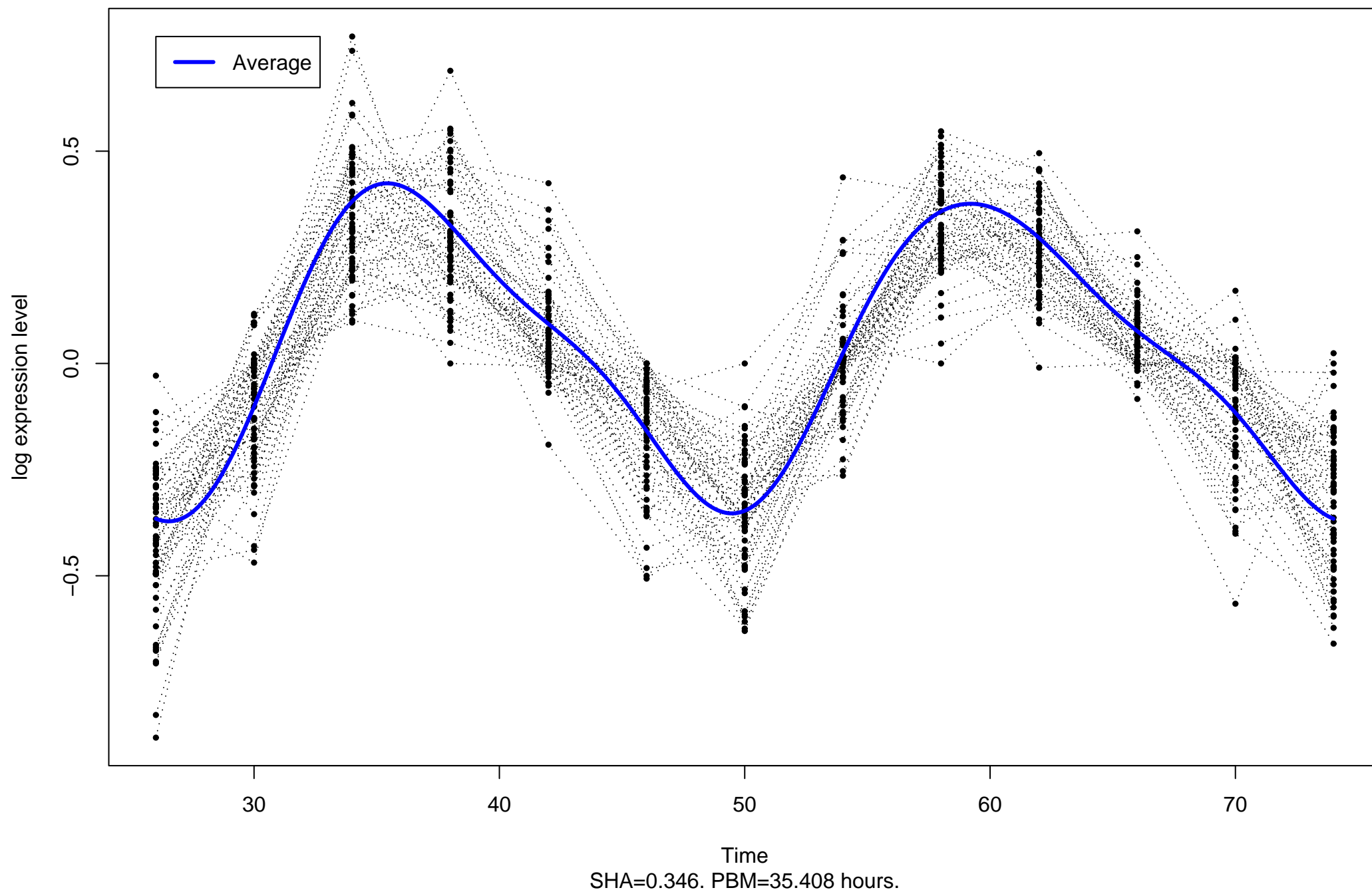
Cluster 14 (325 genes). SHR=0.502.

Time
SHA=0.233. PBM=34.544 hours.
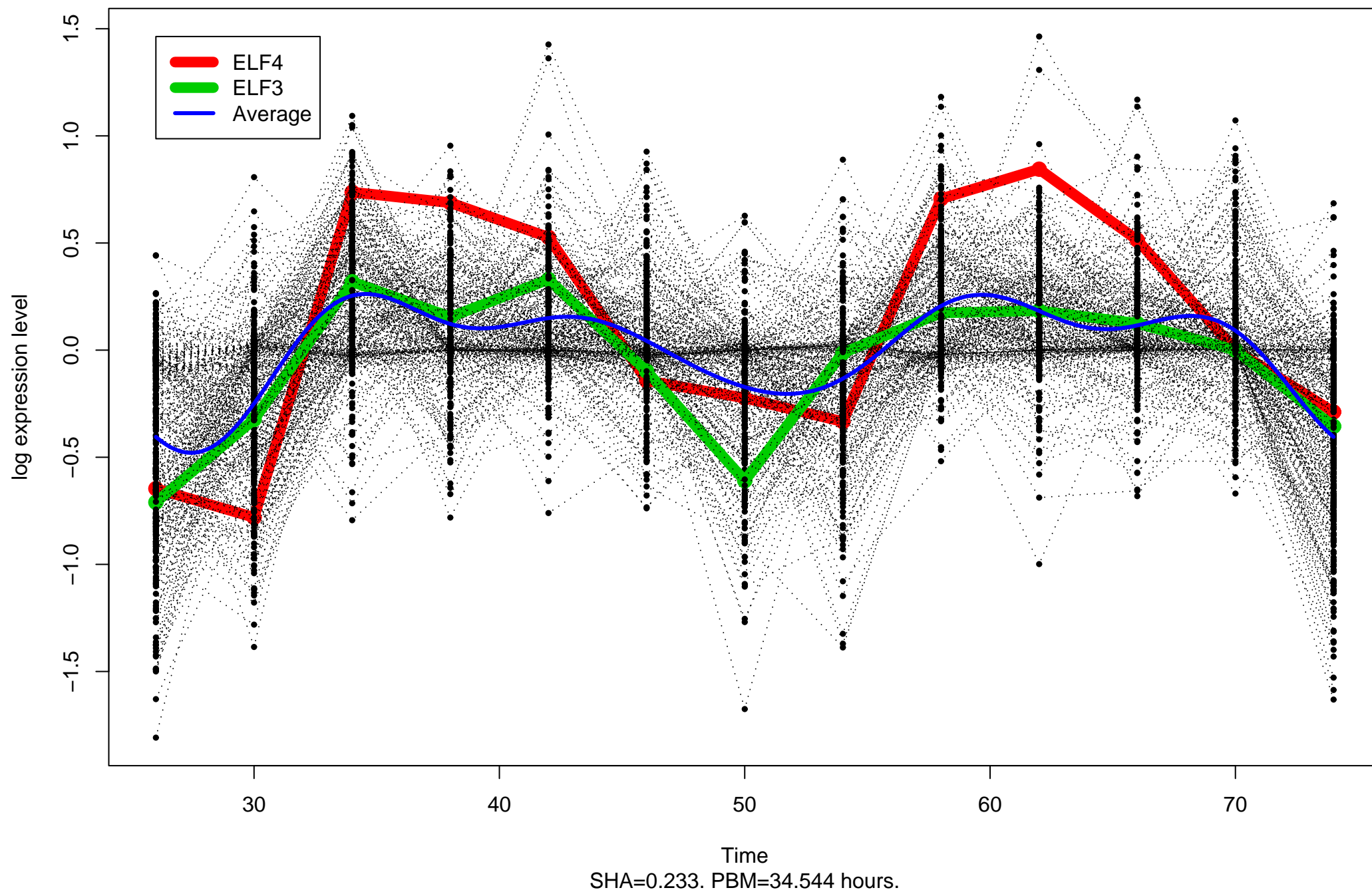
Cluster 15 (26 genes). SHR=0.686.

Time
SHA=0.441. PBM=48.944 hours.
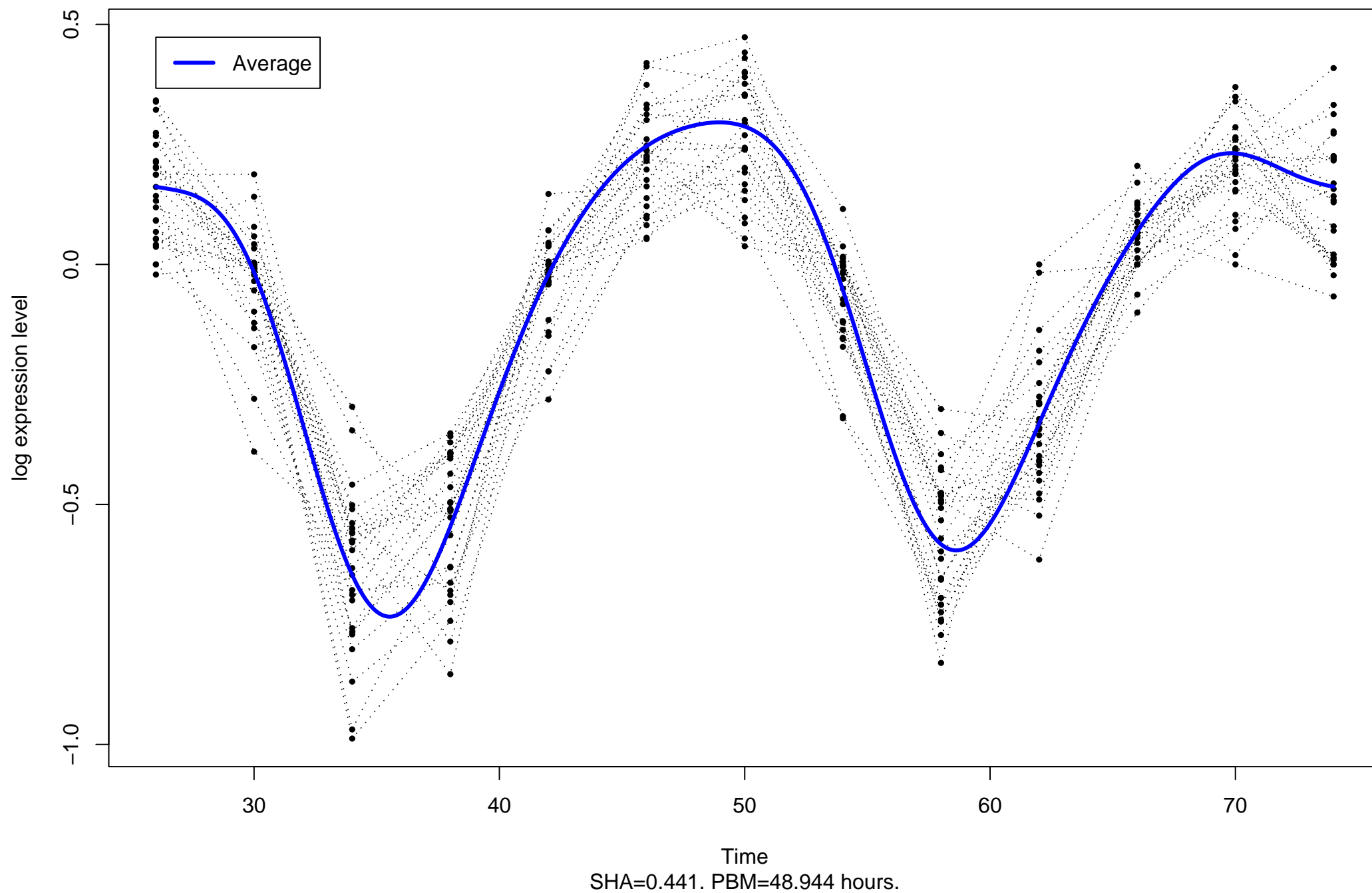
Cluster 16 (63 genes). SHR=0.7.

log expression level

Time
SHA=0.383. PBM=45.728 hours.
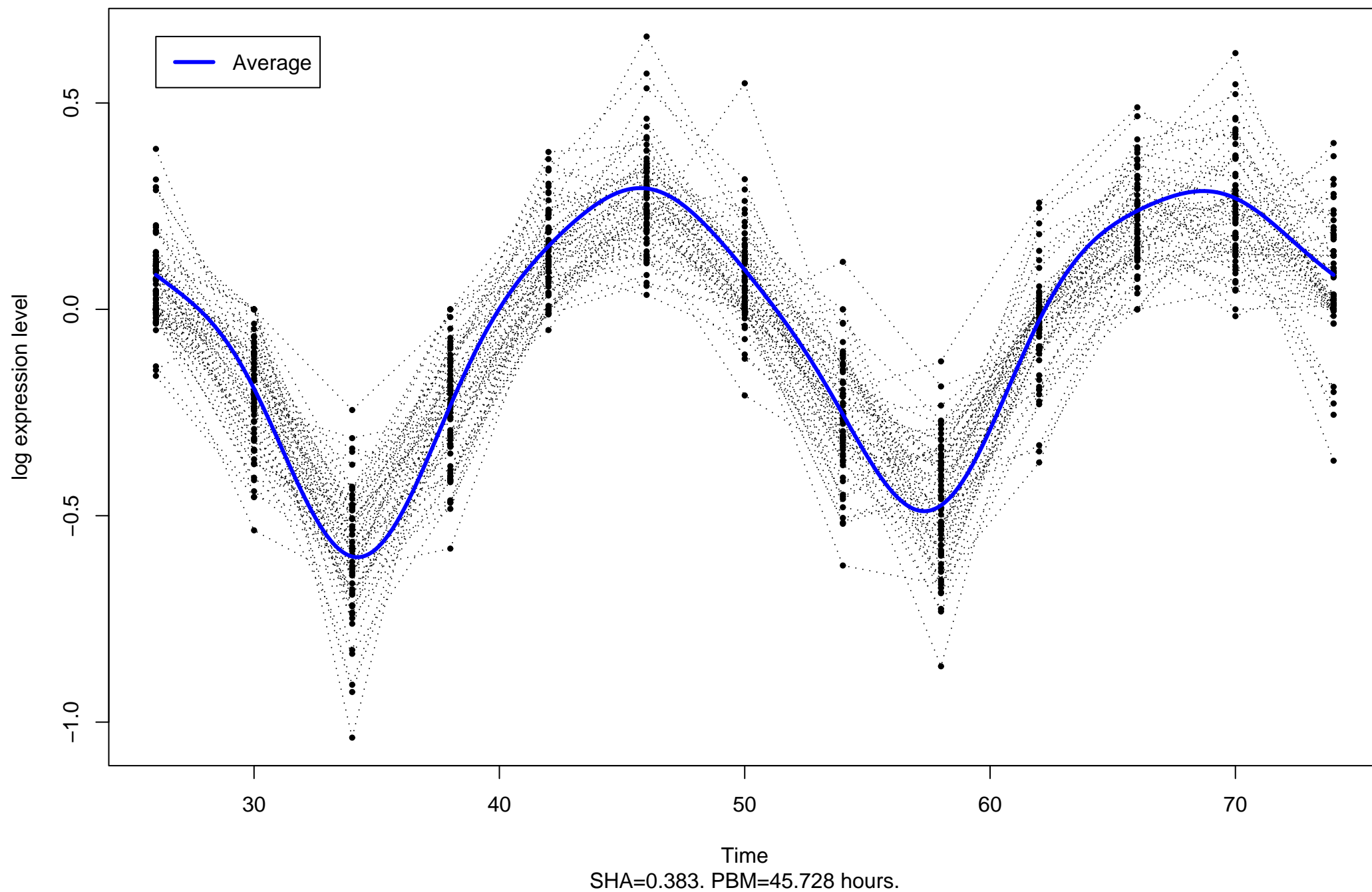
Cluster 17 (126 genes). SHR=0.73.

Time
SHA=0.534. PBM=44.96 hours.
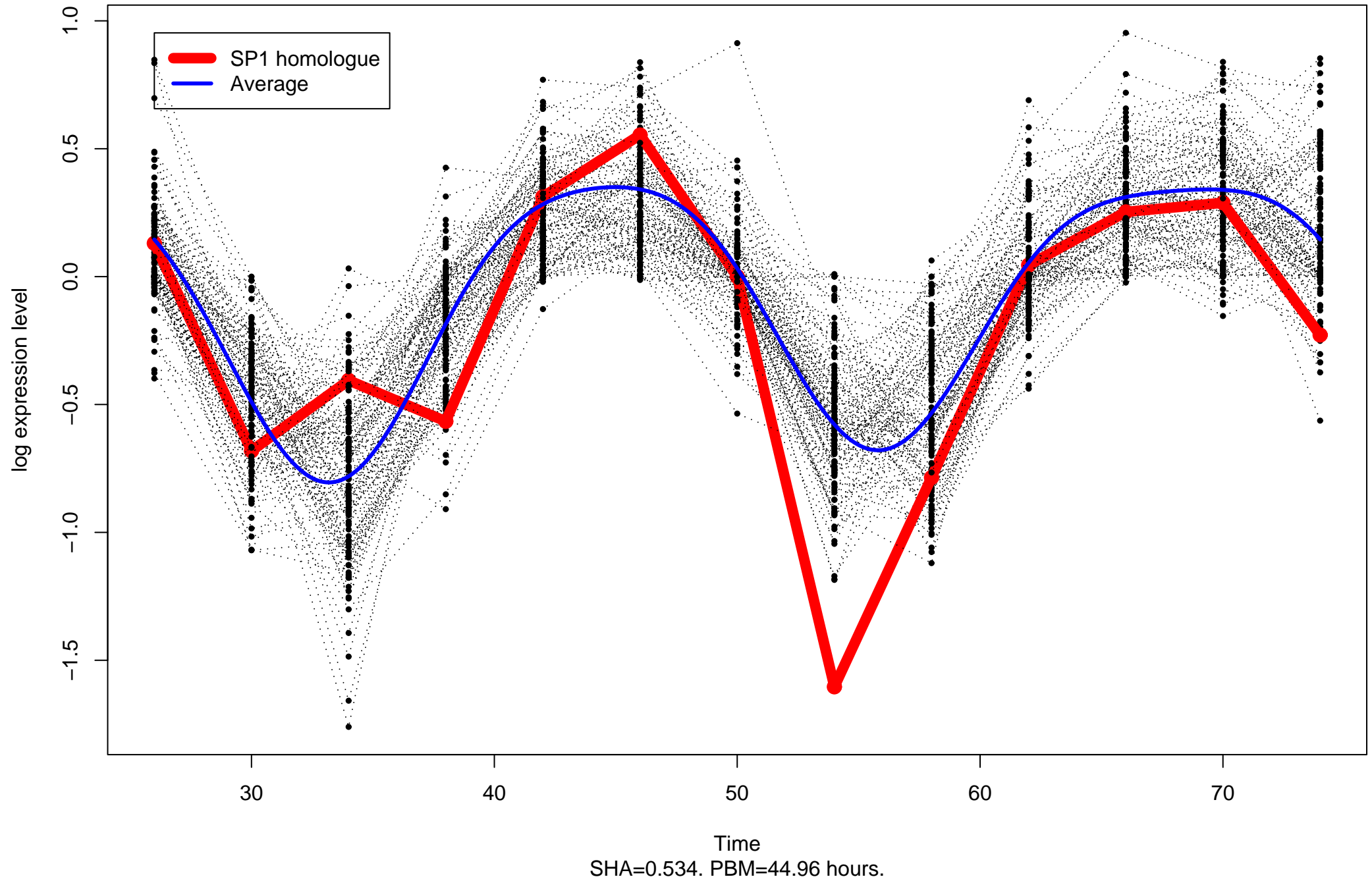
Cluster 18 (59 genes). SHR=0.76.

Time
SHA=0.731. PBM=46.832 hours.
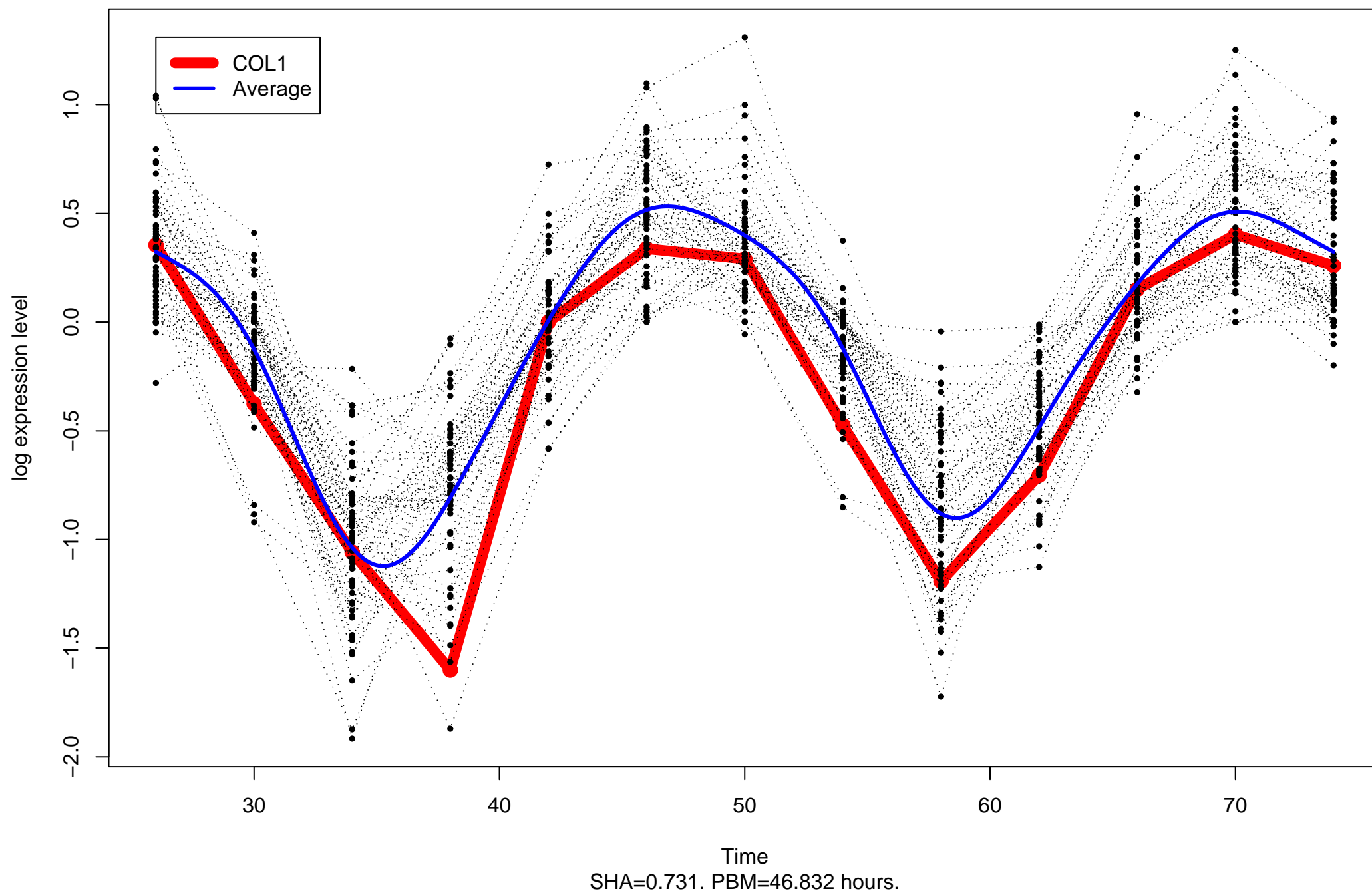
Cluster 19 (20 genes). SHR=0.668.

Time
SHA=0.537. PBM=50 hours.
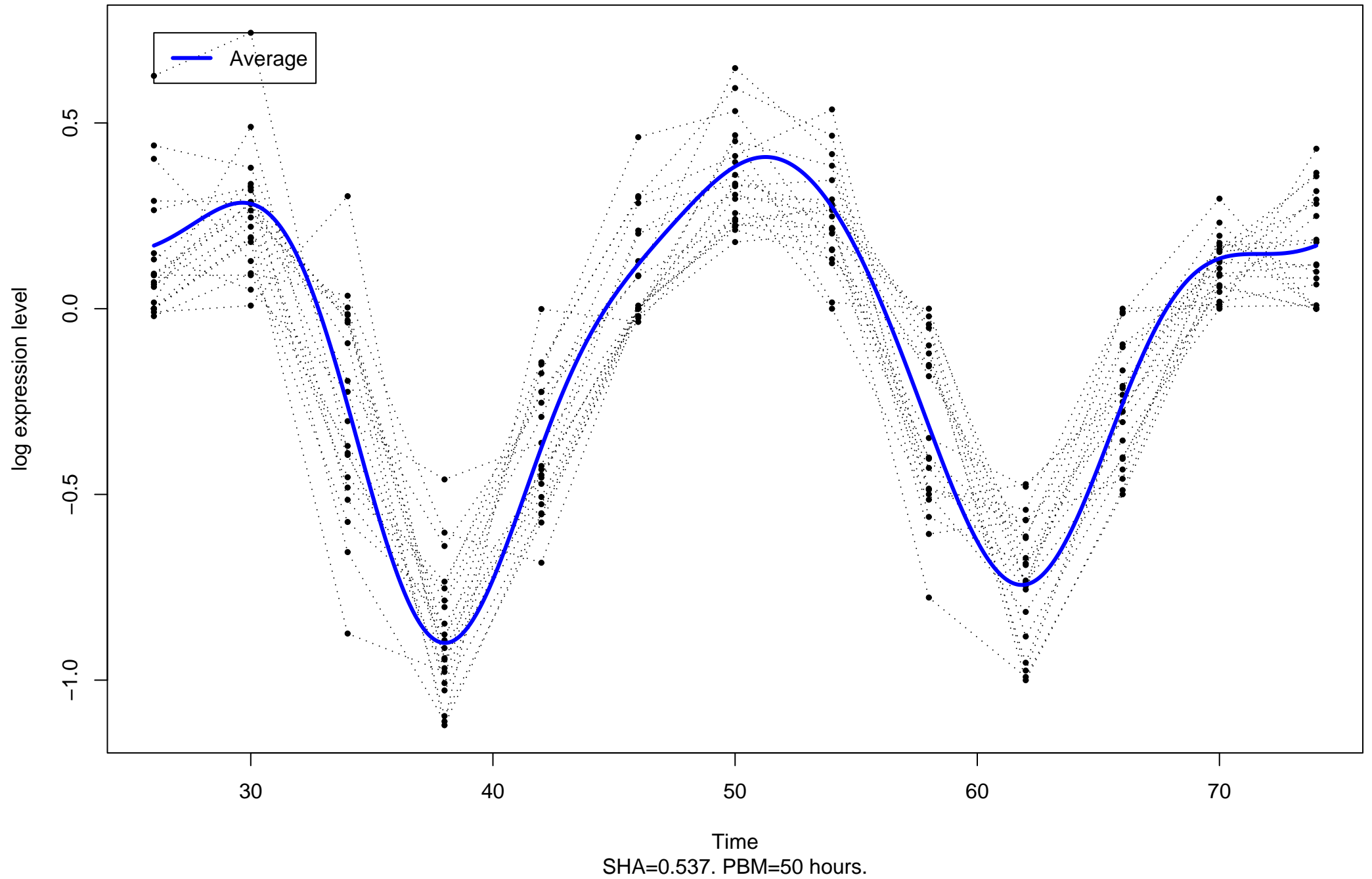
Cluster 20 (24 genes). SHR=0.802.

Time
SHA=1.595. PBM=46.928 hours.
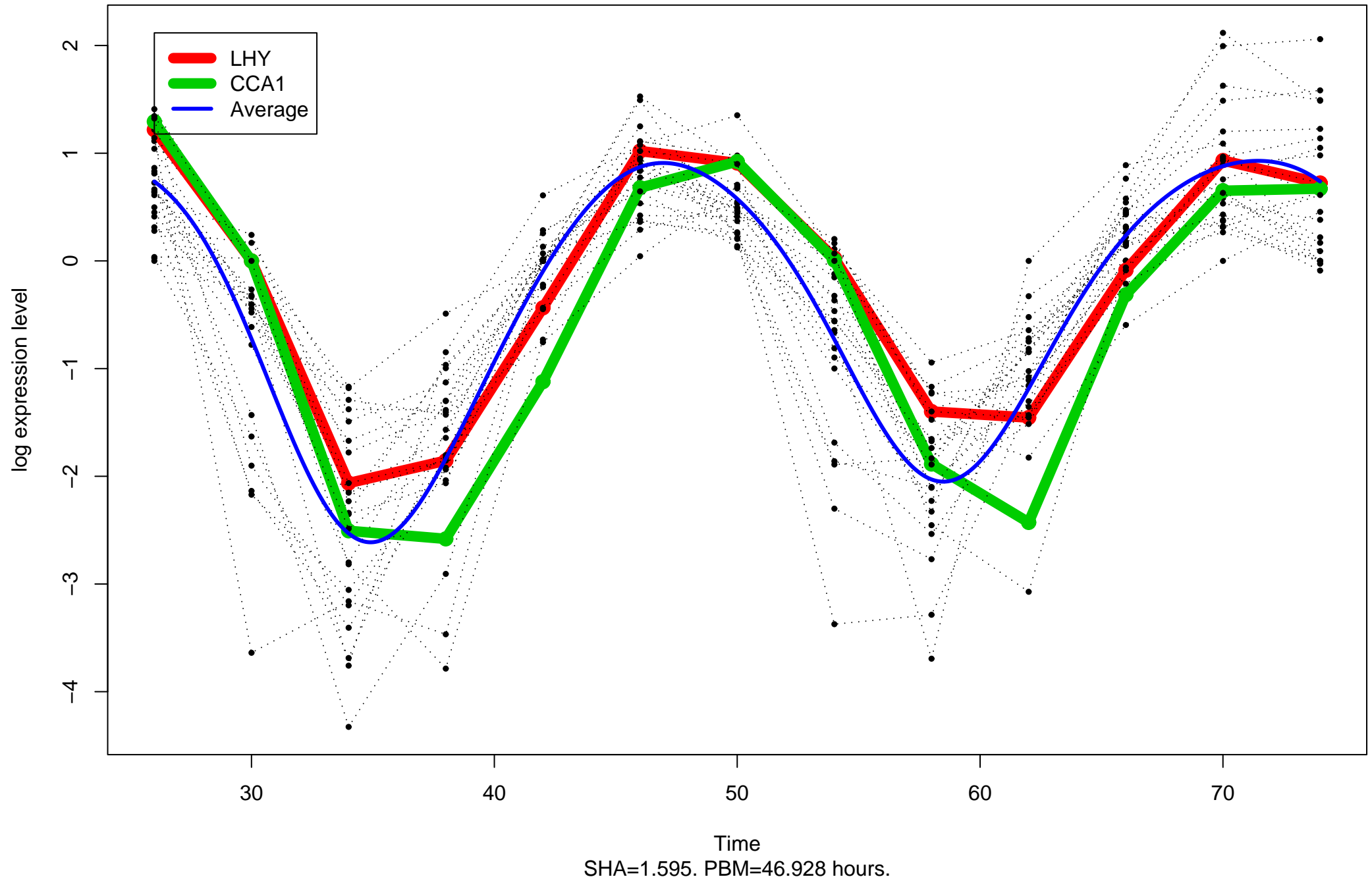
Cluster 21 (34 genes). SHR=0.702.

Time
SHA=0.84. PBM=42.416 hours.
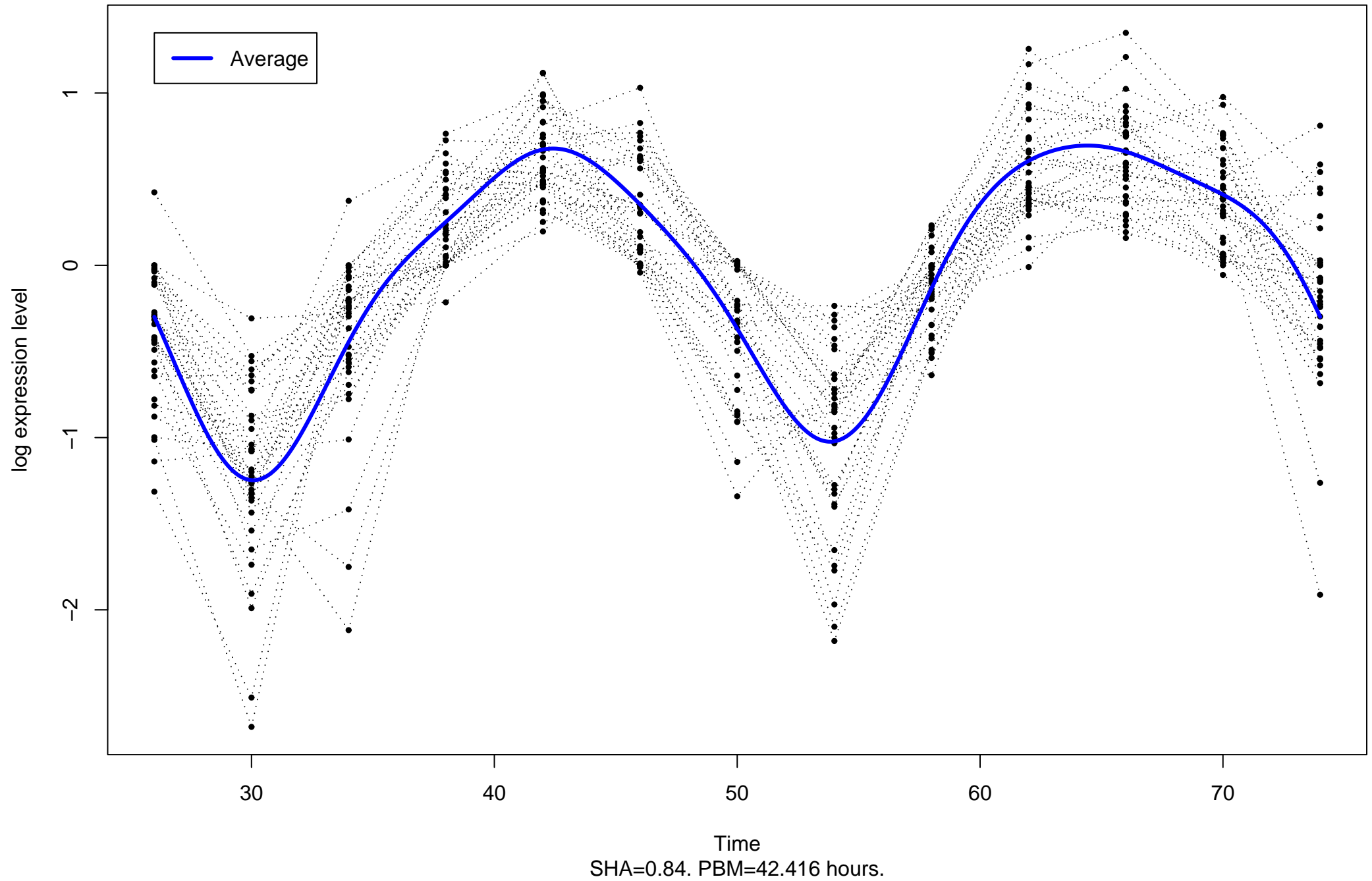
Cluster 22 (58 genes). SHR=0.762.

Time
SHA=0.955. PBM=34.112 hours.
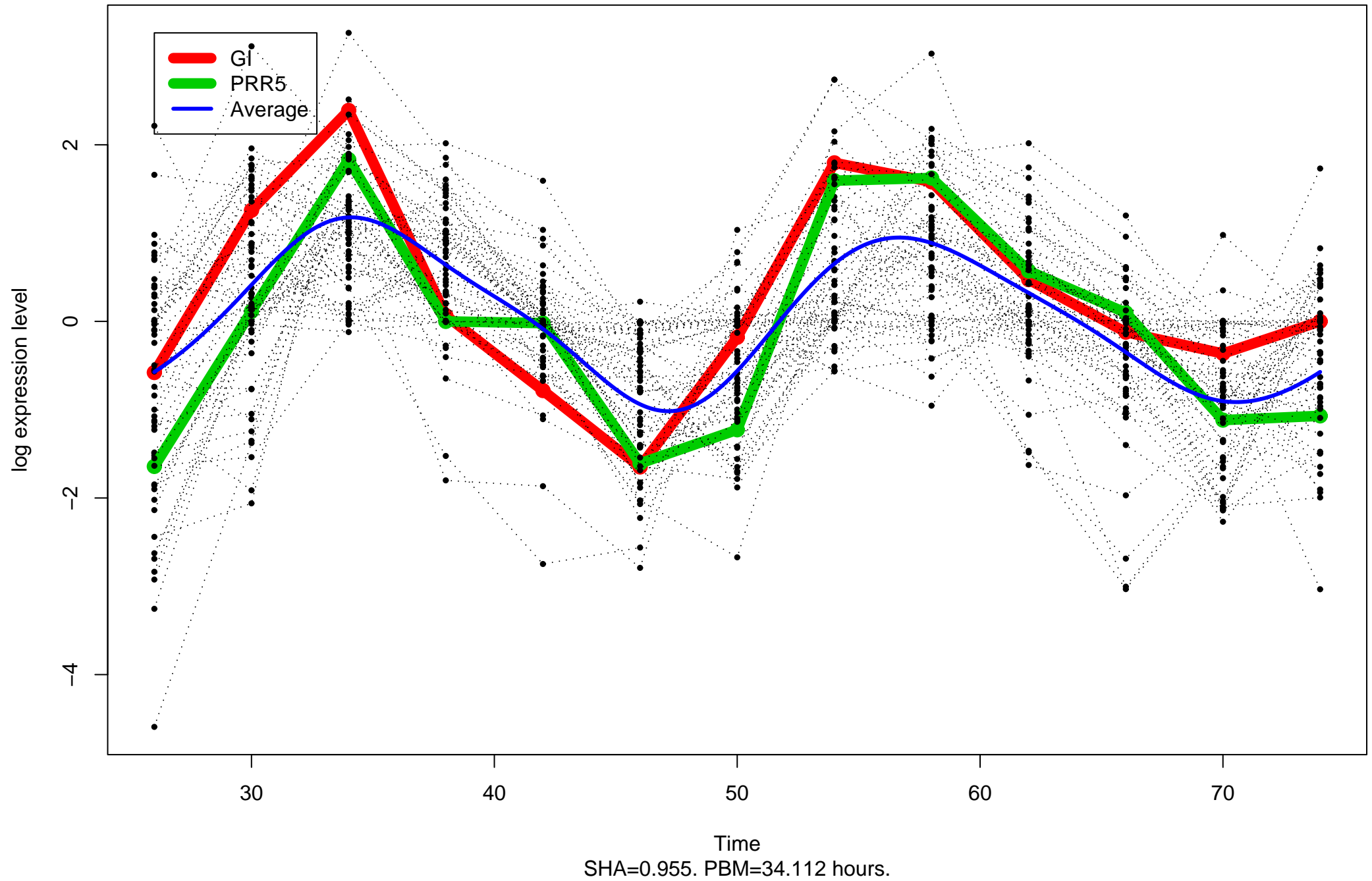
Cluster 23 (30 genes). SHR=0.783.

log expression level

Time
SHA=1.056. PBM=30.176 hours.
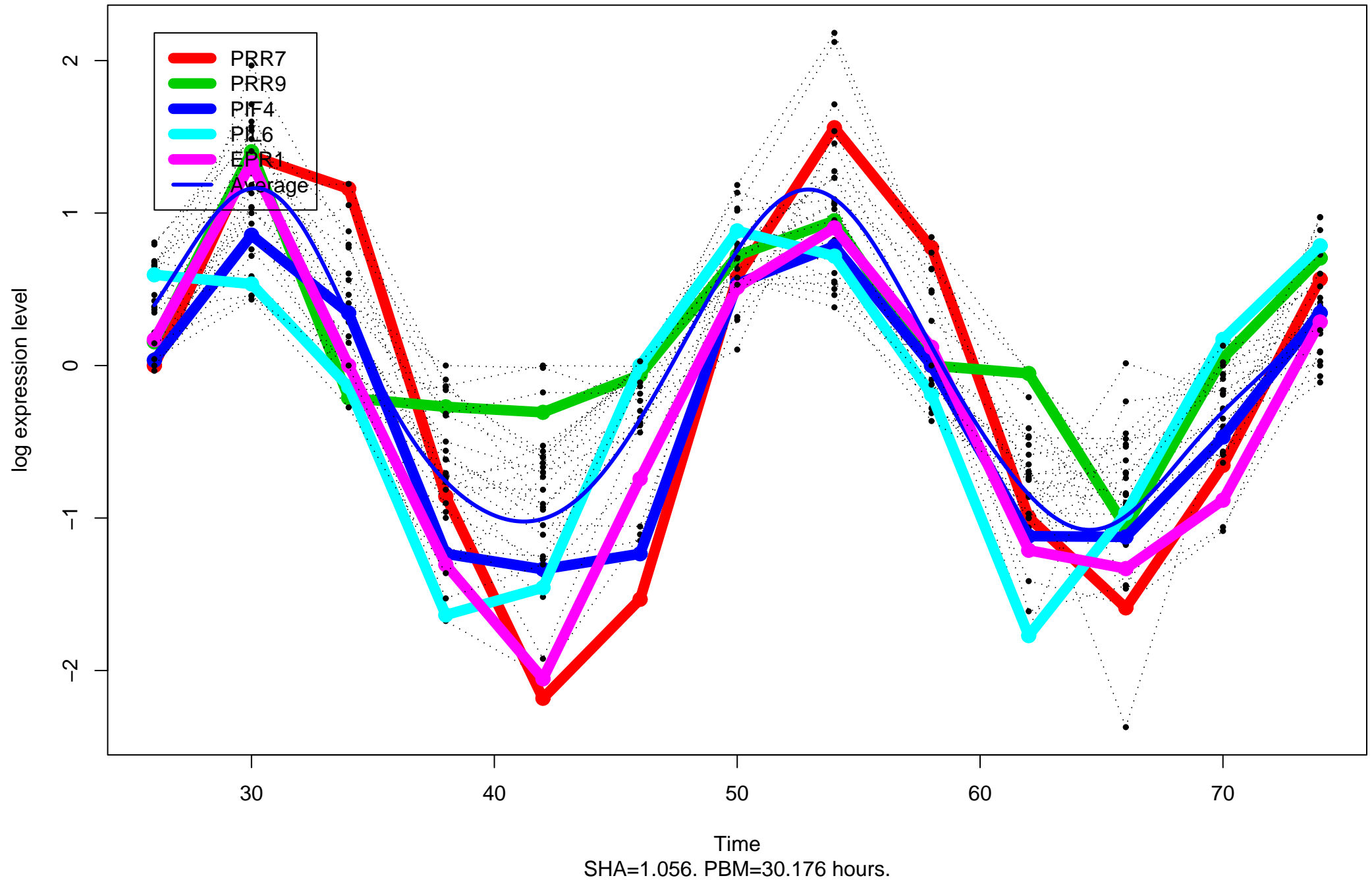
Cluster 24 (21 genes). SHR=0.387.

Time
SHA=0.37. PBM=26 hours.
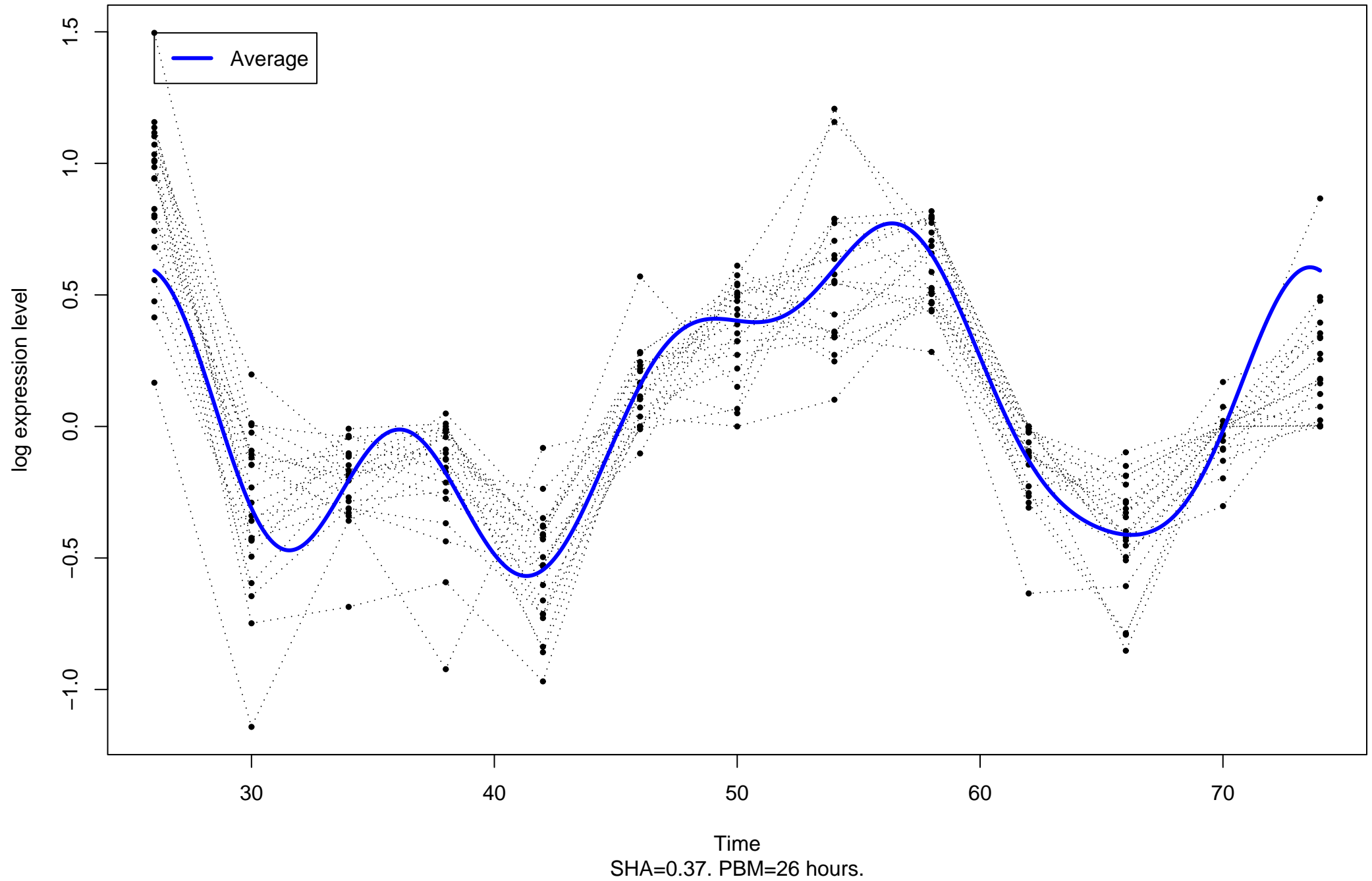
Cluster 25 (38 genes). SHR=0.645.

Time
SHA=0.697. PBM=35.12 hours.
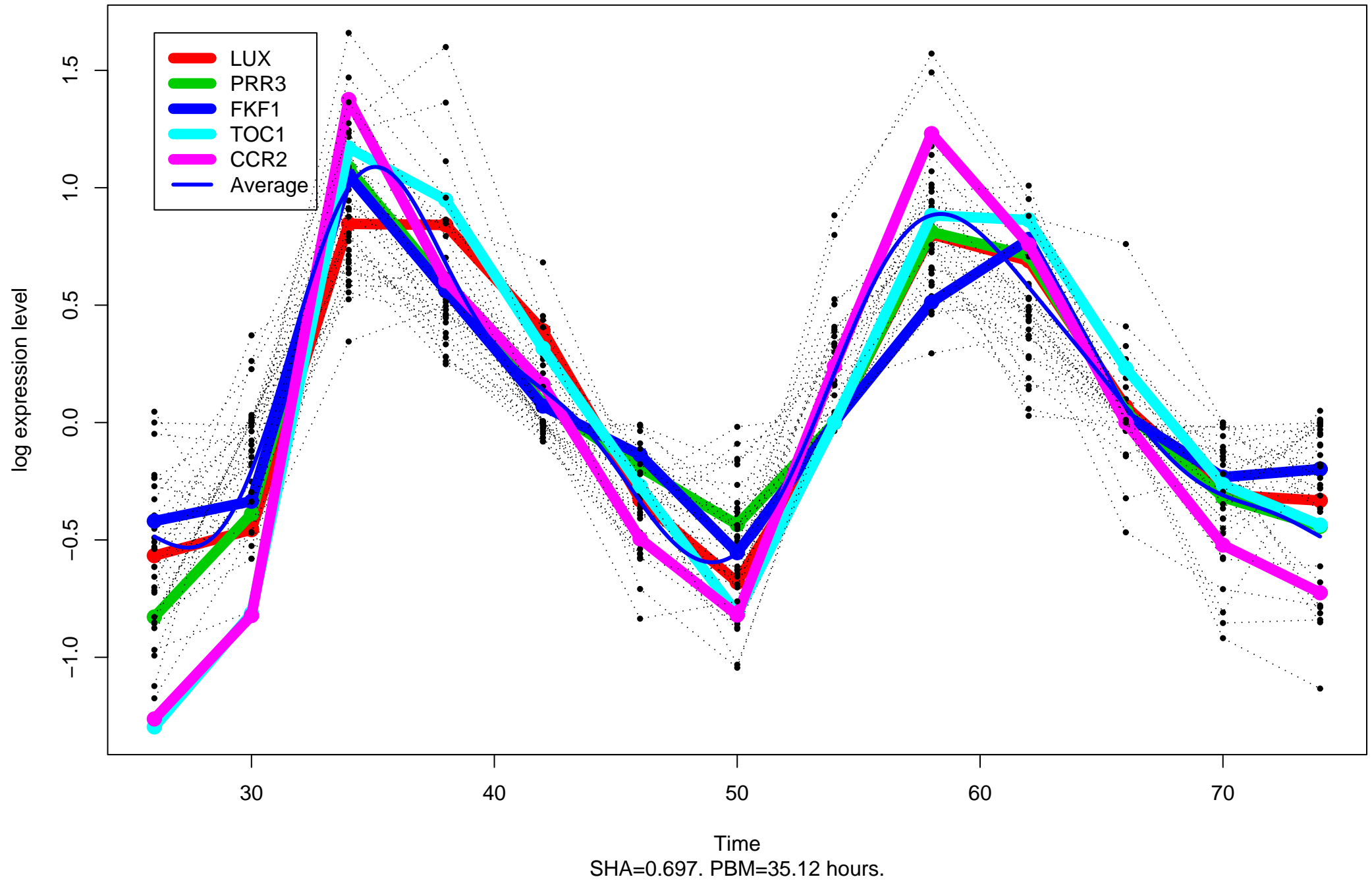
Cluster 26 (131 genes). SHR=0.716.

Time
SHA=0.619. PBM=33.152 hours.
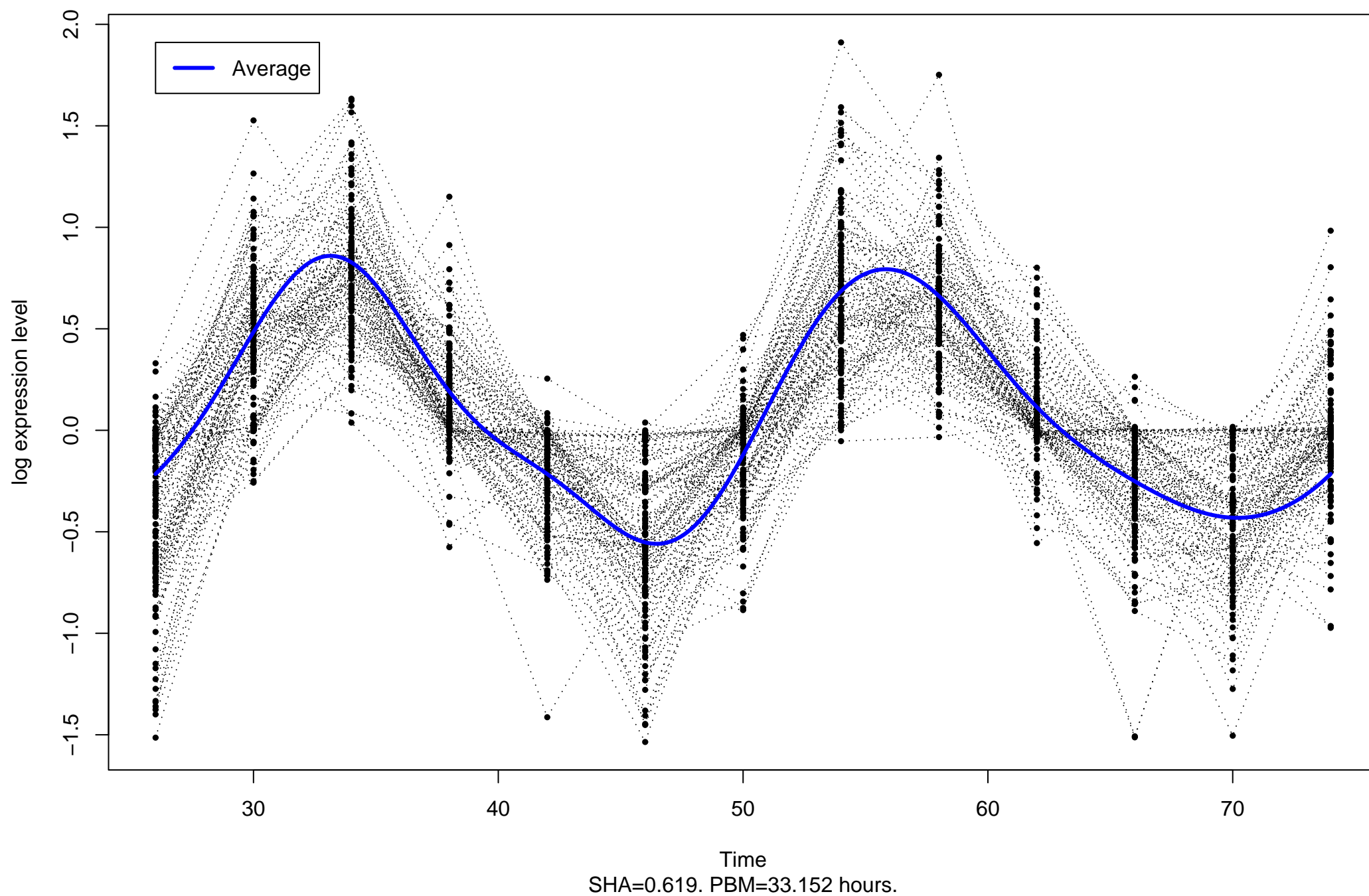
Cluster 27 (100 genes). SHR=0.703.

Time
SHA=0.522. PBM=30.176 hours.
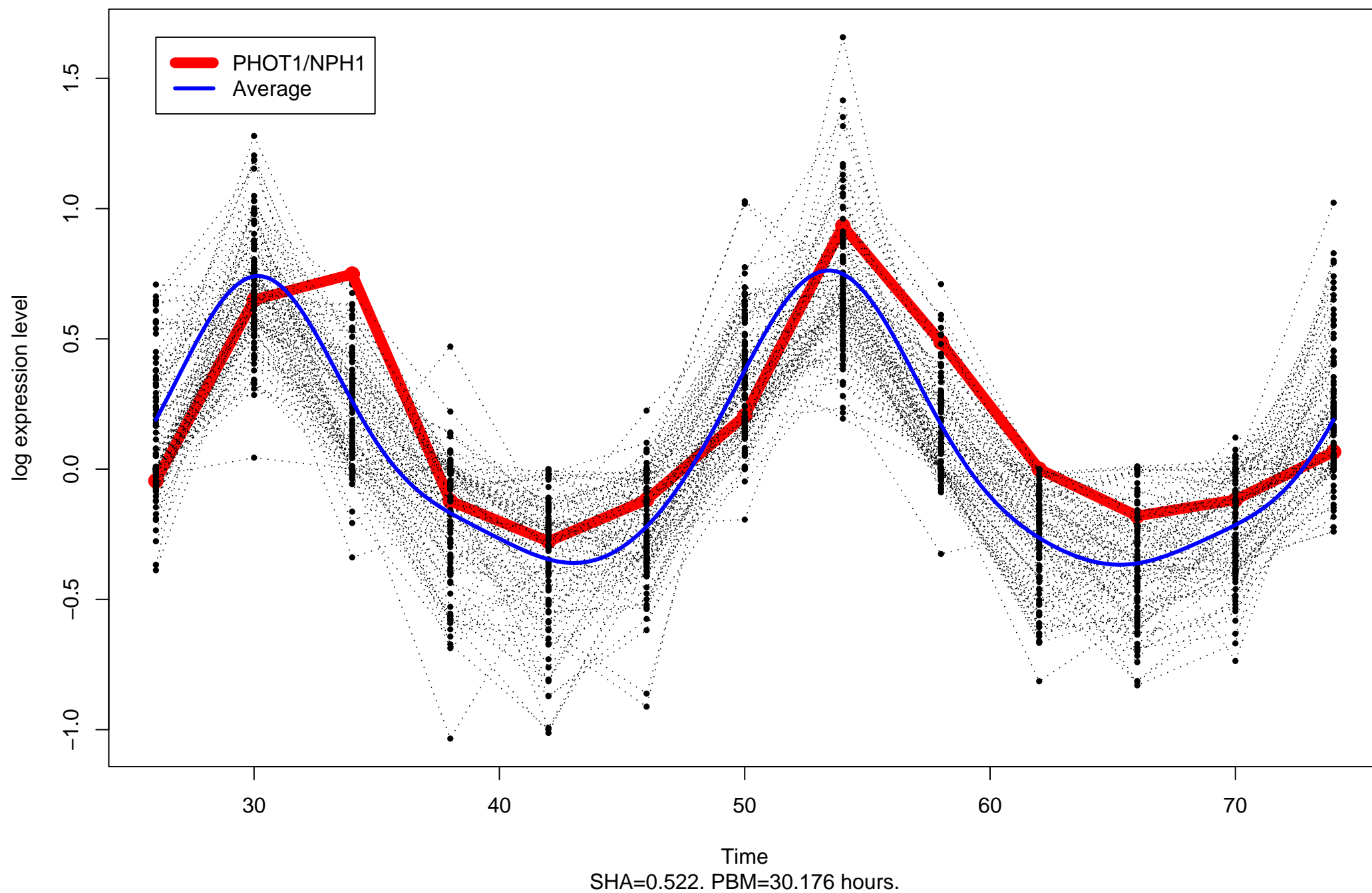
BFC vs COSOPT
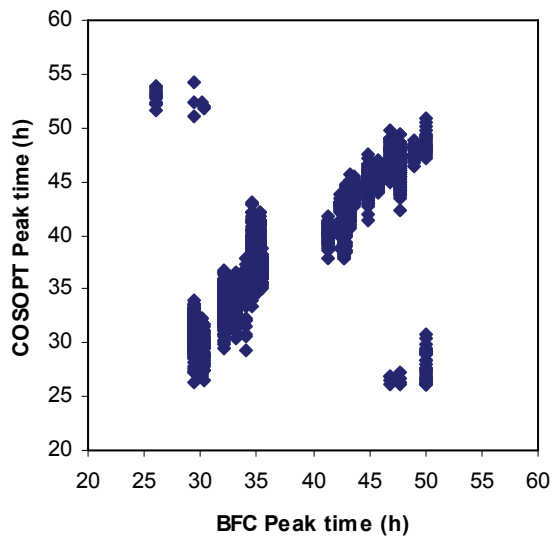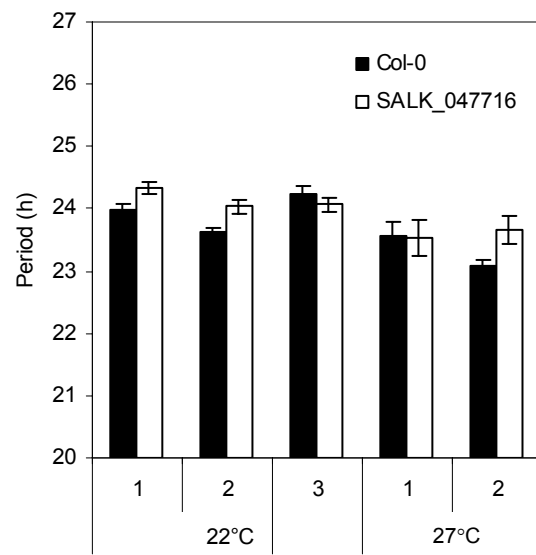
Rank	Affy ID	AGI/Identifier	Fold Change	
1	250476_at	At5g10140	113.3	*FLC*
2	258327_at	At3g22640	0.0361	
3	249053_at	At5g44440	0.0495	
4	255546_at	At4g01910	0.0691	
5	246432_at	At5g17490	0.0698	
6	246299_at	At3g51810	0.071	
7	266503_at	At2g47780	0.0746	
8	248520_at	At5g50600	0.0746	
9	259314_at	At3g05260	0.075	
10	256931_at	At3g22490	0.08	
11	258224_at	At3g15670	0.0803	
12	267579_at	At2g42000	0.0805	
13	263753_at	At2g21490	0.0814	
14	247061_at	At5g66780	0.094	
15	253707_at	At4g29200	0.099	
16	257234_at	At3g14880	0.0996	
17	267075_at	At2g41070	0.107	
18	257947_at	At3g21720	0.107	
19	250868_at	At5g03860	0.112	
20	250882_at	At5g04000	0.112	
21	256139_at	At1g48660	0.119	
22	246273_at	At4g36700	0.124	
23	255471_at	At4g03050	0.129	
24	250648_at	At5g06760	0.133	
25	264494_at	At1g27470	0.134	
26	265091_s_at	At1g03495	7.361	
27	267431_at	At2g34870	0.14	
28	262001_at	At1g33790	0.142	
29	253152_at	At4g35690	0.143	
30	255007_at	At4g10020	0.144	
31	263138_at	At1g65090	0.147	
32	260556_at	At2g43620	0.148	
33	252137_at	At3g50980	0.148	
34	256464_at	At1g32560	0.152	
35	259167_at	At3g01570	0.154	
36	263492_at	At2g42560	0.155	
37	249039_at	At5g44310	0.159	
38	245070_at	At2g23240	0.161	
39	260668_at	At1g19530	0.166	
40	246242_at	At4g36600	0.171	
41	249937_at	At5g22470	0.171	
42	258339_at	At3g16120	0.171	
43	257853_at	At3g12960	0.176	
44	256898_at	At3g24650	0.178	
45	247095_at	At5g66400	0.181	
46	255550_at	At4g01970	0.182	
47	248125_at	At5g54740	0.184	
48	250083_at	At5g17220	5.327	
49	251838_at	At3g54940	0.188	
50	254283_s_at	At4g22870	5.304	
51	264888_at	At1g23070	0.19	

52	263377_at	At2g40220	0.19	
53	256924_at	At3g29590	5.231	
54	264612_at	At1g04560	0.193	
55	249246_at	At5g42290	0.2	
56	265379_at	At2g18340	0.205	
57	260994_at	At1g12130	0.208	
58	262580_at	At1g15330	0.209	
59	258932_at	At3g10150	0.211	
60	245335_at	At4g16160	0.212	
61	259076_at	At3g02140	0.213	
62	245465_at	At4g16590	0.213	
63	261936_at	At1g22600	0.217	
64	263161_at	At1g54020	0.22	
65	266670_at	At2g29740	0.222	
66	265211_at	At2g36640	0.223	
67	265891_at	At2g15010	0.227	
68	262069_at	At1g80090	0.236	
69	264215_at	At1g65340	0.239	
70	248915_at	At5g45690	0.24	
71	266544_at	At2g35300	0.241	
72	258347_at	At3g17520	0.242	
73	255905_at	At1g17810	0.243	
74	266274_at	At2g29380	0.244	
75	262128_at	At1g52690	0.245	
76	256416_at	At3g11050	0.245	
77	267321_at	At2g19320	0.245	
78	259217_at	At3g03620	0.249	
79	250624_at	At5g07330	0.249	
80	248096_at	At5g55240	0.25	
81	262734_at	At1g28640	0.252	
82	245624_at	At4g14090	3.96	
83	258498_at	At3g02480	0.253	
84	265672_at	At2g31980	0.254	
85	249215_at	At5g42800	3.932	
86	254634_at	At4g18650	0.259	
87	251620_at	At3g58060	0.262	
88	256354_at	At1g54870	0.265	
89	247582_at	At5g60760	0.267	
90	267263_at	At2g23110	0.267	
91	265255_at	At2g28420	0.269	
92	261305_at	At1g48470	0.27	
93	263907_at	At2g36270	0.271	
94	258240_at	At3g27660	0.271	
95	249780_at	At5g24240	0.273	
96	255547_at	At4g01920	0.273	
97	254440_at	At4g21020	0.274	
98	257059_at	At3g15280	0.275	
99	253870_at	At4g27530	0.276	
100	257994_at	At3g19920	0.281	
101	260458_at	At1g68250	0.282	
102	248736_at	At5g48110	0.283	
103	263174_at	At1g54040	0.284	
104	256338_at	At1g72100	0.292	
105	267509_at	At2g45660	0.294	*AGL20*

106	249983_at	At5g18470	0.296
107	256340_at	At1g72070	0.297
108	265084_at	At1g03790	0.299
109	245233_at	At4g25580	0.299
110	248869_at	At5g46840	0.303
111	252019_at	At3g53040	0.304
112	246582_at	At1g31750	0.306
113	256827_at	At3g18570	0.307
114	245024_at	atpA	0.309
115	262347_at	At1g64110	0.311
116	253874_at	At4g27450	0.312
117	250118_at	At5g16460	0.313
118	255521_at	At4g02280	0.315
119	248969_at	At5g45310	0.315
120	253895_at	At4g27160	3.16
121	245381_at	At4g17785	3.155
122	248050_at	At5g56100	0.32
123	253494_at	At4g31830	0.322
124	248435_at	At5g51210	0.322
125	247904_at	At5g57390	0.322
126	251100_at	At5g01670	0.323
127	253008_at	At4g38210	0.324
128	248352_at	At5g52300	0.327
129	259042_at	At3g03450	0.328
130	247023_at	At5g67060	0.329
131	248722_at	At5g47810	0.331
132	256938_at	At3g22500	0.332
133	266357_at	At2g32290	0.332
134	254635_at	At4g18670	2.992
135	251137_at	At5g01300	0.339
136	256766_at	At3g22231	2.924
137	248622_at	At5g49360	0.342
138	245052_at	At2g26440	0.343
139	250781_at	At5g05410	0.345
140	252914_at	At4g39130	0.347
141	255056_at	At4g09820	2.875
142	253930_at	At4g26740	0.349
143	259573_at	At1g20390	0.35
144	245970_at	At5g20710	0.351
145	255676_at	At4g00490	0.352
146	259526_at	At1g12570	2.844
147	250199_at	At5g14180	0.352
148	254203_at	At4g24150	0.352
149	255048_at	At4g09600	0.355
150	258586_s_at	At3g04320	0.359
151	263158_at	At1g54160	2.781
152	264782_at	At1g08810	2.78
153	259432_at	At1g01520	0.36
154	253154_at	At4g35710	0.363
155	247421_at	At5g62800	0.364
156	259813_at	At1g49860	2.747
157	246872_at	At5g26080	2.745
158	251238_at	At3g62430	2.743
159	247269_at	At5g64210	0.365

160	263881_at	At2g21820	0.365
161	264079_at	At2g28490	0.37
162	248185_at	At5g54060	2.695
163	253847_at	At4g28010	0.371
164	260037_at	At1g68840	2.69
165	256114_at	At1g16850	0.373
166	254806_at	At4g12430	0.377
167	247437_at	At5g62490	0.377
168	250746_at	At5g05880	0.377
169	264400_at	At1g61800	0.377
170	249111_at	At5g43770	0.382
171	266778_at	At2g29090	0.383
172	248084_at	At5g55470	0.383
173	245628_at	At1g56650	2.607
174	245523_at	At4g15910	0.384
175	255479_at	At4g02380	0.384
176	265236_s_at	At2g07714	2.574
177	256071_at	At1g13640	0.389
178	265611_at	At2g25510	2.566
179	263103_at	At2g05290	2.542
180	265179_at	At1g23650	2.53
181	250180_at	At5g14450	0.396
182	259935_at	At1g71250	0.399
183	249772_at	At5g24130	0.4
184	257243_at	At3g24230	2.499
185	259578_at	At1g27990	0.402
186	245119_at	At2g41640	0.407
187	267036_at	At2g38465	0.409
188	247128_at	At5g66110	0.41
189	266143_at	At2g38905	0.41
190	263385_at	At2g40170	0.411
191	259802_at	At1g72260	0.413
192	245161_at	At2g33070	0.414
193	247718_at	At5g59310	0.417
194	261169_at	At1g04920	0.419
195	259561_at	At1g21250	2.375
196	249013_at	At5g44700	0.421
197	267286_at	At2g23640	0.424
198	250155_at	At5g15160	2.359
199	266654_at	At2g25890	0.424
200	248231_at	At5g53770	0.425
201	265447_at	At2g46570	2.354
202	267089_at	At2g38300	2.354
203	250561_at	At5g08030	2.352
204	266154_at	At2g12190	2.339
205	251509_at	At3g59010	2.337
206	260917_at	At1g02700	0.429
207	248505_at	At5g50360	0.43
208	251580_at	At3g58450	0.431
209	262373_at	At1g73120	0.431
210	266292_at	At2g29350	2.315
211	267076_at	At2g41090	2.305
212	247326_at	At5g64110	2.304
213	256472_at	At1g42610	2.299

214	263947_at	At2g35820	0.436
215	263730_at	At1g60090	0.436
216	247913_at	At5g57510	2.285
217	255579_at	At4g01460	0.438
218	244914_at	orf107e	2.275
219	264007_at	At2g21140	2.272
220	251012_at	At5g02580	0.44
221	262675_at	At1g75930	2.27
222	261135_at	At1g19610	0.443
223	265572_at	At2g28210	2.256
224	267361_at	At2g39920	0.444
225	263191_at	At1g36120	2.245
226	260241_at	At1g63710	2.244
227	251235_at	At3g62860	0.447
228	255294_at	At4g04750	2.226
229	267337_at	At2g39980	0.45
230	263401_at	At2g04070	2.222
231	266690_at	At2g19900	0.451
232	257885_at	At3g16970	2.211
233	264606_at	At1g04660	0.454
234	248372_at	At5g51850	0.454
235	266415_at	At2g38530	0.454
236	257488_s_at	At4g00070	2.202
237	265885_at	At2g42330	0.455
238	255763_at	At1g16730	0.458
239	260915_at	At1g02660	0.459
240	246813_at	At5g27190	2.179
241	260220_at	At1g74650	2.175
242	254384_at	At4g21870	0.46
243	266462_at	At2g47770	0.461
244	250165_at	At5g15290	0.461
245	256571_at	At3g30730	2.162
246	256290_at	At3g12203	0.463
247	256554_at	At3g31380	2.159
248	258603_at	At3g02990	0.464
249	245944_at	At5g19520	0.464
250	262124_at	At1g59660	2.148
251	254805_at	At4g12480	2.148
252	263625_at	At2g04920	2.145
253	265301_s_at	At2g13960	0.466
254	250646_at	At5g06720	0.466
255	257670_at	At3g20340	0.467
256	257859_at	At3g12955	0.468
257	259782_at	At1g29680	0.469
258	249364_at	At5g40590	2.128
259	244953_s_at	nad6	2.124
260	250780_at	At5g05290	0.471
261	244977_at	petD	2.123
262	257244_at	At3g24240	0.471
263	252073_at	At3g51750	0.471
264	264943_at	At1g76910	2.114
265	253767_at	At4g28520	0.473
266	267409_at	At2g34910	0.474
267	251466_at	At3g59340	0.475

268	252417_at	At3g47480	2.098
269	258168_at	At3g21570	2.095
270	251438_s_at	At3g59930	0.478
271	265693_at	At2g24350	2.094
272	255581_at	At4g01490	2.078
273	255189_at	At4g07350	2.078
274	259364_at	At1g13260	0.482
275	264187_at	At1g54860	0.482
276	251511_at	At3g59180	2.073
277	254155_at	At4g24480	0.483
278	251731_at	At3g56350	0.484
279	250769_at	At5g05680	0.485
280	266688_at	At2g19660	0.485
281	263501_s_at	At2g07673	2.058
282	266637_at	At2g35600	2.053
283	255086_at	At4g09300	2.049
284	255527_at	At4g02360	0.488
285	256913_at	At3g23870	0.489
286	256296_at	At1g69480	0.489
287	245875_at	At1g26240	2.041
288	252706_at	At3g43770	2.041
289	252487_at	At3g46660	0.49
290	248494_at	At5g50770	0.491
291	245453_at	At4g16900	2.032
292	262977_at	At1g75490	0.492
293	265621_at	At2g27300	0.494
294	257358_at	At2g40990	2.026
295	264433_at	At1g61810	0.494
296	245982_at	At5g13170	0.495
297	251983_at	At3g53210	0.495
298	244957_at	orf157	2.019
299	249082_at	At5g44120	0.496
300	254213_at	At4g23590	0.496
301	259509_at	At1g43930	2.01
302	264958_at	At1g76960	2.009
303	250345_at	At5g11940	2.008
304	255512_at	At4g02195	0.498
305	255577_at	At4g01410	0.499
306	264623_at	At1g09000	0.499
307	263175_at	At1g05510	0.499
308	249619_at	At5g37500	0.499
309	247136_at	At5g66170	0.499
310	255045_at	At4g09690	2.002
311	249353_at	At5g40420	0.501
312	249390_at	At5g40130	1.995
313	253293_at	At4g33905	1.994
314	246786_at	At5g27410	0.502
315	257008_at	At3g14210	1.99
316	263276_at	At2g14100	0.504
317	255840_at	At2g33520	0.504
318	254095_at	At4g25140	0.504
319	253161_at	At4g35770	0.506
320	260012_at	At1g67865	0.507
321	246888_at	At5g26270	1.97

322	264166_at	At1g65370	0.508
323	253433_s_at	At4g32490	1.96
324	256477_at	At1g42690	1.96
325	249947_at	At5g19200	0.511
326	255589_s_at	At4g01590	0.511
327	258765_at	At3g10710	0.512
328	248916_at	At5g45840	0.512
329	250152_at	At5g15120	0.512
330	263789_at	At2g24560	0.513
331	249532_at	At5g38780	0.514
332	266787_at	At2g28990	1.946
333	250908_at	At5g03680	1.945
334	262185_at	At1g77950	0.514
335	248337_at	At5g52310	0.515
336	245655_at	At1g56530	1.943
337	255703_at	At4g00040	0.515
338	266585_at	At2g14930	1.936
339	257057_at	At3g15310	1.935
340	254245_at	At4g23240	1.935
341	248830_at	At5g47150	1.935
342	245034_at	At2g26390	1.934
343	256561_s_at	At3g31330	1.934
344	255300_at	At4g04870	0.518
345	258914_at	At3g06360	1.93
346	255632_at	At4g00680	0.519
347	253529_at	At4g31520	1.925
348	253556_at	At4g31100	0.52
349	256069_at	At1g13740	0.521
350	245265_at	At4g14400	1.918
351	257368_at	At2g29860	1.917
352	252501_at	At3g46880	1.916
353	245053_at	At2g26450	1.915
354	264144_at	At1g79320	0.523
355	254870_at	At4g11900	1.911
356	263966_s_at	At2g13000	1.911
357	259126_at	At3g02280	0.524
358	265747_s_at	At2g06645	1.906
359	262765_at	At1g13150	1.904
360	251654_at	At3g57140	0.525
361	266499_at	At2g06970	1.901
362	260662_at	At1g19540	0.526
363	244937_at	ndhH	0.526
364	266838_at	At2g25980	0.527
365	251668_at	At3g57010	0.527
366	265603_at	At2g14360	1.895
367	256521_at	At1g66120	1.894
368	249444_at	At5g39370	1.891
369	261221_at	At1g19960	1.89
370	266952_at	At2g34555	1.89
371	266072_at	At2g18700	0.529
372	265397_at	At2g11090	1.887
373	259766_at	At1g64360	1.885
374	247536_at	At5g61650	0.531
375	260470_at	At1g11120	1.884

376	261058_at	At1g01370	1.884
377	266965_at	At2g39510	0.531
378	256499_at	At1g36640	1.881
379	259831_at	At1g69600	0.533
380	260907_at	At1g02570	1.876
381	247731_at	At5g59590	0.533
382	252840_at	At5g32630	1.874
383	251996_at	At3g52840	0.534
384	254710_at	At4g18050	0.534
385	267354_at	At2g39880	1.87
386	256692_at	At3g32050	1.868
387	261342_at	At1g52950	1.868
388	252321_at	At3g48510	0.536
389	251039_at	At5g02020	0.536
390	261907_at	At1g65060	1.865
391	250942_at	At5g03350	1.865
392	265954_at	At2g37260	1.861
393	261603_at	At1g49600	0.539
394	253437_at	At4g32460	0.539
395	260567_at	At2g43820	0.539
396	259360_at	At1g13310	1.854
397	257793_at	At3g26960	1.853
398	261211_at	At1g12780	0.54
399	256940_at	At3g30720	1.852
400	250699_at	At5g06820	1.851
401	247701_at	At5g59900	0.541
402	252316_at	At3g48700	0.542
403	264741_at	At1g62290	0.542
404	245193_at	At1g67810	0.542
405	246855_at	At5g26280	0.543
406	249382_at	At5g40050	1.841
407	259142_at	At3g10200	0.544
408	253684_at	At4g29690	0.544
409	247181_at	At5g65370	1.836
410	246114_at	At5g20250	0.545
411	267357_at	At2g40000	0.546
412	255652_at	At4g00950	1.832
413	256878_at	At3g26460	0.547
414	247463_at	At5g62210	1.828
415	245003_at	psbC	0.547
416	259285_at	At3g11460	0.547
417	265309_at	At2g20290	0.548
418	264049_at	At2g22390	1.826
419	251079_at	At5g02000	1.823
420	250468_at	At5g10120	0.549
421	260849_at	At1g21860	1.822
422	253800_at	At4g28160	1.82
423	257197_at	At3g23800	0.551
424	256589_at	At3g28740	0.551
425	258195_at	At3g13890	1.813
426	251870_at	At3g54510	0.552
427	251767_at	At3g55930	1.812
428	267083_at	At2g41100	0.553
429	256012_at	At1g19250	0.553

430	261799_at	At1g30470	1.808
431	249479_at	At5g38960	1.807
432	261157_at	At1g34510	0.554
433	245151_at	At2g47550	0.554
434	252836_at	At3g42070	1.803
435	263885_at	At2g36940	1.802
436	254274_at	At4g22770	1.801
437	263614_at	At2g25240	0.555
438	252489_at	At3g46710	1.795
439	254046_at	At4g26020	1.793
440	251127_at	At5g01080	1.793
441	255761_at	At1g16770	0.558
442	263784_at	At2g46375	1.792
443	250010_at	At5g18450	0.559
444	265643_at	At2g27390	1.786
445	245472_at	At4g16040	1.784
446	257395_at	At2g15630	0.561
447	258180_at	At3g21480	0.561
448	264160_at	At1g65450	1.782
449	259511_at	At1g12520	0.561
450	251364_at	At3g61300	1.781
451	261647_at	At1g27740	0.562
452	249726_at	At5g35480	1.778
453	265063_at	At1g61500	0.563
454	259371_at	At1g69080	1.776
455	247812_at	At5g58390	1.776
456	256957_at	At3g13420	1.774
457	254534_at	At4g19680	0.564
458	247254_at	At5g64800	1.774
459	246970_at	At5g24900	1.769
460	250826_at	At5g05220	0.566
461	251613_at	At3g57960	1.767
462	248536_at	At5g50140	0.566
463	244972_at	psbB	0.567
464	250589_at	At5g07700	1.764
465	256154_at	At3g08490	1.761
466	264411_at	At1g43240	1.761
467	264083_at	At2g31230	1.76
468	245278_at	At4g17730	0.569
469	265002_at	At1g24400	1.758
470	254914_at	At4g11290	0.569
471	245025_at	atpF	0.57
472	245539_at	At4g15220	0.57
473	260926_at	At1g21360	0.57
474	246297_at	At3g51760	1.754
475	264762_at	At1g61460	1.752
476	266125_at	At2g45050	0.571
477	256349_at	At1g54890	0.572
478	266165_at	At2g28190	0.572
479	252989_at	At4g38420	1.747
480	246229_at	At4g37160	0.573
481	257100_at	At3g25010	1.743
482	263497_at	At2g42540	0.574
483	263032_at	At1g23850	0.574

484	266393_at	At2g41260	0.574
485	247769_at	At5g58910	1.74
486	253608_at	At4g30290	0.577
487	246925_at	At5g25180	0.578
488	252539_at	At3g45730	0.578
489	266175_at	At2g02450	1.73
490	257548_s_at	At3g26620	1.728
491	266989_at	At2g39330	0.579
492	254499_at	At4g20100	1.727
493	258878_at	At3g03170	0.579
494	246293_at	At3g56710	1.725
495	246740_at	At5g27810	1.725
496	246687_at	At5g33370	1.723
497	248246_at	At5g53200	1.722
498	248069_at	At5g55650	0.581
499	265622_at	At2g27280	1.721
500	260716_at	At1g48130	0.582
501	247553_at	At5g60910	1.717
502	249838_at	At5g23460	0.582
503	267411_at	At2g34930	0.583
504	254754_at	At4g13210	1.715
505	247951_at	At5g57240	0.584
506	259374_at	At3g16280	1.712
507	252718_at	At3g43940	1.711
508	256352_at	At1g54970	0.585
509	265493_at	At2g15670	1.709
510	245527_at	At4g15960	0.585
511	267195_at	At2g30940	1.708
512	257142_at	At3g20090	1.705
513	247871_at	At5g57530	0.586
514	245979_at	At5g13150	0.587
515	261567_at	At1g33055	0.587
516	248964_at	At5g45340	0.587
517	262995_s_at	At1g54430	1.703
518	249802_at	At5g23770	1.703
519	265644_at	At2g27380	0.587
520	248614_at	At5g49560	0.588
521	251646_at	At3g57780	1.699
522	252286_at	At3g49070	0.589
523	252436_x_at	At3g47330	1.697
524	255606_at	At4g01110	1.697
525	266504_at	At2g47820	1.697
526	261475_at	At1g14550	0.589
527	262099_s_at	At1g59500	0.59
528	262719_at	At1g43590	1.695
529	260144_at	At1g71960	0.59
530	263945_at	At2g36030	1.694
531	248286_at	At5g52870	0.59
532	252576_s_at	At3g45450	0.591
533	250588_at	At5g07660	0.591
534	249944_at	At5g22290	0.591
535	267041_at	At2g34315	0.591
536	262050_at	At1g80130	1.691
537	263944_at	At2g36040	1.69

538	265131_at	At1g23760	0.592
539	263427_at	At2g22260	1.688
540	250860_at	At5g04770	0.593
541	249814_at	At5g23840	0.593
542	245026_at	atpH	0.593
543	263034_at	At1g24020	1.686
544	263384_at	At2g40130	1.685
545	254334_at	At4g22760	0.593
546	267566_at	At2g30760	1.684
547	249675_at	At5g35940	0.594
548	261350_at	At1g79770	1.681
549	255835_at	At2g33420	1.68
550	251548_at	At3g58870	1.679
551	259793_at	At1g64380	0.596
552	247903_at	At5g57340	0.596
553	249773_at	At5g24140	0.596
554	259602_at	At1g56520	1.676
555	251284_at	At3g61840	1.676
556	247793_at	At5g58650	0.597
557	244983_at	rpl16.chloroplast	0.597
558	266431_at	At2g07230	1.675
559	255069_s_at	At4g08990	1.675
560	260742_at	At1g15050	0.597
561	248660_at	At5g48650	1.674
562	253651_at	At4g30030	1.674
563	253931_at	At4g26770	1.674
564	260178_at	At1g70720	1.674
565	245005_at	rps14	1.673
566	247954_at	At5g56870	0.598
567	260342_at	At1g69280	0.598
568	263851_at	At2g04460	1.671
569	256302_at	At1g69526	0.6
570	258257_at	At3g26770	0.6
571	255029_x_at	At4g09470	1.665
572	258652_at	At3g09910	0.601
573	247976_at	At5g56830	1.664
574	247897_at	At5g57810	1.663
575	261731_s_at	At1g47780	1.663
576	248251_at	At5g53220	0.601
577	255156_at	At4g07780	1.662
578	245420_at	At4g17410	1.662
579	253492_at	At4g31810	0.602
580	264214_s_at	At1g65330	1.66
581	265786_at	At2g07300	1.659
582	251249_at	At3g62160	0.603
583	246121_at	At5g20370	1.659
584	245037_at	At2g26420	0.603
585	245652_at	At4g13960	1.658
586	258897_at	At3g05730	1.657
587	255238_at	At4g05570	1.656
588	248371_at	At5g51810	0.604
589	247672_at	At5g60220	0.605
590	246794_s_at	At5g27010	0.605
591	251405_at	At3g60330	0.605

592	250151_at	At5g14570	0.605
593	249459_at	At5g39580	1.651
594	248867_at	At5g46830	1.651
595	248725_at	At5g47980	0.606
596	267394_s_at	At2g44540	1.649
597	245009_at	rps4.chloroplast	0.607
598	258939_at	At3g10020	0.607
599	260706_at	At1g32350	1.647
600	249664_at	At5g36810	1.647
601	260088_at	At1g73190	0.607
602	245713_at	At5g04370	0.607
603	262102_at	At1g02980	1.644
604	265913_at	At2g25625	1.642
605	249477_s_at	At5g38930	1.642
606	246103_at	At5g28640	0.609
607	261641_at	At1g27670	0.609
608	253904_at	At4g27140	0.609
609	266978_at	At2g39430	0.61
610	250807_at	At5g05130	0.61
611	266756_at	At2g46950	0.61
612	263173_at	At1g54180	0.61
613	250379_at	At5g11590	1.637
614	260262_at	At1g68470	1.637
615	257842_at	At3g28390	0.611
616	261702_at	At1g32760	0.611
617	252115_at	At3g51600	1.636
618	257247_at	At3g24140	1.635
619	245050_at	psbK	0.612
620	247374_at	At5g63190	0.612
621	266784_at	At2g28960	1.634
622	246321_at	At1g16640	1.634
623	264513_at	At1g09420	0.613
624	249091_at	At5g43860	1.631
625	262013_s_at	At1g35640	1.629
626	247360_at	At5g63450	0.614
627	247660_at	At5g60070	1.629
628	260904_at	At1g02450	1.628
629	263055_at	At2g04600	1.626
630	253488_at	At4g31610	1.626
631	256825_at	At3g22120	1.625
632	264339_at	At1g70290	0.616
633	253515_at	At4g31320	0.616
634	257964_at	At3g19850	1.622
635	252629_at	At3g44970	1.622
636	248570_at	At5g49780	1.62
637	267222_at	At2g43880	0.618
638	267043_at	At2g34330	1.617
639	250471_at	At5g10170	1.617
640	254231_at	At4g23810	0.618
641	265163_at	At1g23580	1.617
642	244999_at	rpoB	0.619
643	264991_s_at	At3g43400	1.616
644	250907_at	At5g03670	0.619
645	248873_at	At5g46450	1.613

646	253097_at	At4g37320	1.613
647	245705_at	At5g04390	0.62
648	245738_at	At1g44130	1.612
649	244949_at	orf116	1.611
650	253902_at	At4g27170	1.611
651	255557_at	At4g01990	0.621
652	248443_at	At5g51310	1.61
653	257945_at	At3g21860	1.61
654	264416_at	At1g43140	1.61
655	253082_at	At4g36230	1.609
656	247959_at	At5g57080	1.608
657	264091_at	At1g79110	1.606
658	263019_at	At1g23870	0.623
659	244940_at	rps12.2	0.623
660	245224_at	At3g29796	1.605
661	256815_at	At3g21380	0.623
662	264758_at	At1g61340	0.623
663	256489_at	At1g31550	1.605
664	260468_at	At1g11100	1.604
665	252163_at	At3g50610	1.603
666	252990_at	At4g38440	0.624
667	246477_at	At5g16770	1.603
668	255651_at	At4g00940	1.603
669	258418_at	At3g16660	1.602
670	262448_at	At1g49450	0.624
671	264765_at	At1g61430	1.602
672	254828_at	At4g12550	0.624
673	265128_at	At1g30860	0.624
674	253103_at	At4g36110	1.602
675	246991_at	At5g67400	0.625
676	249634_at	At5g36840	1.601
677	255422_at	At4g03270	1.6
678	246712_at	At5g28200	1.6
679	248625_at	At5g48880	1.6
680	266149_x_at	At2g12250	1.6
681	250501_at	At5g09640	0.625
682	250400_at	At5g10740	0.626
683	260429_at	At1g72450	0.626
684	255005_at	At4g09990	0.627
685	260160_at	At1g79880	0.627
686	249102_at	At5g43590	1.595
687	264195_at	At1g22690	1.594
688	266661_at	At2g25820	1.594
689	262603_at	At1g15380	1.593
690	260011_at	At1g68110	1.591
691	251084_at	At5g01520	0.629
692	265746_at	At2g06630	1.59
693	253894_at	At4g27150	0.629
694	253682_at	At4g29640	1.589
695	252004_at	At3g52780	1.589
696	255526_at	At4g02350	0.63
697	254743_at	At4g13420	1.587
698	260720_at	At1g48095	1.587
699	257588_x_at	At1g30150	1.586

700	247586_at	At5g60660	0.63
701	247379_at	At5g63360	1.586
702	252533_at	At3g46110	1.586
703	257567_at	At3g23930	1.584
704	252622_at	At3g45310	0.631
705	265369_s_at	At2g06470	1.582
706	251009_at	At5g02640	1.582
707	258064_at	At3g14680	0.633
708	263890_at	At2g37030	0.633
709	265518_at	At2g06040	0.633
710	256368_at	At1g66800	0.633
711	261399_at	At1g79620	0.633
712	249333_at	At5g40990	1.578
713	255122_at	At4g08490	1.577
714	249596_s_at	At5g37950	0.634
715	252282_at	At3g49360	1.576
716	255621_at	At4g01390	1.576
717	263791_at	At2g24520	1.576
718	253461_at	At4g32170	1.576
719	266308_at	At2g27010	0.635
720	259145_at	At3g10170	0.635
721	261663_at	At1g18330	0.635
722	246606_at	At5g35350	1.574
723	266669_at	At2g29750	0.635
724	262644_at	At1g62710	0.635
725	263376_at	At2g20520	0.636
726	250294_at	At5g13380	0.636
727	255918_at	At5g28570	1.573
728	262628_at	At1g06490	0.636
729	254327_at	At4g22490	1.572
730	266269_at	At2g29480	0.637
731	264994_at	At1g67270	1.571
732	255594_at	At4g01660	0.637
733	260640_at	At1g53350	1.57
734	244987_s_at	rpl2.1_chloro	0.637
735	260333_at	At1g70500	0.637
736	244979_at	rps11	0.637
737	254673_at	At4g18430	0.638
738	258002_at	At3g28930	1.568
739	247030_at	At5g67210	0.638
740	246251_at	At4g37220	0.638
741	264682_at	At1g65570	0.638
742	249438_at	At5g40010	1.567
743	246107_at	At5g28700	1.567
744	246871_at	At5g26070	1.567
745	259183_at	At3g01580	1.567
746	249476_at	At5g38910	1.567
747	264564_at	At1g05290	1.566
748	245154_at	At5g12460	1.565
749	267138_s_at	At2g38210	0.639
750	262845_at	At1g14740	0.639
751	266479_at	At2g31160	1.564
752	246184_at	At5g20950	0.639
753	249369_at	At5g40680	0.64

754	251667_at	At3g57150	0.64
755	255375_at	At4g03780	1.563
756	263857_at	At2g04380	1.562
757	262371_at	At1g73160	0.64
758	264318_at	At1g04220	0.64
759	267270_at	At2g02550	1.561
760	256427_at	At3g11090	1.56
761	261249_at	At1g05880	1.56
762	248992_at	At5g45230	1.559
763	247665_at	At5g60130	1.559
764	262046_at	At1g79960	1.559
765	260030_at	At1g68880	1.558
766	248553_at	At5g50170	0.642
767	256970_at	At3g21090	0.642
768	246468_at	At5g17050	1.556
769	246370_at	At1g51920	1.555
770	267585_s_at	At2g42090	1.555
771	263098_at	At2g16005	0.643
772	259694_at	At1g63180	0.643
773	264618_at	At2g17680	1.554
774	252686_at	At3g44420	1.554
775	253602_s_at	At4g30910	0.644
776	267457_at	At2g33790	0.644
777	264519_at	At1g10000	1.551
778	250694_at	At5g06710	0.645
779	248979_at	At5g45080	1.55
780	254941_s_at	At4g10830	1.549
781	253837_at	At4g27850	1.548
782	247914_at	At5g57540	0.646
783	248205_at	At5g54300	0.646
784	258078_at	At3g25870	0.646
785	249136_at	At5g43180	1.547
786	252719_at	At3g43950	1.547
787	263913_at	At2g36570	1.547
788	254056_at	At4g25250	0.647
789	252813_at	At3g42500	1.546
790	250267_at	At5g12930	0.647
791	261283_s_at	At1g35770	1.545
792	246825_at	At5g26260	0.648
793	266347_at	At2g01440	1.544
794	251527_at	At3g58650	1.542
795	262902_x_at	At1g59930	1.542
796	256060_at	At1g07050	1.542
797	259796_at	At1g64270	1.542
798	267192_at	At2g30890	1.541
799	264819_at	At1g03510	0.649
800	252234_at	At3g49780	0.649
801	254513_at	At4g20240	1.54
802	256553_at	At3g31360	1.54
803	246973_at	At5g24970	0.65
804	251698_at	At3g56610	1.54
805	247478_at	At5g62360	0.65
806	260942_s_at	At1g45190	1.537
807	250426_at	At5g10510	0.651

808	254511_at	At4g20220	1.536
809	258832_at	At3g07070	1.536
810	247915_at	At5g57570	1.535
811	253660_at	At4g30140	1.535
812	260092_at	At1g73280	0.652
813	246368_at	At1g51890	1.534
814	249336_at	At5g41070	0.652
815	258397_at	At3g15357	0.652
816	255493_at	At4g02690	0.652
817	260858_at	At1g43770	1.534
818	262364_at	At1g72860	1.534
819	250794_at	At5g05270	1.534
820	266844_at	At2g26120	1.533
821	248790_at	At5g47450	0.653
822	256362_at	At1g66450	0.653
823	259843_at	At1g73570	0.653
824	250778_at	At5g05500	0.653
825	249124_at	At5g43740	1.531
826	245506_at	At4g15700	1.531
827	255956_at	At1g22015	1.53
828	264196_at	At1g22670	1.53
829	263969_at	At2g12940	1.53
830	252661_at	At3g44450	1.529
831	248822_at	At5g47000	0.654
832	259065_at	At3g07520	1.528
833	260515_at	At1g51460	1.528
834	248164_at	At5g54490	0.654
835	265387_at	At2g20670	0.654
836	262462_at	At1g50350	1.527
837	262854_at	At1g20870	1.527
838	253041_at	At4g37870	0.655
839	262527_at	At1g17010	0.655
840	251109_at	At5g01600	0.655
841	267495_at	At2g30420	1.526
842	253003_s_at	At4g38300	1.525
843	260788_at	At1g06260	1.525
844	252057_at	At3g52480	0.656
845	251304_at	At3g61990	0.656
846	260990_at	At1g12180	1.524
847	256670_at	At3g32220	1.523
848	257693_at	At3g12850	1.522
849	263622_at	At2g04870	1.522
850	254625_at	At4g18470	0.657
851	251025_at	At5g02190	1.522
852	245329_at	At4g14365	0.658
853	250982_at	At5g03150	1.521
854	246603_at	At1g31690	1.521
855	260962_at	At1g44980	1.52
856	259182_at	At3g01750	1.52
857	250980_at	At5g03130	1.519
858	246401_at	At1g57560	0.658
859	261600_x_at	At1g49680	1.519
860	254371_at	At4g21760	1.519
861	265842_at	At2g35700	1.519

862	244989_s_at	ycf2.1	1.518
863	251765_at	At3g55880	1.518
864	254411_at	At4g21420	1.518
865	255645_at	At4g00880	0.659
866	264486_at	At1g77180	0.659
867	253514_at	At4g31805	1.516
868	259487_at	At1g15720	1.516
869	261327_at	At1g44830	0.66
870	260642_at	At1g53260	1.515
871	265134_at	At1g51260	1.515
872	267621_at	At2g39680	1.515
873	257941_at	At3g21800	0.66
874	266178_at	At2g02280	1.515
875	256288_at	At3g12270	0.66
876	252475_s_at	At3g46640	0.661
877	266600_at	At2g46070	1.512
878	260424_at	At1g72460	1.512
879	249897_at	At5g22550	0.661
880	255467_at	At4g03010	1.512
881	256919_at	At3g18970	1.512
882	246670_at	At5g29584	1.512
883	246807_at	At5g27100	1.512
884	266539_at	At2g35160	0.662
885	259173_at	At3g03640	0.662
886	252804_at	At3g42370	1.51
887	248212_at	At5g54020	0.662
888	244973_at	psbT	0.662
889	261545_at	At1g63530	1.51
890	250558_at	At5g07990	1.509
891	261598_at	At1g49750	1.509
892	258170_at	At3g21600	0.663
893	260067_at	At1g73780	0.663
894	263963_at	At2g36080	0.663
895	247778_at	At5g58750	1.508
896	251812_at	At3g54970	1.508
897	254520_at	At4g19960	0.663
898	261006_at	At1g26410	1.507
899	250776_at	At5g05320	0.664
900	264093_at	At1g79220	1.506
901	254597_at	At4g18980	1.506
902	267191_at	At2g44110	0.664
903	251124_s_at	At5g01040	0.664
904	257504_at	At1g52250	0.664
905	246380_at	At1g57750	1.505
906	261890_at	At1g80970	1.504
907	261059_at	At1g01250	1.504
908	256108_at	At1g16940	1.504
909	251771_at	At3g56000	0.665
910	267362_at	At2g39910	1.503
911	265548_s_at	At2g07620	1.503
912	245081_at	At2g23280	1.502
913	248509_at	At5g50335	1.502
914	249661_x_at	At5g36650	1.502
915	247418_at	At5g63030	0.666

916	265929_s_at	At2g18570	0.666
917	266737_at	At2g47140	0.666
918	245754_at	At1g35183	1.5
919	250915_at	At5g03790	0.667
920	245501_at	At4g15620	1.5
921	267424_at	At2g34800	1.5
922	262659_at	At1g14240	0.667
923	253796_at	At4g28460	1.499
924	257392_at	At2g24450	1.499
925	254299_at	At4g22920	0.667
926	250415_at	At5g11210	1.498
927	248879_at	At5g46180	0.667
928	261223_at	At1g19950	1.498
929	267595_at	At2g32990	1.498
930	254044_at	At4g25820	0.668
931	267084_at	At2g41180	1.497
932	254269_at	At4g23050	0.668
933	247029_at	At5g67190	0.668
934	255694_at	At4g00050	0.668
935	255450_at	At4g02850	1.496
936	256557_at	At3g31410	1.496
937	262915_at	At1g59940	0.668
938	255875_s_at	At2g40500	1.496
939	246913_at	At5g25830	0.669
940	263554_at	At2g16410	1.495
941	254552_at	At4g19900	0.669
942	261596_at	At1g33080	1.495
943	260427_at	At1g72430	0.669
944	261745_at	At1g08500	0.669
945	264240_at	At1g54820	1.494
946	254308_at	At4g22410	1.494
947	247682_at	At5g59650	1.494
948	254718_at	At4g13580	0.67
949	254548_at	At4g19870	1.492
950	258503_at	At3g02500	1.492
951	264631_at	At1g65630	1.492
952	249202_at	At5g42580	0.67
953	266048_at	At2g40790	0.67
954	250277_at	At5g12940	0.671
955	252685_at	At3g44410	0.671
956	266837_x_at	At2g25990	0.671
957	264754_at	At1g61400	1.489
958	258204_at	At3g13960	0.671
959	263572_at	At2g17060	1.489
960	250887_at	At5g04450	1.488
961	262374_s_at	At1g72930	1.487
962	258252_at	At3g15720	0.673
963	255049_at	At4g09610	0.673
964	257507_at	At1g29600	1.487
965	255637_at	At4g00750	0.673
966	261814_at	At1g08310	0.673
967	244997_at	rpoC2	0.673
968	252597_at	At3g45360	1.486
969	256347_at	At1g54923	1.486

970	249607_at	At5g37280	0.673
971	265511_at	At2g05540	0.674
972	264800_at	At1g08800	0.674
973	260312_at	At1g63880	1.483
974	257416_at	At2g17750	1.483
975	263395_at	At2g20510	1.482
976	253859_at	At4g27657	0.675
977	250292_at	At5g13220	0.675
978	264489_at	At1g27370	1.481
979	254043_at	At4g25990	0.675
980	257203_at	At3g23730	0.675
981	252280_at	At3g49260	1.481
982	260166_at	At1g79840	1.481
983	251756_at	At3g55820	1.48
984	258545_at	At3g07050	0.676
985	252598_at	At3g45380	1.479
986	264415_at	At1g43160	0.676
987	265117_at	At1g62500	0.676
988	250665_at	At5g06980	0.676
989	250748_at	At5g05710	0.676
990	262803_at	At1g21000	0.677
991	253998_at	At4g26010	0.677
992	245162_at	At2g33240	1.477
993	266286_at	At2g29170	1.477
994	265561_s_at	At2g05510	0.678
995	261216_at	At1g33030	1.476
996	250157_at	At5g15180	0.678
997	247217_s_at	At5g65050	1.476
998	267565_at	At2g30750	1.475
999	252908_at	At4g39670	1.475
1000	259608_at	At1g27960	0.678

Supplementary Table 1 - *FLC* responsive genes

Table showing list of 1000 genes showing greatest change in expression between *FRI*; *FLC* and *fri*; *flc* genotypes. Ranked according to fold change. Affymetrix probe ID and AGI number (or other identifier) shown for each gene (Note: where probe set targets multiple genes only single AGI number given). Fold change based on difference between average expression values of two biological replicates and expressed in terms of induction or repression in the *FRI*; *FLC* genotype. *FLC* and *AGL20* highlighted to right of table.

Affy ID	AGI	Gene Symbol	BFC Cluster	Notes
259432_at	At1g01520	LCL3	18	Transcription factor (myb)
265611_at	At2g25510		18	
265954_at	At2g37260	TTG2	18	Transcription factor
252661_at	At3g44450		18	
252629_at	At3g44970		18	Electron transport
252316_at	At3g48700		18	
250794_at	At5g05270		18	Flavonoid biosynthesis
245982_at	At5g13170		18	
248625_at	At5g48880	PKT1	18	acetyl-CoA C-acyltransferase activity
247463_at	At5g62210	ATS3	18	
265091_s_at	At1g03495/At1g03940		20	Transferase activity
245624_at	At4g14090		20	UDP-glycosyltransferase activity
254283_s_at	At4g22870/At4g22880		20	putative anthocyanidin synthase
250083_at	At5g17220	ATGSTF12	20	toxin catabolism
249215_at	At5g42800	DFR	20	Anthocyanin biosynthesis
264091_at	At1g79110		21	
253859_at	At4g27657		21	
253097_at	At4g37320	CYP81D5	21	Electron transport
256060_at	At1g07050		22	CONSTANS-like protein-related
262603_at	At1g15380		22	Carbohydrate metabolism
252813_at	At3g42500		22	
254805_at	At4g12480	PEARLI 1 1	22	Lipid transfer
253161_at	At4g35770	SEN1	22	
248509_at	At5g50335		22	
247954_at	At5g56870		22	beta-galactosidase activity
247478_at	At5g62360		22	Pectinesterase inhibitor activity
261663_at	At1g18330	EPR1	23	Transcription factor (myb)
266072_at	At2g18700	ATTPS11	23	Transferase activity
265387_at	At2g20670		23	
253874_at	At4g27450		23	
252475_s_at	At3g46640/At5g59570	LUX/-	25	Transcription factor (myb)
254043_at	At4g25990	CIL	25	

Supplementary Table 2 - *FLC* clock candidate genes

List of 32 genes scored as *FLC* responsive and also in the top six highest amplitude BFC clusters. AGI numbers and gene symbols shown for each gene, along with BFC cluster number and notes on gene functions (from TAIR annotations).